INCOHIS

INCOHIS 2022 AUTUMN

NOVEMBER 25 - 26, 2022
İSTANBUL / TÜRKİYE

INTERNATIONAL CONGRESS OF NEW HORIZONS IN SCIENCES PROCEEDINGS BOOK

www.incohis.com
info@incohis.com

INCOHIS 2022 AUTUMN

INTERNATIONAL CONGRESS OF NEW HORIZONS IN SCIENCES PROCEEDINGS BOOK

NOVEMBER 25 - 26, 2022

İ.T.Ü. MTAL (MESLEKİ VE TEKNİK ANADOLU LİSESİ)

İSTANBUL / TÜRKİYE

www.incohis.com

info@incohis.com

ISBN: 978-605-70762-9-8

EDITORS

- Prof. Dr. Ali DENİZ, Istanbul Technical University
- Prof. Dr. Hüseyin TOROS, Istanbul Technical University
- Lecturer Mustafa OF, Kocaeli University
- Lecturer İsmail KILIÇASLAN, Kocaeli University

SUPPORTERS

Dear participants,

INCOHIS 2022 AUTUMN Congress is an internationally recognized academic event. With this congress, where face-to-face and remote participation is supported, you will have the opportunity to present your scientific publications. Our congress, which is attended by respected names in the scientific community, is a candidate congress to bring new horizons to science.

Participants from 20 different countries applied to the congress. Participants presented their papers for two days with the duration of the congress.

We are also grateful to the esteemed participants, our keynote speakers, our referees for their support and contributions to the success of this congress. Thank you for attending our academic event and supporting us.

The INCOHIS congress will be held every year by raising its target higher. It will reach out to wider communities and increase the number of papers and participants.

Any kind of feedback about the congress is very important to us. You can reach our congress from our web page, info@incohis.com e-mail address and official social media accounts.

17.12.2022

INCOHIS ORGANIZING COMMITTEE

KEYNOTE SPEAKERS

Prof.Dr. Arbnor Pajaziti
University of Prishtina "Hasan Prishtina", Faculty of Mechanical Enginerring, Department of Mechatronics, Kosovo

Assoc.Prof.Dr. Flora Merko
Aleksandër Moisiu University Durrës, Albania

Assoc.Prof.Dr. Etleva Dashi
Assoc. Prof. Dr. Etleva Dashi. Agriculture University of Tirana, Albania

Assoc.Prof.Dr. Lyudmyla Symochko
Uzhhorod National Ůniversity, Ukraine, Coimbra University, Coimbra, Portugal

Assoc.Prof.Dr. Edmond Hoxha
Polytechnic University Of Tirana, Albania

Assoc. Prof. Dr. Mehboob Nagarbawdi
Aki's Poona College Of Arts, Science Commerce, India

PTech. Dr. Noor Zaitun Yahaya
Universiti Malaysia Terengganu, Malaysia

Dr. Ahmad Ali
Department of Life Sciences, University of Mumbai, India

TABLE OF CONTENTS

ELECTROMAGNETIC COMPATIBILITY (EMC) SIMULATION AND APPLICATION IN AUTOMOTIVE ELECTRONICS

Alperen YAZAR[1] and Metin HÜNER[2]

1 Istanbul Technical University, Istanbul/Turkey, yazar20@itu.edu.tr

2 Istanbul Technical University, Istanbul/Turkey, metinhuner@itu.edu.tr

Abstract - To ensure electromagnetic compatibility in automotive electronics, some standards and design methods should be considered during design. One of these standards is UNECE R10 which defines conducted and radiated emissions. In this study, a power supply was designed and simulated that meets the conducted emission standards by UNECE R10 with CISPR 25.

Keywords: EMC, EMI, LTspice, Automotive electronics, Artificial network (AN), Conducted emissions, Noise, CISPR 25.

I. Introduction

EMC is the ability of an electronic component to operate successfully in the electromagnetic field and not affect other systems or components. A system can be affected from environment via radiated or conducted emissions. UNECE R10 is the international standard which defines the maximum emission limits for conducted and radiated emissions. Radiated emissions are measured by high frequency range antennas and spectrum analyzer in shielded rooms. So, radiated emissions cannot be simulated by LTspice. Unlike that, conducted emissions are measured by AN (Artificial Network) and spectrum analyzer. Therefore, using AN model, conducted emissions can be estimated by LTspice. AN model for UNECE R10 is shown in Figure 1 according to the UN Regulation No. 10 [1].

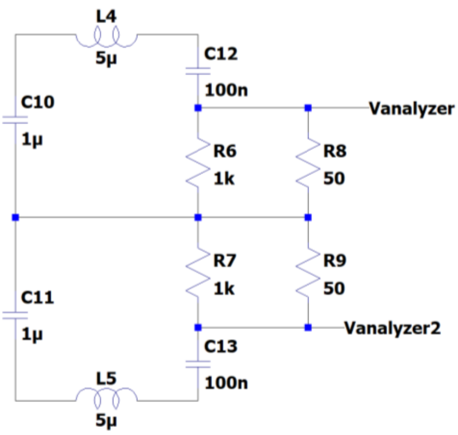

Figure 1: AN model

In a system, there may number of components such as electronic control unit (ECU), advanced driver assistance systems (ADAS), human media interface (HMI), battery management systems (BMS). All these components are supplied by low voltage battery which is 12V or 24V in automotive. So, whole components are connected via power supply line. Every single component should work properly.

Conducted emissions are the noise which is generated by a component to power supply line. Conducted emissions can be defined as differential-mode noise and common-mode noise. In differential-mode noise, noise current and current from main power supply line have same path. Differential-mode noise current path is shown in Figure 2.

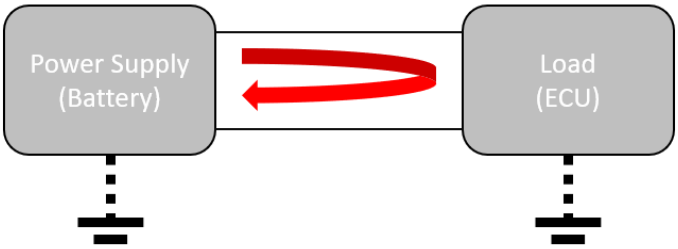

Figure 2: Differential-mode noise current path

Common-mode noise is generated by leakage current on stray capacitances or isolated grounded systems. Such ash, low voltage is used in automotive generally. With low voltage battery, hybrid vehicle or electric vehicle (EV) has high voltage batteries. So, high voltage batteries have different grounding. These high voltage and low voltage grounds are connected via stray capacitors. Common-mode noise current path is shown in Figure 3.

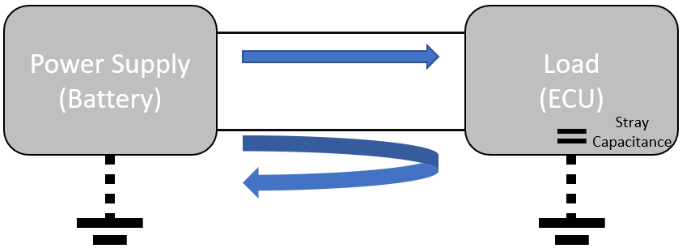

Figure 3: Common-mode noise current path

Conducted emissions are measured by AN and spectrum analyzer. Test environment is shown in Figure 4.

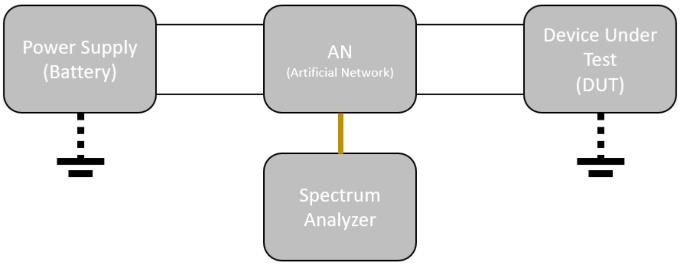

Figure 4: Conducted emissions test environment

In this work, a power supply of an electronic control unit (ECU) was designed and simulated to observe conducted emissions (differential-mode and common-mode noises) via LTspice.

II. Literature

EMI specifications are defined for different fields. According to the UNECE R10, CISPR 25 can be defined main EMI standards for automotive. Main electronic components which are existed in an automotive must comply with the CISPR 25 standards [2]. To test CISPR 25, shielded room is needed but there are some ways to estimate the results such as LTspice and MW Studio. [3]. Unlike CISPR 25, CISPR 22 covers the multimedia equipment which are used as external systems in the automotive [2].

To estimate common-mode and differential-mode noises, AN model can be considered as a resistor. So, equivalent circuit can be built with resistors [4]. Despite this approach, real AN model can be built with low-pass filters [5].

Common-mode and differential-mode noises can be reduced by using some filters. These filters have inductor and capacitors basically to block noises from DC-DC converter to main power supply line. To analyze attenuation level, current and voltage methods can be used. Current method is more efficient way because it has not source impedance. So, noise can be simulated as current source [6].

III. Design and simulation method

In automotive electronics, every single component should be AEC-Q (Automotive Electronics Council) qualified. AEC-Q qualified component ensure the work properly in stressed environments such as high temperature range and vibration. So, designed power supply has AEC-Q qualified active and passive components. Electronic control units have different modules such as power supply module, communication module, microcontroller module, input-output module etc. Generally, input voltage of all sub-modules is 5V. So, power supply module has a switch-mode power supply which generates 5V from battery voltage. For this work, LT8640A from Analog Devices is used [7]. It is a step-down converter with high-efficiency and ultra-low EMI (Electromagnetic Interference) emissions, and it can provide 5A from 5V output to microcontroller and others. Switching frequency also is adjustable. To use similar inductance, switching frequency is set to 1MHz via R_T resistance. Also, all passive components have not basic spice-models due to get realistic results. Capacitors and inductors are modelled with parasitic. To get 250mA from output, 20Ω load resistance is used. Also, electromagnetic compatibility tests are observed in continuous mode due to avoid start-up noises.

To observe differential-mode and common-mode emissions, “Vanalyzer” and “Vanalyzer2” nets are transformed from time domain to frequency domain via FFT analysis. LTspice FFT analysis has range with dBV scale but CISPR 25 defines the limits with dBμV. So, this conversation is actualized as in (1).

$$1dBV = 120dB\mu V \tag{1}$$

Differential-mode calculations are simulated with formula which shown as in (2).

$$Vdm = \frac{V(Vanalyzer) - V(Vanalyzer2)}{2} \tag{2}$$

Common-mode calculations are simulated with formula which shown as in (3).

$$Vcm = \frac{V(Vanalyzer) + V(Vanalyzer2)}{2} \tag{3}$$

IV. Simulations and filter design

Typical application schematic of LT8640A with AN model is designed in LTspice as shown in Figure 5.

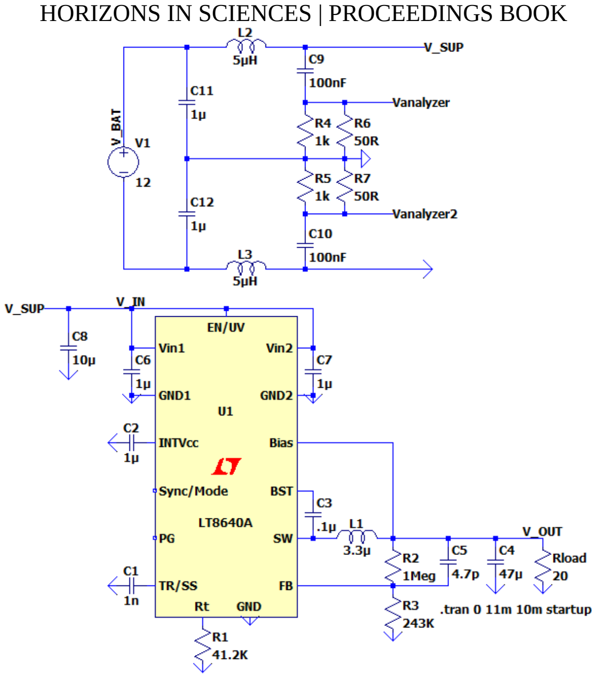

Figure 5: Typical application schematic with AN model

Differential-mode (red trace) and common-mode noises (blue trace) are simulated in frequency domain which shown in Figure 6. CISPR 25 limits are also shown as grey trace.

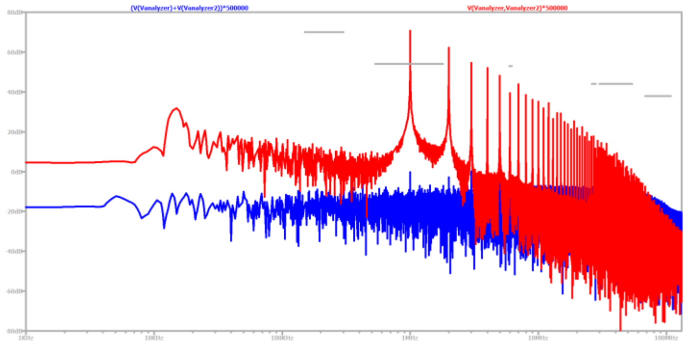

Figure 6: Differential-mode and common-mode noises of typical application schematic

As shown, differential-mode and common-mode noises exceed the limits around 1MHz which is switching frequency. In power supply systems, to prevent exceeding of the limits, common-mode chokes and LC low-pass filters are used. Common-mode choke is based on two coupled inductors [8]. In this system, common-mode noise is not detected. So, LC low-pass filter must be designed to block differential-mode noise.

To find attenuation rate, input of power supply can be simulated as current source and AN can be simulated as 100Ω basically [6]. Simulation schematic is shown in Figure 7.

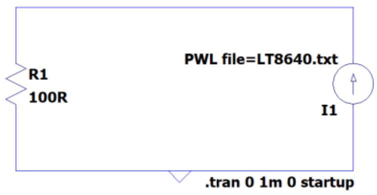

Figure 7: Simulation schematic for FFT analysis

Noise levels can be estimated on frequency domain via FFT analysis. FFT analysis (red trace) shows the frequency levels which exceed the limits (grey trace). Simulation results are shown in Figure 8.

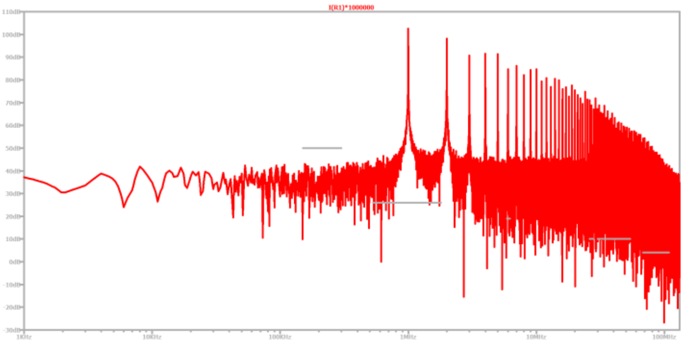

Figure 8: FFT analysis for differential-mode noise

To decrease differential-mode noise, second order LC filter can be used. According to the CISPR 25 current probe method Class 5 section, limit is 26dBμA. Unfortunately, power supply has 100dBμA noise level at 1MHz. So, the attenuation rate should be around 80dBμA.

Second order low-pass filters have -40dB/dec attenuation rate [9]. Second order low-pass filter should be designed to get -80dB/dec attenuation rate at 1MHz according to the Figure 9.

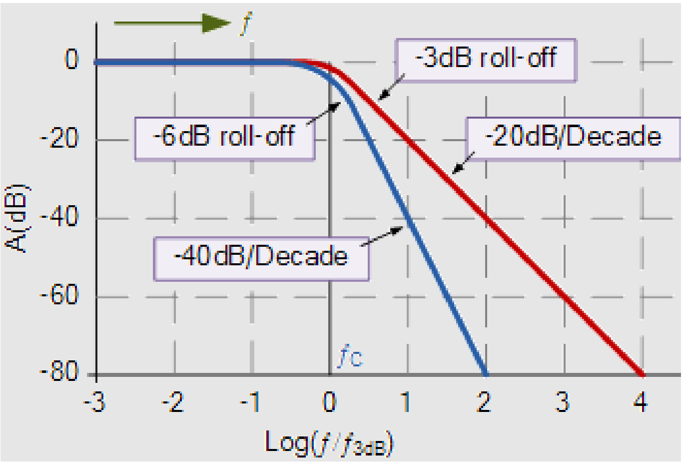

Figure 9: Attenuation graph for low-pass filters [9]

The formula shown in (4) can be used to find the cut-off frequency of the low-pass filter.

$$\log\left(\frac{f}{f3dB}\right) = 2 \qquad (4)$$

During selecting inductor, current limits, power loss and impedance should be considered. LC filter values can be calculated following formula (5). So, cut-off frequency should be around 10kHz.

$$f3dB = \frac{1}{2\pi\sqrt{(LC)}} \qquad (5)$$

In general applications, inductance may be selected as 10μH. So, capacitor value can be calculated via formula which is shown in (6) [6].

$$f3dB = \frac{1}{2\pi\sqrt{(LC)}} = \frac{1}{2\pi\sqrt{(10\mu\mathrm{H} * 22\mu F)}} = 10.73kHz \quad (6)$$

Same typical application schematic is re-simulated with LC low-pass filter. Typical application schematic with LC low-pass filter is shown in Figure 10.

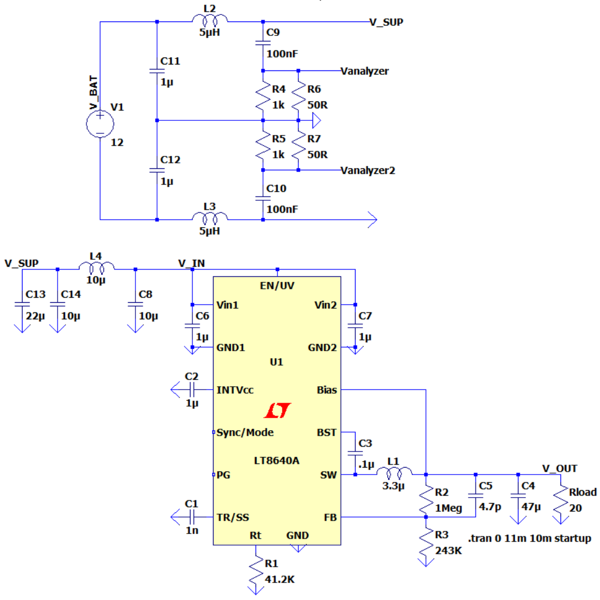

Figure 10: Typical application schematic with AN model and LC low-pass filter

LC low-pass filter should be placed to power supply line. Because, for all components connected to the main power supply line to continue to operate properly, differential mode noise from the step-down converter must be filtered.

Differential-mode (red trace) and common-mode noises (blue trace) are re-simulated with LC low-pass filter in frequency domain which shown in Figure 11. CISPR 25 limits also shown as grey trace.

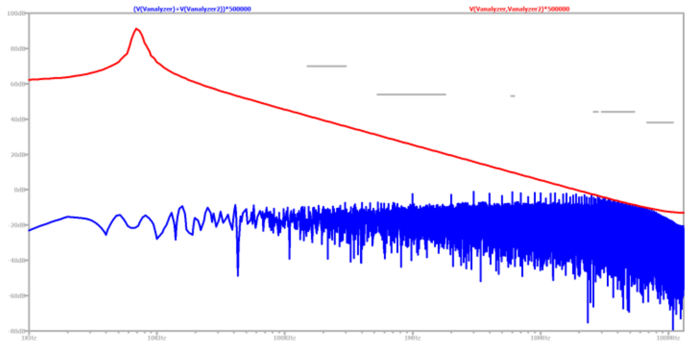

Figure 11: Differential-mode and common-mode noises of typical application schematic with LC low-pass filter

V. Conclusion

During the DC-DC converter design, EMC standards and design methods should be considered. In this work, a step-down convertor for automotive grade technology equipment was simulated and designed. Common-mode and differential-mode noises are estimated via LTspice using AN model.

Exceeding the conducted emission limits is suppressed by the second-order LC low-pass filter design.

REFERENCES

[1] *United Nations Regulation No. 10*, pp. 42, November 2019
[2] *Texas Instruments Application Note SLYY136*, Texas Instruments, February 2018
[3] *Automotive Component EMC Testing*, Vicente Rodriguez, March 2022
[4] *Design of EMI Filters for DC-DC converter*, J. L. Kotny, T. Duquesne, N. Idir, France, 2010
[5] *Anticipate EMC with LTSPICE*, Wurth Electronics, May 2020
[6] T*exas Instruments Application Note AN2162*, Texas Instruments, November 2021
[7] *Analog Devices Data Sheet LT8640/8640-1*, Analog Devices, March 2022
[8] *ST Microelectronics Application Note AN4511*, ST Microelectronics, June 2016
[9] www.electronics-tutorials.ws/filter/second-order-filters

SUSTAINABILITY OF HOUSEHOLD WATER TREATMENT METHODS FOR ARSENIC REMOVAL IN AFGHANISTAN (CASE STUDY)

Abdul Wahed Ahmadi[1], Mehmet EminArgun[2] , Ajit P. Annachhatre[3]

[1& 2] Konya Technical University, Faculty of Engineering and Natural Sciences, Environmental Engineering Department, Konya, Turkey

[3]Asian Institute of Technology (AIT), Department of Energy, Environment and Climate Change, Pathum Bangkok, Thailand

Abstract

Arsenic contamination in groundwater is an huge risk and big problem on a global scale in the many countries. Over fifty million people in more than seventy countries are affected by arsenic pollution in drinking water. The main sources of arsenic contamination in groundwater are considered to be anthropogenic, gelogenic (geothermal) and biogenic. Therefore, as groundwater is one of the main important drinking water sources in Afghanistan and it is highly susceptible to be contaminated by any of these sources, the need for suitable and sustainable water filtration and treatment technologies for arsenic removal is sensed. Currently, 78% of the population relies on groundwater which is mainly being taken using household tub wells in order to access safe drinking water. Recently, the high level of arsenic contamination of groundwater in Afghanistan becomes a critical problem. According to a study on water quality in Afghanistan, 459 out of 746 water point samples showed high level of arsenic contamination (around 61%) and it exceeds the World Health Organization (WHO) standard. The main goal of this research study is the comparative evolution of the current arsenic removal technologies and methods in developing countries such as Afghanistan. Additionally, it is critically review the current state of arsenic contamination of groundwater in Afghanistan in order to suggest sustainable household arsenic removal methods. For this purpose, the three most popular household arsenic removal technologies such as Sono Sand Filter, Kanchan Arsenic Removal and Arsenic Bio Sand Filter already tested in a study area (Nawalparasi district of Nepal). Based on the tests, samples analysis report and assessment of existing household arsenic removal technologies; it has been shown that the Arsenic Bio Sand Filter (ABSF) is the most effective method. In this method removal of arsenic is done with an effectiveness of 95 %. Additionally, the method is very effective for removal the pathogens, bacteria, iron, and turbidity reduction. Finally, the outcome of this study will assists the authorities and decision makers to develop some mitigation policies for controlling potential contamination of arsenic in the groundwater, which will lead to improve the public health by reducing arsenic related diseases.

Keyword: Arsenic, Contamination, Household, Groundwater.

Emails: ahmadi267071@gmail.com
Phone: +905313187462

Introduction

Arsenic pollution in groundwater has been recognized as a global problem since 1990 and over 150 million people in more than seventy countries worldwide are affected by arsenic poisoning drinking water. For example, in Bangladesh over thirty million people and in India over twenty million people, are at risk (Nordstrom, 2002). Therefore, as groundwater is one of the main important drinking water sources in Afghanistan and it is highly susceptible to be contaminated by any of these sources, the need for sustainable water filtration and technology for arsenic treatment is sensed. Currently, 78% of the population relies on groundwater, which is mainly being taken using household tub wells in order to access safe drinking water. Recently, the high levels of arsenic contamination of groundwater in Afghanistan become a critical problem. According to a study on water quality in Afghanistan, 459 out of 746 water point samples showed high level of arsenic contamination (around 61%) and it exceeds the World Health Organization (WHO) standard. In addition, arsenic pollution and it`s problem in groundwater is natural and geological origin in different cities of Afghanistan. (Ahmad, 2001).

According to Rahman 2009, Afghanistan is a landlocked country in the Central Asia and it has a population of 32.5 million, with 79 % of the population living in rural areas and the 42 % of its population in rural area and 78 % in urban area access to improved safe drinking water sources and arsenic contamination of groundwater in Afghanistan is a problem of existing groundwater especially drinking water and water supply systems where people have been using groundwater such as wells water sources. However, the contamination of arsenic is also the main environmental health management problem particularly in Panjshir, Ghazni, Logher, Parwan Midanwardek, Farah, Kabul, Maymamna and Jalal abad provinces in Water, Sanitation and Hygiene Monitoring "WASH" sector. The arsenic contaminated groundwater in Afghanistan mostly have been used for domestic purpose such as drinking can cause adverse effect on human health at the study area. According to a study about the water quality in different provinces of Afghanistan with "746" samples from DWPs" drinking water points" it has been carried in the district of Ghazni province "Khawja Omari district" it is in the center of Ghazni and also in another region such as Jaghato district of the Miydan Wardak province, the results shows that level of arsenic concentration in groundwater at the study areas 61% of DWPs samples exceeded then the value of the "WHO" guideline of 10 ppb of arsenic and 38% of analyzed water samples exceeded the Afghanistan drinking water quality standard "ADWQS" of 50 ppb (Safi & Kohistani, 2016). However, mostly the Afghanistan's drinking water resources for domestic purpose and for agricultural are as follows: Groundwater (wells ,shallow wells and depth wells ,springs) 78 %, Surface Water 18 % (lakes, rivers and canals) and other 4 % rainy water snow, hail and etc (Peter *et al.*, 2009).

Ghazni and Midanwardek provinces are the best example as many sources of arsenic contamination in groundwater. There are annually a lot of diseases including cancer and skin diseases happening on people in Afghanistan due to the high range of arsenic contamination in groundwater. Arsenic is now evident that in groundwater is a problem around the world because several regions in the world are above the WHO's maximum permissible. Increasing the level of arsenic in groundwater have been related to human health diseases and mortality from drinking water consumption. Therefore, Arsenic is carcinogenic metal which can impacts the major organs such as urinary tract, kidneys and liver (Safi & Kohistani, 2016).

Usually, 78% of the Afghan people for their household using groundwater from shallow wells for domestic purpose specially for drinking and each family has at least a shallow well with depth of 3 to 15 meter in their yards. Since the groundwater is one of the main and important sources of drinking water in Afghanistan so it is susceptible to these contaminations and problems. Groundwater pollution with arsenic occurs when man-made products and activities become unsafe and unfit for human use and it really can effect on human health. The source arsenic pollution and contamination of groundwater in Afghanistan is natural, geological and human activities.

Furthermore, arsenic contamination of the groundwater in Afghanistan is also a serious problem; the major problem is most severe in the many regions especially in Ghazni province (Brammer & Ravenscroft, 2009).

According to a study on water quality in different cities of Afghanistan such as Ghazni, Panjshir and Midanwardek, the result from 1756 water point samples showed that high level of arsenic contamination in groundwater (around 61% in Ghazni and 38% in Panjshir) which is exceeds than the WHO standard (Fig-1) (WHO, 2001). So in this study, it focuses to find the sustainable method to remove Arsenic from the water which already contaminated**.**

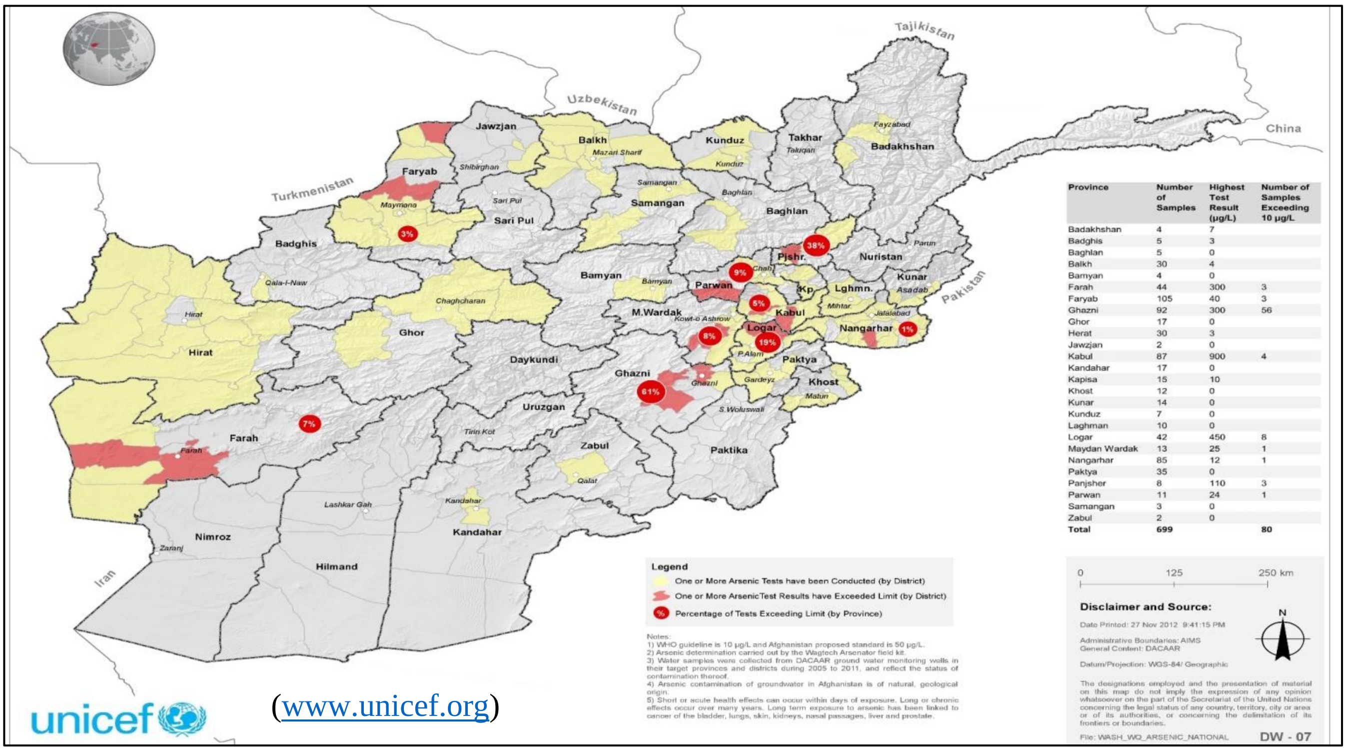

Fig.1: Level of Arsenic Contaminant of Groundwater in the Different Regions of Afghanistan

The basic and general objective of this research is to critically review the current problem of arsenic contamination of groundwater in Afghanistan and to suggest sustainable arsenic removal method to solve this problem. Specific objectives are as follows:

1. To review the global arsenic pollution in groundwater and its effect on human health and environment.

2. To assessment the current situation of technology for household water treatment using in developing countries.

3. To identify and recognize the most suitable and sustainable arsenic removal technology for Afghanistan.

Methodology

The procedure and method for this study, including the reviewed about the arsenic problem in the Asian, American, African and European continents including of the Afghanistan country, as well as, it stated the arsenic contamination of groundwater in developing countries, reviewed various arsenic treatment technologies used in developing countries and finally it tried to have an evaluation the between reviewed technologies and then it was selected the most suitable methods and technology which is recommended in Afghanistan.

Data Analysis

Data analysis process, in this study was both qualitative and quantitative techniques and the source of data were the primary and secondary. The data collected form the research work, Published and unpublished reports and documents, Journal, articles, guidelines and policy documents to find out the groundwater contamination and its possible causes by arsenic and primary data including the questionnaires, interviews, observations and sampling were analysis with the statement of analysis and analysis of data did by Excel, SSPS and X-connect software in this study. However, the standard methods is a joint publication of the American Public Health Association (APHA), American Water Works Association (AWWA), and the Water Environment Federation (WEF) and the Atomic Absorption Spectroscopy (AAS) has been selected for analysis of my samples taken from wells water to identify and detect the concentration of arsenic in both raw water (before filtration) and filtered water (after filtration) in the ENPHO laboratory.

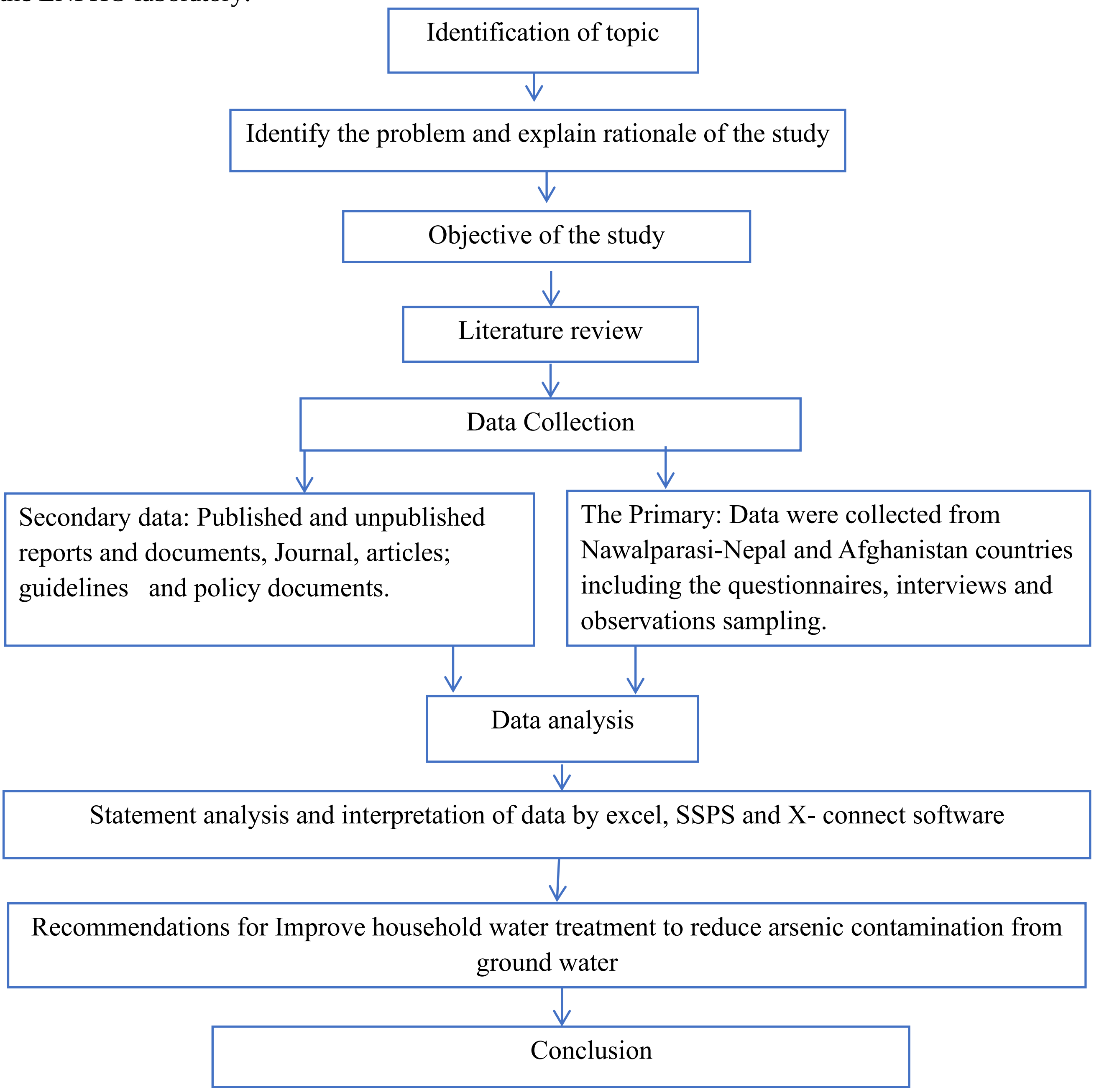

Results and Discussion

Samples Analysis Report & Water Test Result in the Study Area

The results & report from analysis of samples showing that groundwater and well water in the Bhairahawa village of Nawalparasi district Kathmandu city in Nepal has contaminated with arsenic more than the WHO, Guild line Value (GV) and NDWS.

Table 1 *Samples Analysis Report & Water Test Result in ENPHO Lab*

No-Sample	Type of Water	Parameter	Concentration in Raw water	Efficiency Removal	WHO GV	Unit	Source of Water samples
1126	RW	Ar	0.07	Very good	0.01	mg/L	Well water (groundwater)
1127	FW	Ar	0.05		0.01	mg/L	Kanchan Filter
1128	RW	Ar	0.83	Not good	0.01	mg/L	Well water (groundwater)
1129	FW	Ar	0.23		0.01	mg/L	Sono Arsenic Filter
1130	RW	Ar	0.39	Excellent	0.01	mg/L	Well water (groundwater)
1131	FW	Ar	0.005		0.01	mg/L	Arsenic Bio Sand Filter

Note: Raw water (RW), Arsenic (Ar)

The report of WHO and ENPHO shown in 2015 that this water has also others contamination such as bacteria and other chemicals such as iron, fluoride, nitrate, and etc.

Table 2 *Overall Water Quality Test Result and Removal Efficiency by ABSF*

Water quality parameters	Range of concentration in raw water	% of Raw water Exceeding the NDWQS	Removal efficiency by ABSF (%)
AS (PPb)	91.57	80 – 54	83
Fecal coliform (cfu/100 mg)	72.86	90	97
Iron (mg/L)	0 -5	79	100
Hardness (mg/L)	19-664	1	7
pH	6- 7.5	40	----------
Phosphate (mg/L)	0 – 2	80	75

The summary of water quality test result, removal efficiency by the arsenic bio sand filter and the percentages of raw water exceeding the NDWQS in 57% samples that token by the ENPHO from Nepal. In this case, most wells are contain arsenic concentration up to the WHO and NDWQS (Danglol, 2016).

Comparison between test result and WHO guideline

The comparison between the result from Environmental Public Health Organization laboratory experiment indicated that most samples have Arsenic concentration higher than the WHO and NDWQS GV (0.01mg/L & 0.05 mg/L) and bacteriological contamination is mostly higher the standard. The groundwater especially wells water are contaminated with pathogens, especially arsenic is to much higher from shallow wells water because it is up to 0.05 mg/L (WHO, 2015).

The survey results showing that out of 6 samples, 3 samples from raw water and 3 samples also from filtered water, the raw water have Arsenic concentration higher than World Health Organization GV 0.05 and filtered Arsenic Bio Sand Filter and Kanchan Arsenic Filter are lower than the WHO and NDWQS, But the range of arsenic concentration in filtered water from Sono Filter is yet higher than the both WHO and NDWQS range. However, the result shows that Arsenic Bio Sand filter is the most suitable technology for household water treatment method especially for removal of arsenic from groundwater.

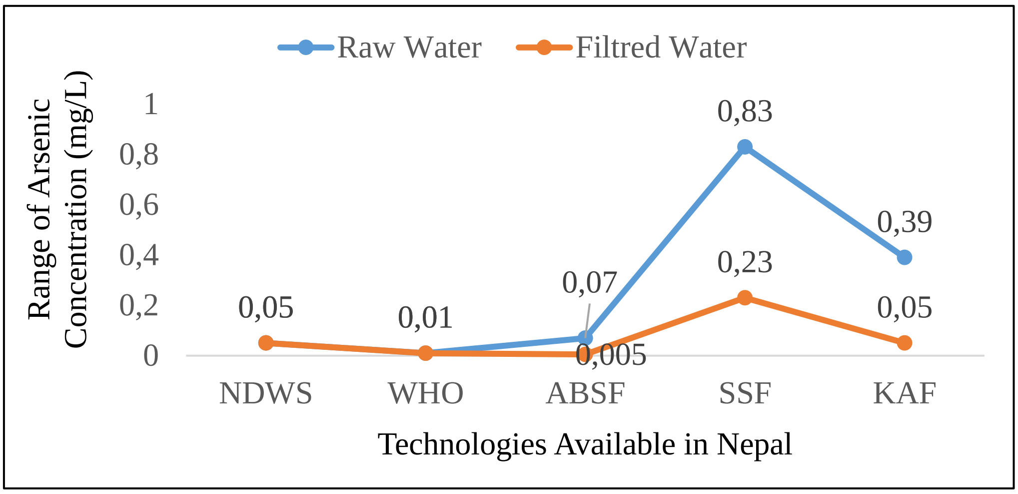

Fig.2: Comparison of Raw Water and Filtered Water with WHO GV and NDWS (WHO, 2015)

The efficiency removal of Arsenic Bio Sand Filter (ABSF) is much higher than the Sono Sand Filter (SSF) & Kanchan Arsenic Filter (KAF) and the efficiency removal of Sono Sand filter is so low. However, according to the result SSF could not remove arsenic concentration from groundwater event to the WHO GV or NDWS. Therefore, classification of these three technologies was based on the removal efficiency Kanchan Arsenic Filter is medium arsenic removal, SSF has low efficiency removal and ABSF is an excellent arsenic removal (Fig.2). (WHO, 2015)

Evaluation of Arsenic Removal Methods

According to this review the primary data in this research, the information is given about the technologies for household arsenic removal from groundwater. The methods and technologies can be used by local well owners (household) and public water suppliers. However, according to available and basic information, a matrix is formed to give an idea on the applicability of the technology for some given situations. The Fundamental information of arsenic chemistry and its processes is important when a community or a household is either looking to install or make a new system for arsenic removal from drinking water or modify an old technology to comply with the new arsenic rule. Thus, based on the finding of this study, it was tried to evaluate those methods and technologies that were studied in literature review according to the cost, removal and treatment efficiency, production, Lifespan and operation and maintenance (Table-1) However, it compares the six most promising arsenic removal methods and technologies in terms of cost-benefits with operations and maintenance costs (Table-2). So, arsenic removal methods and technologies are ranked form one up to ten for each decision driver. For instance, capital costs or mechanical reliability the basis for the ranking of each parameter is shown in the right-most column. The high rank is 10 or excellent which indicates that the methods and technology is more suitable for implementation in household. This type of ranking and analysis has to be performed for impacted system, accounting for the utility preferences and site constraints. However, this analysis system is purely for evaluation purposes (Table-2). The comparison of main arsenic removal technologies, according to all the technologies, regarding to the processes listed in the each of this technology has their advantages , disadvantages and is being refined to be most suitable under the rural conditions (Table-3) and (Table-2).

The comparison and modifications according to the pilot scale implementation of the technology are as following objectives:

1) To improve effectiveness of arsenic removal technologies for using in household.
2) To reduce the capital cost and O&P (operaiton and maintenance) cost of the methods of those technology.
3) To make the technologies UF (user friendly) for household or community.
4) To overcome operation and maintenance problems.

Table 3 *Comparison of Main Arsenic Removal Technologies*

Technology Type	Removal Efficiency %	Benefits	Estimated costs $	
			Capital cost/$	Operating cost/year ($)
Filtration 1-Arsenic BSF	76-90	Can provide 60-80 L/h and high flow rat and minimum maintenance	50-75	10
2-SONO filter	90- 95	Produces 20–30 L/hour for daily ,Without producing toxic wastes, Works without any chemical	35-50	20
Coagulation & flocculation 1-Bucket Treatment Unit	60-90	Low costs and simple chemicals, chemicals normally available	10-20	15-20
2-Three Kolshi Filter	90	A homemade and inexpensive ways to treat drinking water 90% Arsenic removal	15-20	15
Activated alumina 1-Magc-Alcan Filter	80-85	Simple operation and common chemicals Media life span about 1 year	35-50	life span 1 year
2- Shapla Filter	80-90	very efficient removal low maintenance, no daily sludge	10-15	10
Membrane Technology 1-Reverse osmosis (RO)	> 95	Removal of multiple contaminant Well defined, high removal efficiency	300 - 1500	100-200
Ion-exchange 1-READ-F	95	Long media lifespan	50-70	life span 3 year
Oxidation 1-Solar oxidation	60-90	simple method that uses irradiation of water with sunlight	60-70	20-15
Compact conventional TU	90- 94	Good arsenic removal with low cost	800	100-150

Fill and Draw Units	90	Both arsenate and arsenate can be removed by its	600	100-150

Table 4 *Evaluation of Arsenic Treatment Technology Ranking based on Characteristics*

Characteristics	Filtration ABSF	Membrane Technology RO	Oxidation (SOAR)	Ion Exchange (REDA-F)	Activated Alumina Adsorption	Coagulation and flocculation	Scoring Basis
Capital Costs (O&M)	9	5	10	7	7	6	High Score (HS) for low cost technologies and Low Score (LS) for high cost technologies
Ease of Implementation	9	7	8	9	8	9	HS, for methods that are easy to install and operate LS, for cumbersome technologies
Labor Required	9	10	7	7	6	**7**	HS , that can be automated and LS, for labor-intensive technologies
Process Reliability	10	6	8	7	8	8	HS, that have less interference from source water quality and LS, that are highly impacted by co-occurring ions
Mechanical Reliability	9	10	7	6	6	7	HS, for sturdier processes and LS, for processes with more moving parts
Public Acceptance	10	6	9	7	7	8	HS, for technologies that have minimal impact on the neighborhood and LS, for technologies that have lots of interference with neighborhood activities
Residuals Handling	10	8	6	6	8	7	HS, for technologies that produce little or no waste stream
Process Flexibility	10	6	8	8	9	10	HS, for processes that can be readily upgraded or modified and LS, for processes that are difficult to expand
Cumulative Score	77	58	63	57	59	62	High score for technologies that has high removal efficiency with high produce treated water and should be low cost without waste

Selection of the most Suitable Arsenic Removal Technology for Afghanistan

Most Suitable Arsenic Treatment Technology (MSATT) for household and community for a specific water system should be based on careful consideration of many potations and factors including the System Capacity (SC), Site Constraints (SC) (availability of land, power and sewer connection), Residuals Handling Preferences (RHP), Existing Treatment System (ETS), Qualitative Decision Drivers (QDD) (ease of implementation, public acceptance), Capital Cost (CC) and Operation and Maintenance Costs (OMC) .According (Table-5) arsenic bio sand filter has high score than the other six technologies for household arsenic removal, because of their following potations and characteristics:

- The removal efficiency of Arsenic Bio Sand Filter (ABSF) with high removal
- ABSF can remove turbidity, color, some iron, manganese and odor.
- ABSF is a good microbial removal (it can remove over 98.5% bacteria and100% parasites).
- ABSF has high flow rate, up to 60 to 80 liters per hour.
- ABSF has no on-going costs or no need for replaceable parts.
- ABS is also durable and robust.
- ABSF can fabricate from local materials. (It is a good opportunity for local businesses).
- Easy to maintain and water tastes and looks good.
- The capital cost and operation cost are suitable for each household or community.

Regarding to the above attributes of the arsenic bio sand filter and it's this technology, the ABSF, is a good option and it is most suitable for Afghanistan and it is recommended for households and communities which they using for water treatment (Fig-3).

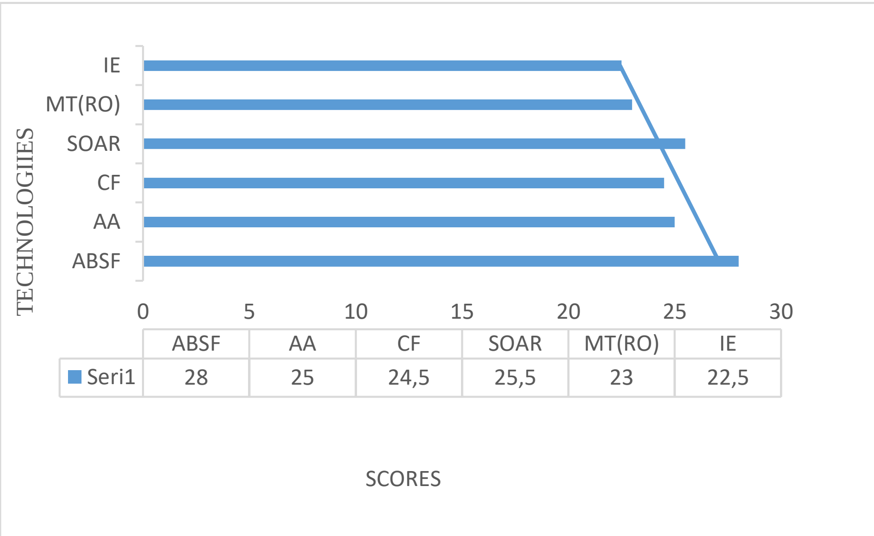

Fig.3: Summary of Ranking System for (ARTs) (WHO, 2015).

Note: IE (Ion Exchange), MT (Membrane Technology), SOAR (Solar Oxidation As removal), CF (Coagulations and Flocculation), AA (Activity Alum), and ABSF (Arsenic Bio Sand Filter).

Conceptual design of technology for a family

The design of this sustainable technology for household arsenic removal was entirely constructed with local available materials as well as local labor. However, in this study design was ABSF to estimated home water use needs for average family members (Table-5).

Table 5 *Average Water Use Estimation in a Family for Various Water Services*

Average water use per person in a estimated family		
Number of People Living at Home	5 person	
Average family income/month	300$	
water use source	Groundwater or Surface water	

(WHO, 2015)

Water contaminated parameter	Bacteria, Viruses, Protozoa Helminths, Turbidity, Iron and Arsenic	
Daily water usage and expense for various water services per person in an estimated family in the case of Afghanistan.	For Drinking	2x5 =10 liters per day
	Cooking	3x5 = 15 liters per day
	Washing hands, brushing teed and shower	15x5 =75 liters per day
	Washing dishes	8 liters per day
	Others	12 liters per day
Total water used in the family		100 liters per day

According to the above table, the average water use was estimated family for various water services and water usage varies enormously; it is only estimation to what technology that was can design for a family in the case of Afghanistan. Therefore, it was mentioned that I did not consider about the water consumption such as flash toilet, cleaning and laundry.
In this case, for the purposes of planning to design a sustainable household water treatment for arsenic removal which it can provide to meet demand of the water consumed in the family as the mentioned technology above has all characteristics that can improve water quality. For the design of such methods, it was consider the following options:

- It may removes arsenic, pathogens, iron and turbidity from both groundwater and surface water.
- It could construct by trained local technicians using local materials that mean it constructed of simple materials available on the local market.
- This method has a good flow rate, 20 -30 L/h. and it need simple thing for their operation and maintenance.
- The construction of the filter can be carried out by local trained technicians.

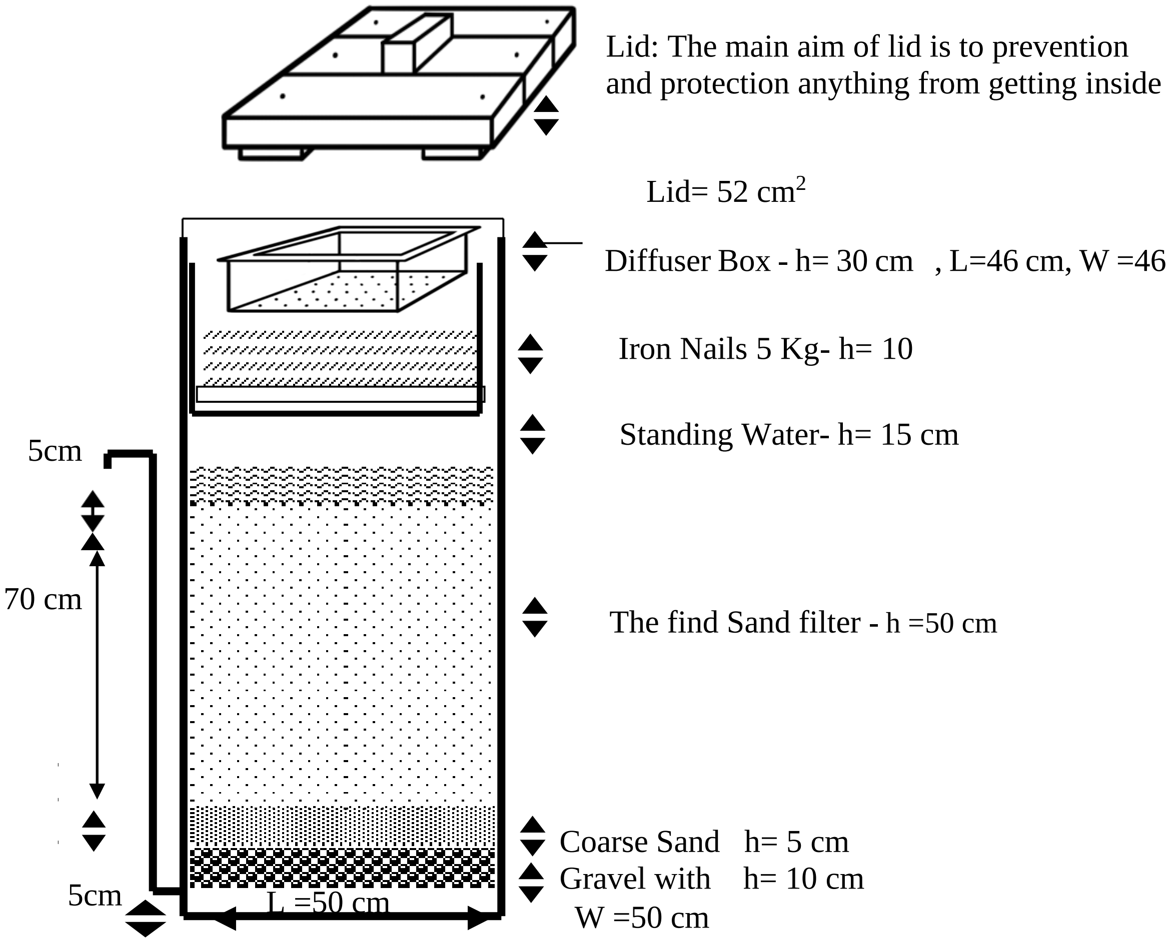

Fig.4: Construction Process of Sustainable Household Arsenic Remove Technology (Arsenic Bio Sand Filter or Absf)

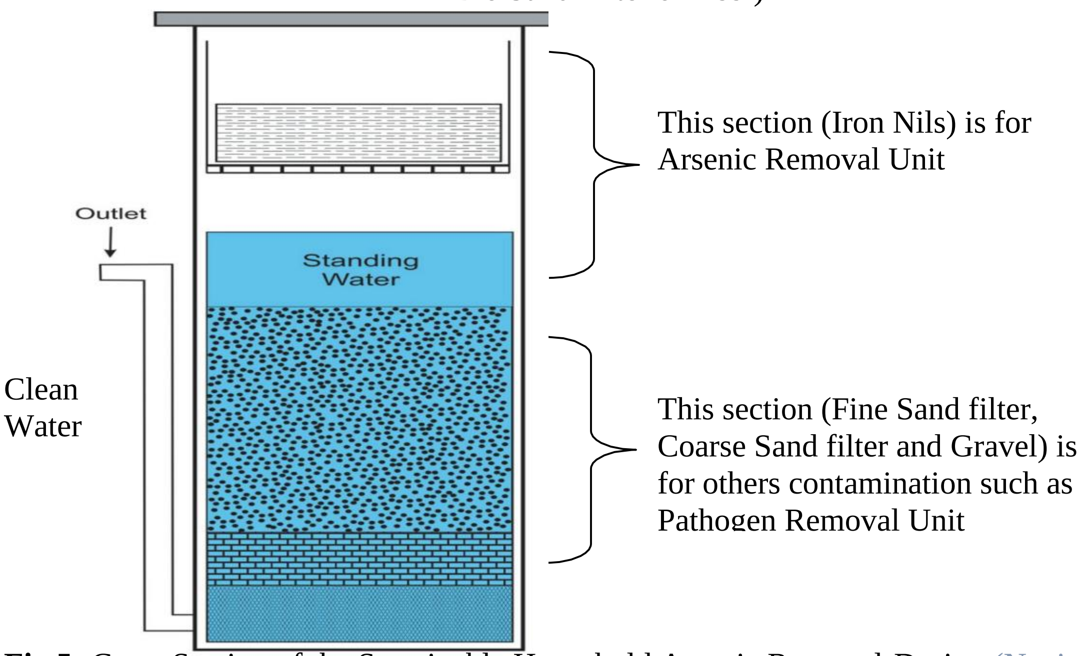

Fig.5: Cross Section of the Sustainable Household Arsenic Removal-Design (Ngai et al., 2006)

Length = 50 cm

Width = 50 cm

High = 120 cm

Filter loading rate = 400 liters/hour/m^2

Flow rate = 0.4 l/min = 24 litters/ hours

Reservoir volume = 12 litters Sand pore volume = 12 litters

Standing water depth = 15 cm

Fig.6: Design of the Sustainable Household Arsenic Bio sand Filter for Arsenic and Pathogen Removal in Afghanistan (Ngai *et al*., 2006)

The details and design of sustainable household arsenic removal technology has been shown in the above figures 4 and 5.Therefore, this Arsenic bio sand filter can be enough for an average family as which estimated (Table-5) According to the design specifications of sustainable arsenic bio sand filter in the above figures, the volume between the surface of still water level into the filter and bottom of diffuser box would be more than 10 litters. By the way, it was observed that the number of users pour more than10 litters of water within the filter at the same time in each use of water for filtering.

The unfiltered water in the other words, influent water mostly passes through the iron nails bed quickly because of arsenic removal, and accumulates in this 10 litter space. Therefore it is due to resistance of water flow within iron nails bed as many less as the resistance to water flow within the FSFL (fine sand filter layer) in the below. In this case, “distance or volume space between the sand layer and diffuser box is reduced”, then a more section of the incoming water about 5 to 10 litter will remain in the player box, instead to accumulate in the space below, it may increase the contact time between the unfiltered water, iron nails, and it may improve the arsenic removal efficiency by iron nails.

However, if the distance or space between the sand filters layer and box could be reduced, after the disturbance to the sand filter layer from the falling force of the incoming water would be reduced. Anyway, the basic activity of the diffuser box is to prevention the top of sand within moving around when we pour and the water into the filter, can prevents bilayers, on that case we can be sure that water drips onto sand evenly across the top of the sand and this way all of the sand could be used to filter the water contaminated with arsenic or others pollutions.

Moreover, the basic purpose of sand into this method also has an excellent role for removal of pathogen, bacteria, helminthes, and turbidity removal. The sand filter usually removes all the mentioned dirt and pollutants from the surface water and groundwater. Therefore, it is best to sand and be prepared correctly for the filter to work excellently. The separation gravel prevents sand from moving down and this relocates and blocks outlet tube and gravel of drainage is also large gravel prevents the small gravel from moving and blocking the outlet tube. The large gravel is too big to get inside the outlet of the mentioned tube. Finally, water that comes out of the outlet tube is safe to drink and the tube could be made from plastic and copper into the safe layer storage, for the safe storage we should have a clean and safe drinking water storage container to collect the filtered water as it flows out of the outlet tube layer.
According to the (Fig-6) here is the calculation of the volume within each part separately as follows:

Diffuser Box: h_6= 30 cm L = 46 cm and W = 46 cm
Iron Nails: h_5= 10 cm
Standing Water: h_4= 15 cm
The find Sand filter – h_1 =50 cm
Coarse Sand diameter: h_2= 5 cm
Gravel with diameter: h_3= 10 cm
According to the above data now we can calculate the volume of each part of the Arsenic Bio Sand Filter.
Volume1 (V_1) = A base x h_1 >> V_1= (0.5m x 0.5m x 0.1m = 0.025m^3 the volume of gravel
V_2 = 0,025m2 x 0.05m = 0.0125 m^3 volume of coarse Sand
V_3 = 0.025 x 0.5 = 0.0125 m^3 the volume of find Sand filter
V_4 = 0.025 x 0.15 = 0.004 m^3 volume of standing water between the sand filter and Iron nails.
V_5 = 0.30m x 0.46m x 0.46m = 0.063m^3 volume of diffuser box in top of Arsenic Bio Sand Filter.

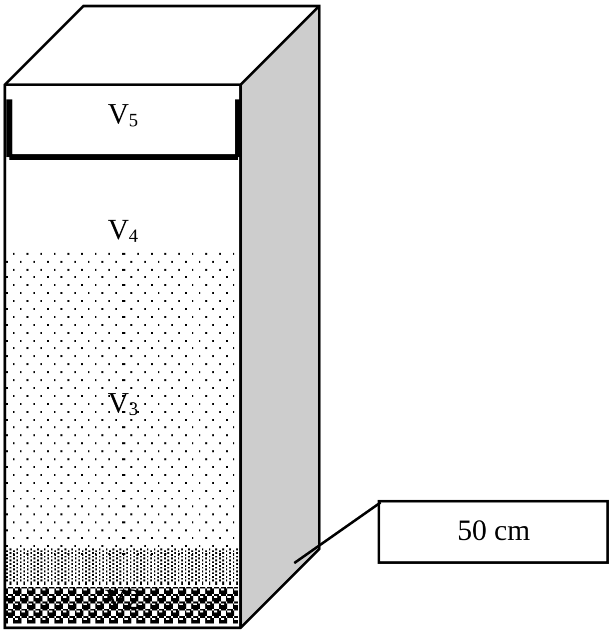

Fig.7: Volume of each Part and Flow Rate of this ABSF, it flows rate is 0.4 L/min = 24 litters/hours (Ngai *et al.*, 2006)

Conclusion

Review to improve the sustainability of water treatment technology for arsenic removal throughout high levels of arsenic contamination groundwater which addresses an alarming problem worldwide. Concentration of Arsenic in groundwater causes health problems with high level of toxicity in drinking water due to, anthropogenic activities, agriculture activities (pesticides, herbicides, seed treatment and fertilizers), industrial activities (timber treatment, electroplating, tannery and paints/chemical) and sewage (wastewater treatment plant, mining and smelting main sources of arsenic pollution in groundwater.

According to a study on water quality in Ghazni and Midanwardek provinces, Afghanistan, 459 out of 746 water point samples showed high levels of arsenic contamination roughly 61% which exceeded the WHO standard (0.01 mg/L). Furthermore, another suitable technology designed for arsenic removal in developing countries is oxidation methods for arsenic treatment from drinking water. This method was controlled oxidation with air and filtration to reduce the concentration of arsenic to low levels. The main difference between Arsenic Bio Sand Filter and Sand Filter are at the Arsenic removal on the surface by iron nails rust when exposed to air and water, as absorbed to ferrous hydroxide particles in the Arsenic Bio Sand Filter method. But in the Sand Filter, there are no iron nails for abrogation of arsenic.

Finally, the major significant finding of the study was the evaluation the existing household arsenic removal was used in developing countries based on ranking system, as a result, the most suitable method selected for household arsenic removal as well as a lot of household water treatment technologies for arsenic removal has been prepared and developed by many NGO and organizations, the sample analysis report from three available arsenic removal methods at study area and this study confirms the Arsenic Bio Sand Filter technology which is the most efficient and appropriate method for arsenic treatment with an excellent flow rate and also this method is recommended for Afghanistan. The design of sustainable household arsenic removal for this study is estimated for one family, it showed effective removal of arsenic with a median removal of 95 %, bacteria removal 88-99 %, helmets up to 100 %, turbidity 80 to 95% and Iron 90-95%.

References

Ahmed, M. F. (2001). *An overview of arsenic removal technologies in Bangladesh and India* (pp. 251–269). University of Engineering & Technology, Dhaka, Bangladesh.

Brammer, H., & Ravenscroft, P. (2009). Arsenic in groundwater: A threat to sustainable agriculture in South and South-East Asia. *Environment International, 35*(3), 647–654. https://doi:10.1016/j.envint.2008.10.004

Dangol, Bipin (2016). An Assessment of the Performance of the Kanchan Arsenic Filter (KAF) in Nawalpa. Department of Water Supply and Sewerage (DWSS). Kathmandu, Nepal

Ngai, T.; Dangol B.; Murcott, S.; Shrestha, R.R. (2006). Kanchan Arsenic Filter. Massachusetts Institute of Technology (MIT) and Environment and Public Health Organization (ENPHO). Kathmandu, Nepal

Nordstrom, D. K. (2002a). Worldwide occurrences of arsenic in groundwater. *Science, 296*(5576), 2143–2145.

Nordstrom, D. (2002b). Public health. Worldwide occurrences of arsenic in groundwater. *Science, 296*(5576), 2143-2145.

Peter, Ravenscroft, Hugh, Brammer & Keith Richards. (2009). *Arsenic Pollution a Global Synthesis: Handbook Center Tehran, For Educational Use*. Retrieved from www.ebookcenter.ir

Rahman, M. M., Naidu, R., & Bhattacharya, P. (2009). Arsenic contamination in groundwater in the Southeast Asia region. *Environmental Geochemistry and Health, 31*(1), 9–21.

Safi, M. H., & Kohistani, A.J. (2016, March). *Arsenic contamination of groundwater in Ghazni and Midan Wardak provinces, Afghanistan, Part 2* (Scientific Investigation Report). Afghanistan: DACAAR.

World Health Organization, Regional Office for South-East Asia (2001, July). *Arsenic contamination in groundwater affecting some Countries in the South-East Asia Region Society* [Report No. SEA-RC54-8]. New Delhi, India: Author. Retrieved from http://apps/10.3390/w3010001

ASSESSMENT OF SHORELINE CHANGES IN KARPEN- QERRET- GOLEM'S AREA

Dr. Sc. Bilbil Nurçe

Polytechnic University of Tirana, Faculty of Civil Engineering, Department of Geodesy

E-Mail: billnurce@gmail.com, bilbil.nurce@fin.edu.al, ORCID: 0000-0001-7179-618X

Prof. Assoc. Edmond Hoxha

Polytechnic University of Tirana, Faculty of Geology and Mining,

Department of Mineral Resource Engineering

E-Mail: ehoxha63@gmail.com, edmond.hoxha@fgm.edu.al, ORCID: 0000-0003-4049-0705

Abstract

Albania's coastline has a length of about 450 *km*, with wide access to the Adriatic and Ionian seas, where various forms of sandy and rocky beaches are combined, with the possibility of touristic use. The study of shoreline changes is concentrated in Karpen-Qerret-Golem's area, as the most frequented beach sector by locals and foreign tourists, as well as in the last three decades as very important area for the development of business in the field of construction.

The purpose of the study is to compare the shorelines shown in the topographic maps of 1:10 000 scale (editions of 1978), on Ortophotos (1994, 2007, 2015, 2018) and 2021's GNSS measurements in the study area, as well determining the direction and rate of the shoreline changes. Since 1978, due to the shoreline erosion it lost over 810 000 m^2, while the rise in sea level, caused by climate change, paints an even more shocking image for the future. The objectives of the study are providing evidence of the shoreline changes in Karpen-Qerret-Golem's area, as well as giving recommendations for stopping or reducing of shoreline erosion in this important sector.

Keywords: Shoreline changes, Erosion, accretion, average rate, lost/gained area, map, Ortophoto, GNSS.

1. INTRODUCTION

The territory of Albania lies in the south-western part of the Balkan Peninsula. The western part of Albania, which is wetted by the waters of the Adriatic and Ionian seas, is represented by beaches, lagoons and partly by marshes. The coastline of Albania influenced by geological, geodynamic, climatic factors, etc. has an irregular configuration, which over time has undergone one-by-one modifications. The coastline of Albania has a north-south extension of about 450 *km*, and it starts in the north with the Buna river (Fig. 1) and ends in the south with Stillo's Cape. This coastline is rich in sandy beaches, capes, sheltered bays, lagoons, small sandy beaches, sea caves, etc.

Based on the morpho-lithological characteristics (Boçi, 1991; Naço and Bedini, 2005 and Pano, 1992), the Albanian coast is divided into two types: a) accumulative coastline, which is wetted by the Adriatic Sea or which extends from the Buna River to "Cold water", Vlore) and b) abrasive coastline, wetted by the Ionian Sea or extending from "Cold water" in Vlora to Stillo's Cape in the south. The "Accumulative" coastal area of the Adriatic represents a length of the coastal area of about 251 *km* or 55.3% of the total coastline of the territory of Albania. In the coastal space of Albania, an important place is occupied by the sector of the Gulf of Durrës, to the south of which is the Karpen-Qerret-Golem beach (Fig. 2).

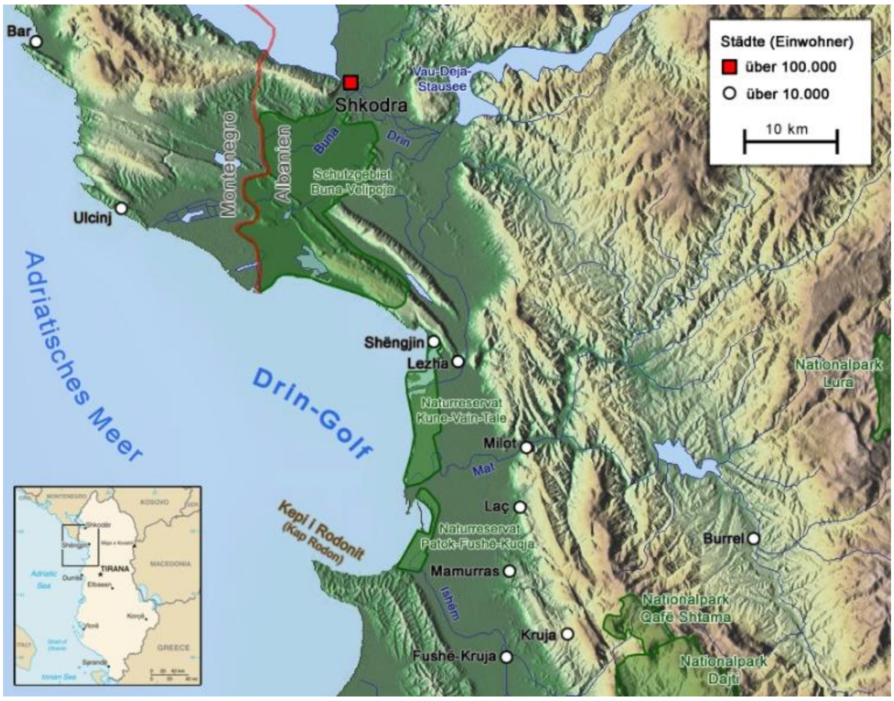

Figure 6. Map of the Gulf of Drin area in Albania (Ekrem Canli: https://commons.wikimedia.org/wiki/File:Dringolf.png)

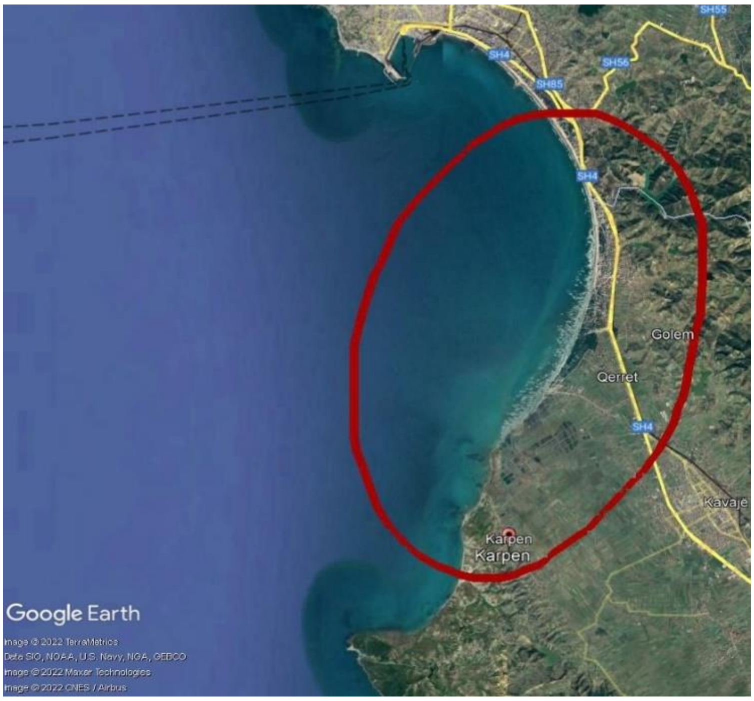

Figure 2. Fragment of the Karpen-Qerret-Golem sector shoreline/costline, Durres (Google Earth 2022)

In the Bay of Durres there are the streams of Lishat (Syneji), Rob's and Golem mountains, several canals which descend from the higher territories in the east (the salt channel-Hydrovor), as well as the Darchi river. Also the river of Shkumbin, which flows south of the bay of Durres, and the river Erzen, which flows north of it, near the Pali's cape, play a primary role in the supply of sediments. These two important water arteries play a primary role for the behavior of sediments in the Durres Bay area. According to studies, sea/ocean levels around the world continue to rise.

Since 1900-1930 the average sea level has increased with an average rate of about 0.6 mm/year, 1930-1992 with 1.2 *mm*/year, 1993-2015 with 3.2 *mm*/year and 2010-2015 with 4.4 *mm*/year (Fig. 3). In the dynamics of the shoreline changes in the Kavaje region in general and for the Karpen-Qerret sector, the following factors have their influence: changes in land use, deforestation and reforestation, desertification, geomorphology of the Durres-Karpen sector, characteristics geological-tectonic and neotectonic of the area, seismic conditions of the area, hydrogeological characteristics of the Karpen-Qerret area, climatic characteristics of the area, wind speed and its direction, precipitation, air temperature, and solar radiation.

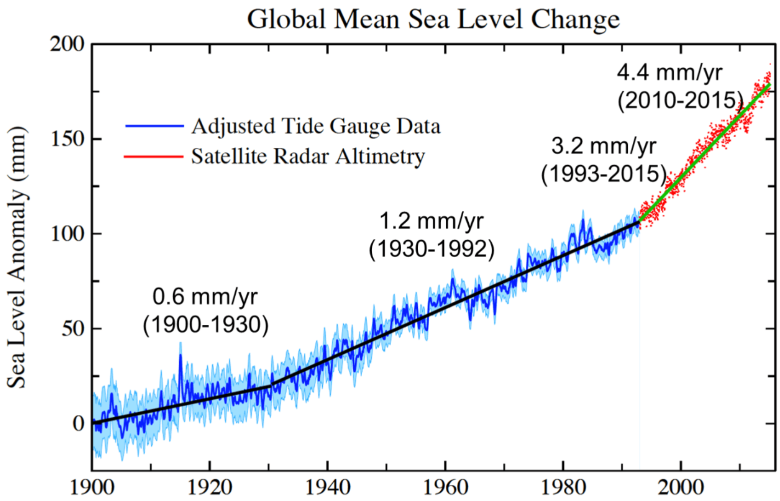

Figure 3. Global water level rise (https://climatefeedback.org/claimreview/global-sea-level-rise-accelerating-despite-heartland-institute-reports-claims-otherwise/)

2. MATERIALS AND METHODS

The first study for the evidence of shoreline changes of our Adriatic coast was carried out in 1963 at the Department of Geodesy (Boçi and Luli, 1989 and Boçi, 1994). The study was based on the position of the shoreline shown in the maps of the Austrian editions of 1916-1918, on the maps of the Italian editions of 1936-1938, on the topographical maps published in Albania in 1962, as well as on detailed surveys carried out in the field. Several factors have affected in the process of changing the position of the shoreline, such as: tides, wind, accumulative and abrasive activity of seas and rivers, as well as climate changes from global warming.

The objectives of the study are: providing evidence of the shoreline changes in the area of Karpen-Qerret-Golem, as well as giving recommendations for stopping or reducing of shoreline erosion in this important sector.

The study presents the assessment of the dynamics and rate of development of the phenomenon of shoreline erosion in time and space, based on the changes of shoreline shown in: a) the topographic maps of 1:10 000 scale (editions of 1978), b) in Ortophotos (1994, 2007, 2015, 2018) and c) GNSS measurements performed.

Figure 4. Fragment from the 1978's Topographical maps of the Karpen-Qerret-Golem area (https://geoportal.asig.gov.al/map/?fc_name=25k_krgjsh&auto=true)

The topographic maps in the scale 1: 10 000 (Fig. 4) were produced based on aerial photography respectively in the years 1968-1989 by the former Topographical Institute of Albania (today the Military Geographical Institute of Albania). These maps are based on the reference ALB-1986 (Ellipsoid of Krassowsky-1941, cartographic projection Gauss-Kryger (TM), central meridian 21^o, distortion scale factor at the central meridian $k_0 = 1$). The theoretical accuracy (M) in the position (N,E) of points on topographic maps in scale 1:10 000, is predicted to be: $M = \pm 0.2\ mm\ x$ Map Scale = $0.2\ mm \cdot 10\ 000 = 2\ m$.

Through the photogrammetric methods, the production of digital Ortophoto maps from the aerial photography is enabled. Since 1994, based on the aerial photographs of 1994, 2007, 2015 and 2018 the respective "Ortophotos" (Fig. 5, Fig. 6) at different levels of accuracy have been produced. The ortophotos of 2007/2015 are produced at three levels of accuracy: LOT-1 covering urban areas, LOT-2 covering all the western low-land and major road corridors and LOT-3 covering all the high-land areas, respectively with resolutions 8 *cm*, 20 *cm* and 40 *cm* based on the reference ITRF-2005/ETRF2000 (WGS84, UTM (Mercator's Universal Traversal), 21^o, $k_0 = 0.9996$). The accuracy of the orthophoto according to (Aerosistemi" SRL and Hansa Luftbild Sensorik und Photogrammetrie GmbH, October 2015; Geofoto SRL, 2007 and PASCO CORPORATION, Japan and Hansa Luftbild AG, Germany, 2018) is ±20 *cm*.

Figure 5. Fragment from 1994's Ortophoto (left) and 2007's Ortophoto (right) of the Karpen-Qerret area (https://geoportal.asig.gov.al/map/?auto=true)

Figure 6. Fragment from 2015's Ortophoto of the Karpen-Qerret area (https://geoportal.asig.gov.al/map/?auto=true)

GNSS observations were collected using Trimble R8 receiver with data collection every 1 *sec* based on the ALBCORS-2019. After processing the GNSS observations using TBC (Trimble Business Center) office software (Trimble Inc. PN 022543-256Q) the coordinates (N,E) on the Albanian modern reference (ETRS89, GRS80, UTM, $k_0 = 0.9996$, $\lambda_0 = 21^o$) are obtained, and a layout of positions was prepared by the software "Autodesk AutoCAD® Civil 3D 2019" (Fig. 7).

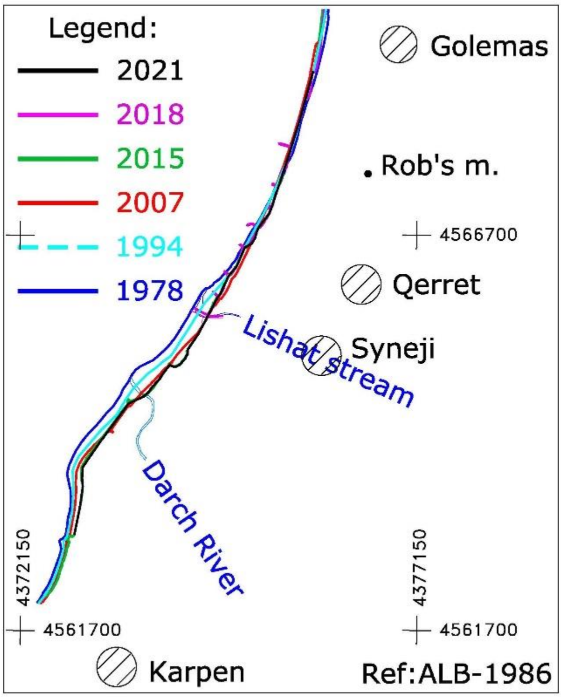

Figure 7 Coastline positions of Karpen-Qerret-Golem (1978-1994-2007-2015-2018-2021)

2.1 Transformation of the GNSS campaign coordinates

To compare the shorelines shown in the topographic maps and Orthophotos of the area chosen in the study, the GNSS positions measured referred to ALBCORS-2019 (ETRS89, GRS80, UTM, k_0=0.9996, λ_0=21º) are transformed into ALB-1986 (Krassowsky-1941, TM, 21º, k_0=1) by the Helmert linear equations (1) and (2) according (Nurçe, 2013):

$$N_{ALB1986\,(TM)} = N_0 + p \cdot N_{ETRF2000\,(UTM)} + q \cdot E_{ETRF2000\,(UTM)} + r \qquad (1)$$

$$E_{ALB1986\,(TM)} = E_0 + q \cdot N_{ETRF2000\,(UTM)} + p \cdot E_{ETRF2000\,(UTM)} + s \qquad (2)$$

with: N_0=4551000.000, E_0=416800.000, p=1.000408598, q=3.11103E07, r=1952.142887, s=97.55894084. While the digital Ortophoto content referred ETRF2000 (WGS84, UTM, 21º, k_0=0.9996) is transformed into ALB-1986 (Krassowsky-1941, TM, 21º, k_0=1) using ArcGIS software through 7- Helmert's Parameters. The accuracy of the transformation is ±20 *cm*, which does not affect our study.

3. RESULTS

From the comparison of the shorelines shown in the 1978's topographic maps, in (1994, 2007, 2015, 2018)'s Orthophotos of different years and 2021's GNSS measurements of Karpen-Qerret- Golem sector with a length of about 7.5 *km* (Fig. 8, left), the shoreline changes due to the erosion/accretion are measured by profiles every 1000 *m* (Fig. 8, right), as well as average rate of the shoreline changes, the lost/gained area and the average rate of lost/gained area due to the shoreline erosion/accretion are computed.

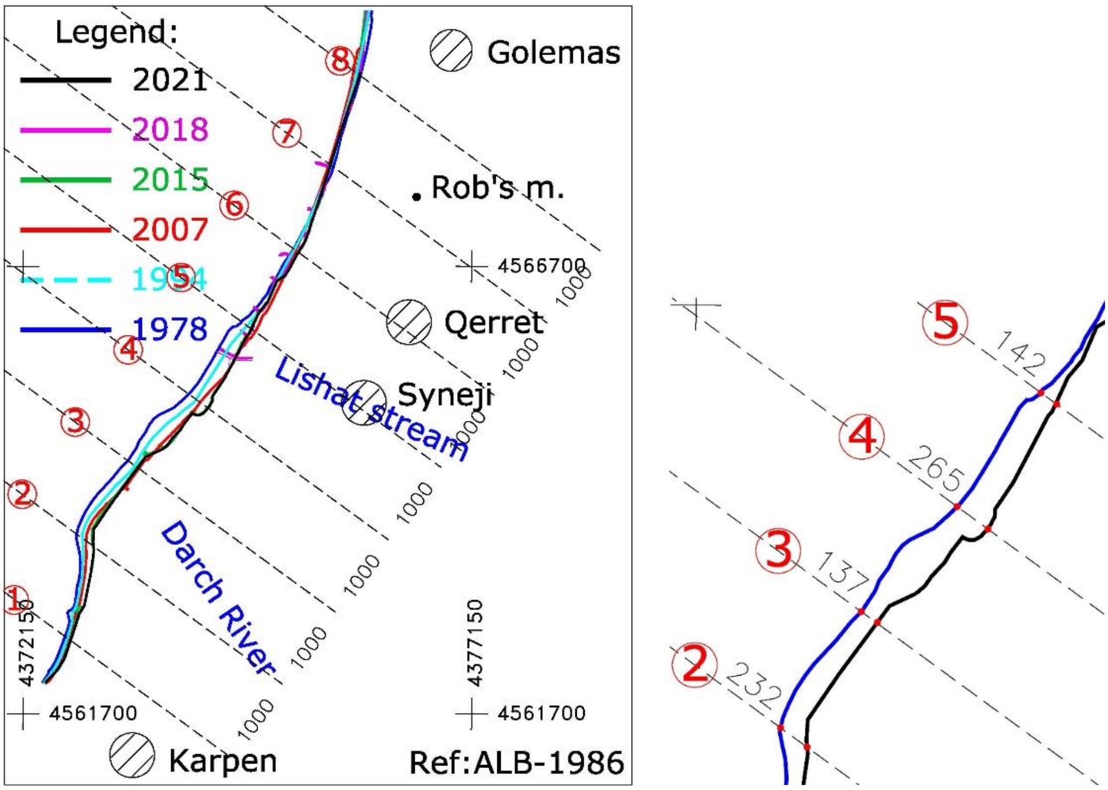

Figure 8. (1978-1994-2007-2015-2018-2021)'s Shoreline changes of Karpen-Qerret-Golem sector

Table 1 and Table 2 show the results of comparison of the shorelines shown in the topographic maps of 1978's 1:10 000 scale and 1994's digital Orthophotos (Fig. 9):

Table 1. Shoreline changes/Average rate/Lost area/Gained area for period 1978-1994

Profiles	1	2	3	4	5	6	7	8
Shoreline changes/profile (*m*)	29	79	93	100	69	12	-32	-45
Average rate (*m*/year/profile)	1.8	4.9	5.8	6.3	4.3	0.8	-2.0	-2.8
Lost area due to the shoreline Erosion (m^2)	-364 943							
Gained area due to the shoreline Accretion (m^2)	50 275							

Table 2. Average change/ Shoreline changes average rate/ Lost/gained area average rate (m^2/year) for period 1978-1994

	Erosion	Accretion
Average change (*m*)	63.7	-38.5
Shoreline changes average rate (*m/year*)	4.0	-2.4
Lost/gained area average rate ($m^2/year$)	-22 809	3 142

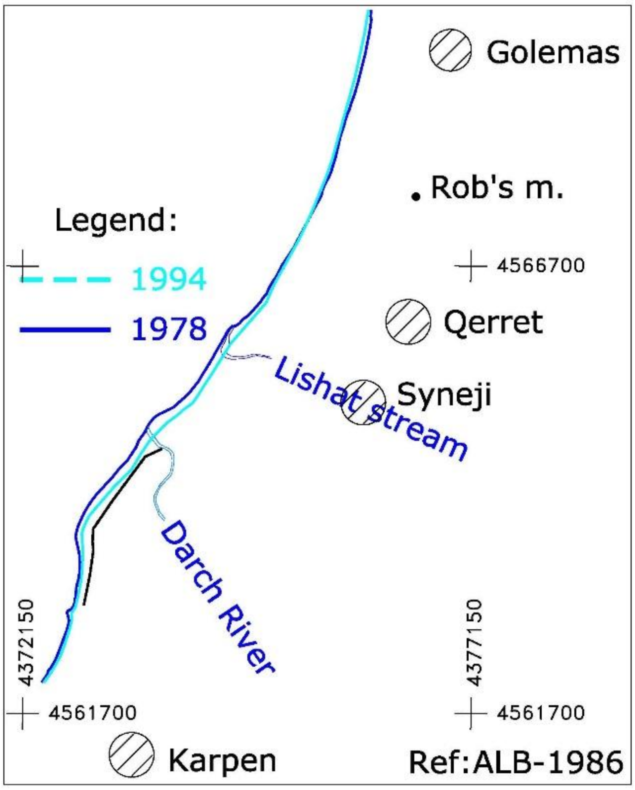

Figure 9. (1978-1994)’s Karpen-Qerret-Golem sector Shorelines

Table 3 and Table 4 show the results of comparison of the shorelines shown in the topographic maps of 1978’s 1:10 000 scale and 2007's digital Orthophotos (Fig. 10):

Table 3. Shoreline changes/Average rate/Lost area/Gained area for period 1978-2007

Profiles	1	2	3	4	5	6	7	8
Shoreline changes/profile (*m*)	63	138	151	157	185	33	-59	-89
Average rate (*m*/year/profile)	2.2	4.8	5.2	5.4	6.4	1.1	-2.0	-3.1
Lost area due to the shoreline Erosion (m^2)	-720 351							
Gained area due to the shoreline Accretion (m^2)	79 759							

Table 4. Average change/ Shoreline changes average rate/ Lost/gained area average rate (m^2/year) for period 1978-2007

	Erosion	Accretion
Average change (*m*)	121.2	-74
Shoreline changes average rate (*m/year*)	4.2	-2.6
Lost/gained area average rate (*m^2/year*)	-24 840	2 750

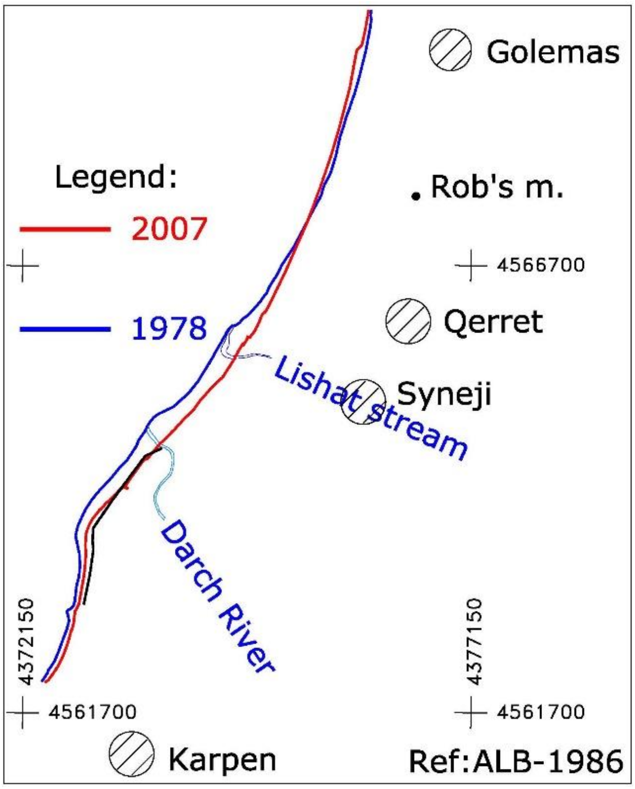

Figure 10. (1978-2007)'s Karpen-Qerret-Golem sector Shorelines

Table 5 and Table 6 show the results of comparison of the shorelines shown in the topographic maps of 1978's 1:10 000 scale and 2015's digital Orthophotos (Fig. 11):

Table 5. Shoreline changes/Average rate/Lost area/Gained area for period 1978-2015

Profiles	1	2	3	4	5	6	7	8
Shoreline changes/profile (*m*)	77	226	127	259	128	69	-52	-50
Average rate (*m*/year/profile)	2.1	6.1	3.4	7.0	3.5	1.9	-1.4	-1.4
Lost area due to the shoreline Erosion (m^2)	-807 135							
Gained area due to the shoreline Accretion (m^2)	41 885							

Table 6. Average change/ Shoreline changes average rate/ Lost/gained area average rate (m^2/year) for period 1978-2015

	Erosion	Accretion
Average change (*m*)	147.7	-51
Shoreline changes average rate (*m/year*)	4.0	-1.4
Lost/gained area average rate (*m^2/year*)	-21 814	1 132

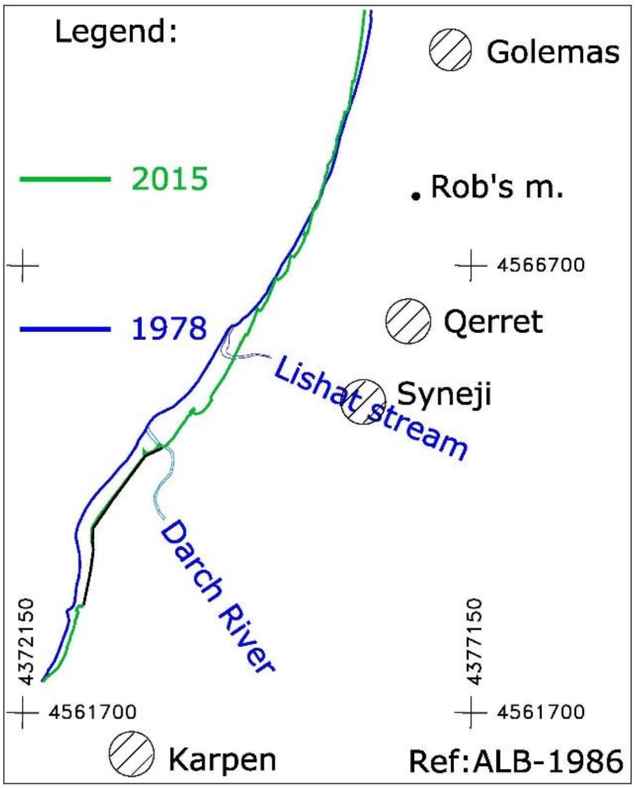

Fig. 11: (1978-2015)'s Karpen-Qerret-Golem sector Shorelines

Table 7 and Table 8 show the results of comparison of the shorelines shown in the topographic maps of 1978's 1:10 000 scale and 2018's digital Orthophotos (Fig. 12):

Table 7. Shoreline changes/Average rate/Lost area/Gained area for period 1978-2018

Profiles	1	2	3	4	5	6	7	8
Shoreline changes/profile (*m*)	No data				144	70	-46	-17
Average rate (*m*/year/profile)	No data				3.6	1.8	-1.2	-0.4
Lost area due to the shoreline Erosion (m^2)	-152 865							
Gained area due to the shoreline Accretion (m^2)	39 095							

Table 8. Average change/ Shoreline changes average rate/ Lost/gained area average rate (m^2/year) for period 1978-2018

	Erosion	Accretion
Average change (*m*)	107.0	-31.5
Shoreline changes average rate (*m/year*)	2.7	-0.8
Lost/gained area average rate (*m^2/year*)	-3 822	977

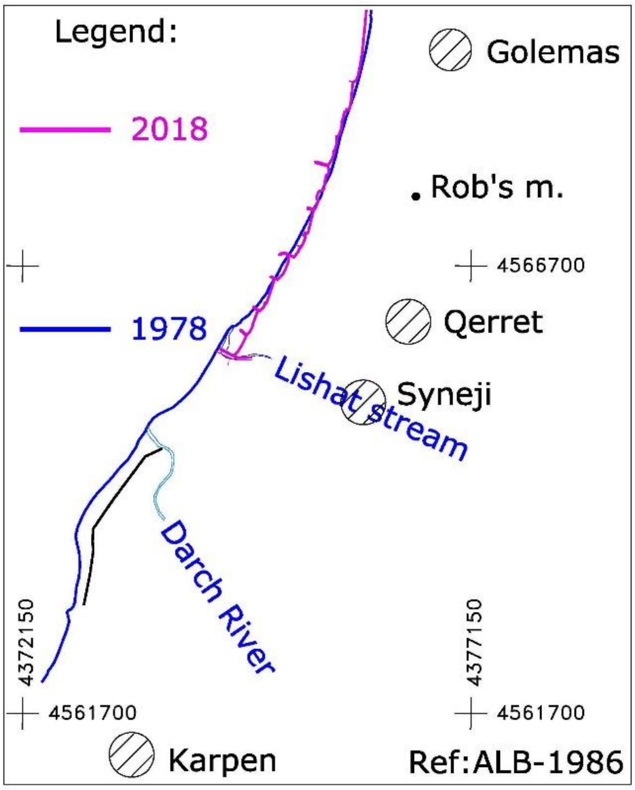

Figure 12. (1978-2018) Karpen-Qerret-Golem sector Shorelines

Table 9 and Table 10 show the results of comparison of the shorelines shown in the topographic maps of 1978's 1:10 000 scale and 2021's GNSS field measurements (Fig. 13):

Table 9. Shoreline changes/Average rate/Lost area/Gained area for period 1978-2021

Profiles	1	2	3	4	5	6	7	8
Shoreline changes/profile (*m*)	83	232	137	265	142	62	-44	-11
Average rate (*m*/year/profile)	1.9	5.4	3.2	6.2	3.3	1.4	-1.0	-0.3
Lost area due to the shoreline Erosion (m^2)	-846 585							
Gained area due to the shoreline Accretion (m^2)	30 152							

Table 10. Average change/ Shoreline changes average rate/ Lost/gained area average rate (m^2/year) for period 1978-2021

	Erosion	Accretion
Average change (*m*)	153.5	-27.5
Shoreline changes average rate (*m/year*)	3.6	-0.6
Lost/gained area average rate ($m^2/year$)	-19 688	701

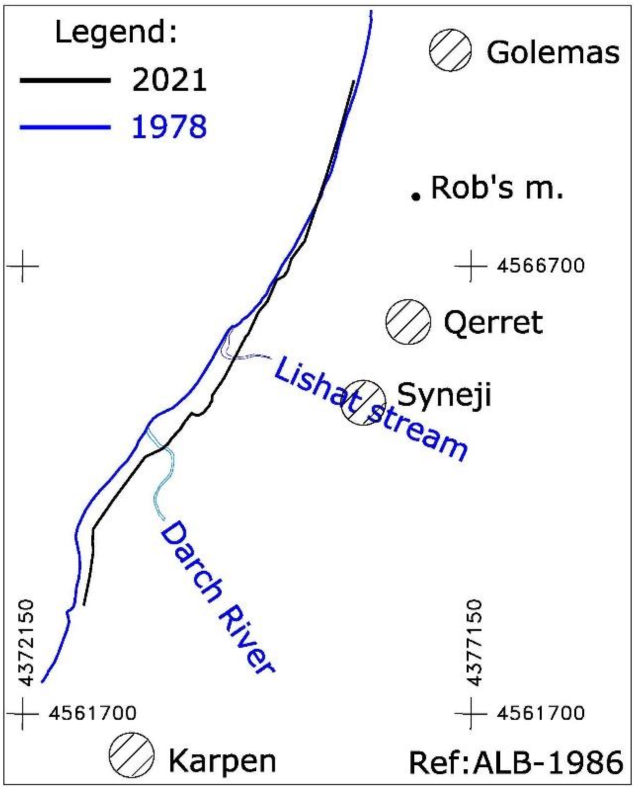

Figure 13. (1978-2021)'s Karpen-Qerret-Golem sector Shorelines

4. DISCUSSION

1. The study shows the shoreline changes due to the erosion/accretion, average rate of the shoreline erosion/accretion, the lost/gained area due to the shoreline erosion/accretion and average rate of lost/gained area due to the shoreline erosion/accretion.
2. From the comparison of the shorelines shown in the topographic maps, in orthophotos of different years and GNSS measurements of Karpen-Qerret- Golem sector with a length of about 7.5 km, the Erosion phenomenon was found in the segment Darch stream (Karpen)-Golem beach with a length of about 5.5 km, as well as Accretion in the segment Golem beach to the north with a length of about 2 km.
3. The results obtained from the comparison of the shoreline changes in the area of Karpen-Qerret-Golem for the period 1978-2021, show that this sector has been constantly under the influence of sea erosion, where after 1980 it has increased significantly.
4. From the analysis carried out, it resulted that the use of complex geodetic methods for the study of the shoreline changes, together with the information obtained from satellite images and GNSS measurements, would enable the study of the shoreline changes with the highest accuracy, in conformity with European standards and studies.

5. CONCLUSION

1. The existence of sea erosion on the shoreline of our country and its intensification in some sectors of the coast make it necessary to control/monitoring of the shoreline of Albania by responsible/specialized institutions.
2. To re-evaluate oceanographic indicators such as: waves, direction and length of waves, winds, tidal currents, etc. we emphasize that after 1990's, there are no permanent data and measurements for

these indicators. Unfortunately a number of meteorological stations located along the coast do not work.

3. Protective measures should be taken by responsible local and governmental bodies as well as by scientific institutions.
4. The study should also be carried out in other areas such as Shengjin - Patok Beach - Ishmi River, Drac - Rinia, Spille - Karavasta Lagoon.

ACKNOWLEDGEMENTS

The authors did not receive funds, grants, or other support from any organization for the submitted work. The data presented in this study are openly available in link (https://geoportal.asig.gov.al/map/?fc_name=25k_krgjsh&auto=true), (https://geoportal.asig.gov.al/map/?auto=true). This research is part of the continuous qualification of the Academic Staff. Bilbil Nurçe thanks his daughter Ina, for her insightful comments and suggestions. All the material is owned by the authors and/or no permissions are required.

REFERENCES

Aerosistemi SRL and Hansa Luftbild Sensorik und Photogrammetrie GmbH, (October 2015) TECHNICAL REPORT “Digital aerial photography of Republic of Albania territory, production of oriented images, LiDAR data, DTM, orthophotos and training”.

B. Nurçe, (2013) Dissertation Thesis, Study of the development of geodetic coordinate references of Albania.

Geofoto SRL, (2007) Aerial photography final technical report.

N, Pano, (1992) Dinamica del litorale Albanese -sintese delle conoscense, Aut del diciannovesimo convegno AlGI, p. 3-18.

P. Naço and E. Bedini, (2005) Geology, coastline, actual risks along the segment Divjaka-Kepi i Rodonit, Albania. Abstract. Conference on Marine Environment, 6-7 June 2005, Tirana, Albania.

PASCO CORPORATION, Japan and Hansa Luftbild AG, Germany, (2018) Digital aerial photography work for project on geospatial information for sustainable land development in Tirana-Durres area.

S. Boçi and N. Luli, (1989) The study of changes in the coastline from a topographic point of view.

S. Boçi (1991) Some problems, which arise from the topo-geomorphological study of the Adriatic coast in the implementation of its protection from erosion and the acquisition of new lands.

S. Boçi, (1994) Evolution and environmental problems of the Albanian coast, Bulletin Soc/era Geological ltaliana, 113, p. 7-14.

EVALUATION OF THE COORDINATE TRANSFORMATION MODELS BETWEEN THE ETRF2000, EPOCH2008.0 AND ALB1986 REFERENCES

Dr. Sc. Bilbil Nurçe

Polytechnic University of Tirana, Faculty of Civil Engineering, Department of Geodesy

E-Mail: billnurce@gmail.com, bilbil.nurce@fin.edu.al, ORCID: 0000-0001-7179-618X

MSc. Eduart Blloshmi (PhD in process)

Polytechnic University of Tirana, Faculty of Civil Engineering, Department of Geodesy

E-Mail: eduartblloshmi@yahoo.com, eduart.blloshmi@fin.edu.al

MSc. Bledar Sina (PhD in process)

Polytechnic University of Tirana, Faculty of Civil Engineering, Department of Geodesy

E-Mail: sina_bledar@yahoo.com, bledar.sina@fin.edu.al

Abstract

Several GNSS measurement campaigns have been carried out in Albania (October 1994, February 1998, September 1998) for the connection of the State Geodetic Network with the Global or European Reference System. Based on the results of the latest GNSS measurement campaign of Fall 2007-Spring 2008 the best relationship until now between the local and ETRF references was found.
Aim of this study is to present the different transformation models applied in the Albania, as well as the test results of the transformation models in different areas.
Since, the models of the transformed planimetric coordinates referred ETRF2000 into ALB1986, are not officially approved it recommended to be applied for the topographic mapping of the territory of Albania up to a scale of 1: 5000. These models can be improved if we will carry out additional measurements at the existing points of the horizontal control network referred to ALB1986.

Keywords: GNSS, coordinate transformation, ITRF/ETRF/ALB reference.

1. INTRODUCTION

The first GPS measurement campaign in Albania carried out on period of October 6-21, 1994 by the former ITU (Military Topographic Institute, today MGIA) in collaboration with the DMAAC (United States Defense Mapping Agency Aerospace Center, now NIMA). The aim was to transform the State Geodetic Network (ALB1986) into the WGS84 (World Geodetic System 1984). 24 points of triangulation (order I/II) and 11 points of state leveling (order I) observed. Relative positions have resulted in standard deviations of up to 10 cm for (N,E,h), while standard deviations for data displacement parameters from the Krasovsky- 1941 ellipsoid to WGS84 have resulted (Geodesy and Geophysics Department, Geodetic Surveys Division, (October 1994):

$$\sigma(N)= \pm 0.5\ m, \qquad \sigma(E)= \pm 0.3\ m, \qquad \sigma(h)= \pm 0.6\ m$$

whereas the transformation parameters and the corresponding accuracies are:

$$\Delta X= 24\text{ m} \pm 4\text{ m}, \qquad \Delta Y= -130\text{ m} \pm 4\ m, \qquad \Delta Z= -92\text{ m} \pm 4\ m$$

The second GPS measurement campaign carried out on February 1998 by the PMU (Project Management Unit) in collaboration with the Department of Civil Engineering Geodesy of the University of Wisconsin, Florida, USA. The aim was to connect the State Geodetic Network (ALB1986) with the International Reference System (ITRF). Standard deviations for the calculated (X,Y,Z) and ellipsoidal (φ,λ,h) coordinates in WGS84, ITRF96, Epoch1998.0 are in the range of 1-2 *cm*. Standard deviations for the recalculated point coordinates of the GPS campaign of October 1994, in WGS84, ITRF96, Epoch1998.0 are in the range under of 10 *cm*. Standard deviations for the 2-D transformation parameters (19 common points) between the coordinates in the local reference ALB1986 (Gauss-Kruger projection) and the reference WGS84, ITRF96, Epoch1998.0 (UTM-34N projection) have resulted (Greening and Barnes, April 1998):

- 4-Parametric linear Helmert: $\sigma_0 = \pm 0.155\ m$, $|v|\max = 0.342\ m$.
- Polynomial transformation: $\sigma_0 = \pm 0.113\ m$, $|v|\max = 0.288\ m$.

For the transformation of the GPS ellipsoidal height differences (Δh) referred to WGS84 into so called orthometric height differences (ΔH), it is recommended to perform according to the equation: $\Delta H=\Delta h-\Delta N$, ΔN is calculated referring to the geoidal model EGM96, but not knowing the difference between the vertical reference data of Albania and the geoid EGM96 the transformation model is always recommended to be used in relative sense in plain and hilly areas (Greening and Barnes, April 1998). No information given regarding the accuracy of the transformation of the ellipsoidal heights h referring to the WGS84 ellipsoid to the so-called orthometric height H.

In the framework of the CRODYN project, on September 1998, the third GPS measurement campaign carried out by the former ITU (Military Topographic Institute, today MGIA) in cooperation with the Federal Agency for Cartography and Geodesy of Germany. The purpose of this GPS measurement campaign was to connect the State Geodetic Network (ALB1986) with the European Reference System ETRS89 (ETRF1989). After processing, the standard deviations for the point coordinates in ITRF96, Epoka1998.7 resulted in ± 2 *mm* in plan and ± 6.5 *mm* in height. For the transformation of coordinates from the global reference ITRF96 to the European reference ETRS89, the 7-Parameters are (EUREF Publication No. 8, 1999):

$T_X = 4.1\ cm$, $T_Y = 4.1\ cm$, $T_Z = -4.9\ cm$, $D=10^{-8}\ ppm$,

$R_X = 0.20''$ (0.0012"/year), $R_Y = 0.50''$ (0.0012"/year), $R_Z = -0.65''$ (0.0012"/year)

where, (T_X,T_Y,T_Z) are the transformation parameters from ITRF96 to ETRS89, (R_X,R_Y,R_Z) are the rotation parameters from ITRF96 to ETRS89.

In the period autumn 2007 - spring 2008, the fourth GNSS measurement campaign is carried out by IGUS (Military Geographical Institute of Albania) in cooperation with the Military Geographical Institute of Florence (IGUF), Italy. The aim was to find the transformation parameters from the European reference system (ETRF2000, Epoch 2008) to local (ALB1986). GNSS surveys were carried out at approximately 150 points in the state triangulation and leveling networks (Fig. 1). Once the coordinates of the points are calculated in ITRF2005, then transformed into ETRF2000, Epoch2008.0 (Maseroli, January 2010).

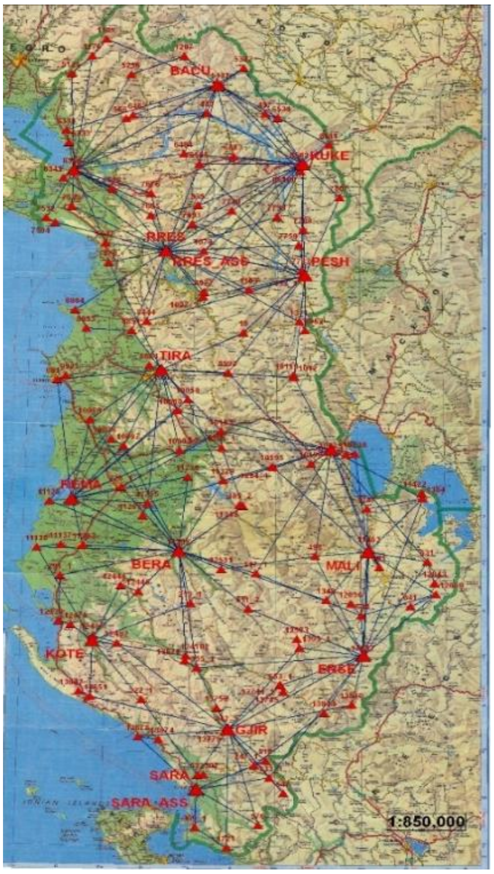

Figure 1. Scheme of the points measured autumn 2007 - spring 2008 (Maseroli, January 2010)

Based on the evaluation of the differences ($\Delta\varphi = \varphi_{ALB1986} - \varphi_{ETRF2000}$, $\Delta\lambda = \lambda_{ALB1986} - \lambda_{ETRF2000}$), with the help of a "*pseudo-interpolation*" algorithm, an approximate correlation surface was calculated through a *horizontal least squares regression* model:

$$aX_i + bY_i + c \approx Z_i$$

Interpolating the residuals $v_i = Z_i - (aX_i + bY_i + c)$ with the *minimum curvature algorithm* via the function: $g(X_i,Y_i) \approx v_i$ produced the residuals w_i:

$$w_i = v_i - g(X_i,Y_i) = Z_i - f(X_i,Y_i)$$

and

$$f(X_i,Y_i) = aX_i + bY_i + c + g(X_i,Y_i)$$

Function g called "*Spline in tension*" has come out as an approximate solution of the *biharmonic differential* equation:

$$(1 - \lambda) \nabla 2 (\nabla 2g) - \lambda \nabla 2g = 0$$

(λ is the distortion parameter of an elastic surface in tension).

The coordinates for the measured points - not vertices of the respective grids ($\Delta\varphi$,$\Delta\lambda$) are calculated according to the relations:

$$\varphi_{ALB1986} = \varphi_{ETRF2000} + \Delta\varphi_{ETRF2000 - ALB1986}, \qquad \lambda_{ALB1986} = \lambda_{ETRF2000} + \Delta\lambda_{ETRF2000 - ALB1986}$$

or

$$\varphi_{ETRF2000} = \varphi_{ALB1986} + \Delta\varphi_{ALB1986 - ETRF2000}, \qquad \lambda_{ETRF2000} = \lambda_{ALB1986} + \Delta\lambda_{ALB1986 - ETRF2000}$$

The transformation of the positions (N,E) referred ETRS89, ETRF2000, Epoch2008.0 into the reference ALB1986 is realized through the program ALBACO or 7-P Helmert, calculated based on 90 common points (Table 1):

Table 1. 7-P Helmert for the transformation of $(N,E)_{ETRS89,\ ETRF2000,\ 2008.0}$ to $(N,E)_{ALB1986}$

T_X (*m*)	T_Y (*m*)	T_Z (*m*)	S (*ppm*)	R_X (")	R_Y (")	R_Z (")
44.183	0.58	38.489	8.2703	2.3867	2.7072	- 3.5196

but the accuracy of the transformation from ETRS89, ETRF2000, Epoch2008.0 to ALB1986 through 7-P Helmert has resulted: σ_0= 18 *cm* (with confidence level of 68%) and σ_0 = 40 *cm* (with confidence level of 85%).

2. MATERIALS AND METHODS

2.1 The linear interpolation polynomial proposed

Department of Geodesy of the Faculty of Civil Engineering for the transformation of coordinates from ETRF2000 to ALB1986, has proposed linear equations of Helmert transformation of the form (Nurçe, 2013):

$$N_{ALB86} = N_0 + p\cdot N_{ETRF2000} - q\cdot E_{ETRF2000} + r \qquad (1)$$

$$E_{ALB86} = E_0 + q\cdot N_{ETRF2000} + p\cdot E_{ETRF2000} + s \qquad (2)$$

or in vector form:

$$\begin{bmatrix} N_{ALB86} \\ E_{ALB86} \end{bmatrix} = \begin{bmatrix} N_0 \\ E_0 \end{bmatrix} + \begin{bmatrix} p & -q \\ q & p \end{bmatrix} \cdot \begin{bmatrix} N_{ETRF2000} \\ E_{ETRF2000} \end{bmatrix} + \begin{bmatrix} r \\ s \end{bmatrix} \qquad (3)$$

with: N_0 = 4551000, E_0 = 416800, coefficients p = 1.000408598, q = 3.11103E-07, r = 1952.142887, s=97.55894084.

For the transition from ETRF2000 to ALB86, we also used transforming polynomials of the form (Nurëe, 2013):

$$N_{ALB1986} = N_{ETRF2000} + (a_2 + n\cdot a_3 + e\cdot a_4 + q\cdot a_5 - p\cdot a_6) \qquad (4)$$

$$E_{ALB1986} = E_{ETRF2000} + (a_1 + e\cdot a_3 - n\cdot a_4 + p\cdot a_5 - q\cdot a_6) \qquad (5)$$

or in vector form:

$$\begin{bmatrix} N_{ALB1986} \\ E_{ALB1986} \end{bmatrix} = \begin{bmatrix} N_{ETRF2000} \\ E_{ETRF2000} \end{bmatrix} + \begin{bmatrix} 0 & 1 & n & e & q & -p \\ 1 & 0 & e & -n & p & -q \end{bmatrix} \begin{bmatrix} a_1 \\ a_2 \\ \vdots \\ a_6 \end{bmatrix} \qquad (6)$$

with: $n = 10^{-5}\cdot N_{ETRF2000}$, $e = 10^{-5}\cdot E_{ETRF2000}$, $p = e^2 - n^2$, $q = 2\cdot e\cdot n$, a_1 = -33.94098357, a_2 = 86.36090734, a_3 = 40.95349125, a_4 = 1.718666252, a_5 = -0.019183782, a_6 = 0.001022946.

3. RESULTS

3.1 GNSS Field Survey

For the real control of the transformation model treated above, static GNSS measurements performed, in four different areas (Fig. 2), at the points referred ALB1986, which not used to derive the transformation models in plan and height during the autumn 2007-spring 2008 GNSS campaign.

Figure 2. Test areas of transformation models of (N,E) (illustrated by Google.com)

Tables 2, 3, 4, 5, 6 give the 3-D coordinates (φ,λ,h) and (N,E,h) in the reference ETRF2000, Epoch2021.5, respectively for the areas: (a) Berat, (b) Tepelena, (c) Shkodra, (d) Tirana and (e) Kukes-Peshkopi.

TABLE 2. COORDINATES OF POINTS (Φ, Λ, H) MEASURED IN THE BERAT AREA (ETRF2000, EPOCH2021.5)

Point No.	Catalogue No.	φ_{GRS80} *(dd.mmssssss)*	λ_{GRS80} *(dd.mmssssss)*	N(UTM) (m)	E(UTM) (m)	h_{GRS80} *(m)*
1	124102	40.20143351	19.58410227	4465698.118	413197.659	396.109
2	12495	40.22195190	19.59384661	4469542.423	414596.896	351.93
3	12494	40.22220782	19.56300923	4469673.174	410155.525	498.424
4	12488	40.24025350	19.57356906	4472752.258	411738.915	709.341
5	12574	40.25122421	19.59560811	4474863.366	415072.611	632.069
6	12477	40.26345737	19.55393890	4477472.939	409054.295	842.152
7	12471	40.28008705	19.57466647	4480097.995	412083.878	736.033
8	12470	40.28016748	19.55003796	4480169.824	408168.270	896.533
9	12563	40.29100403	20.01017197	4482178.214	416701.043	884.696
10	12461	40.30118997	19.55355413	4484175.072	409045.153	950.894
11	12453	40.31524148	19.5522422	4487278.143	408774.225	1029.756
12	12450	40.32371241	19.5942460	4488584.478	414907.823	910.296
13	12448	40.34081603	19.57019816	4491435.518	411166.401	750.701

14	12522	40.34333564	20.01065042	4492146.143	416924.677	935.317
15	12431	40.36394722	19.54435582	4496140.653	407969.200	988.542
16	12423	40.38469466	19.58102194	4500012.850	412871.565	656.799
17	11298	40.42276650	19.56427155	4506843.073	410898.076	276.159

TABLE 3. COORDINATES OF POINTS (Φ, Λ, H) MEASURED IN THE TEPELENA AREA (ETRF2000, EPOCH2021.5)

Point No.	Catalogue No.	φ_{GRS80} *(dd.mmssssss)*	λ_{GRS80} *(dd.mmssssss)*	N(UTM) (m)	E(UTM) (m)	h_{GRS80} *(m)*
1	12444	40.34597428	19.42581380	4493288.856	391347.586	638.864
2	13745	40.12439585	20.21571331	4451503.764	446038.629	613.000
3	518	39.58092635	20.17556353	4424578.555	440117.606	644.893
4	576	39.44244274	20.16120659	4399168.328	437453.094	492.205
5	535	41.55478862	20.00103364	4642481.469	417329.229	318.906
6	566	42.14025747	19.42169868	4676575.013	393120.968	393.313
7	631	40.40259895	20.56068384	4502558.360	494526.228	887.526
8	1103	41.37583967	20.12510392	4609315.714	434547.091	851.367

TABLE 4. COORDINATES OF POINTS (Φ, Λ, H) MEASURED IN THE SHKODRA AREA (ETRF2000, EPOCH2021.5)

Point No.	Catalogue No.	φ_{GRS80} *(dd.mmssssss)*	λ_{GRS80} *(dd.mmssssss)*	N(UTM) (m)	E(UTM) (m)	h_{GRS80} *(m)*
1	6343	42.00130142	19.22569567	4651443.067	366047.193	72.0951
2	6344	42.00400046	19.25089825	4652218.780	369099.761	75.2734
3	6407	42.04096554	19.36315503	4658412.345	384905.152	254.583
4	6440	42.03019511	19.33504968	4656385.359	381168.975	180.236
5	6447	42.00391688	19.32222729	4652015.927	379065.759	90.7896
6	6592	42.0437555	20.24554509	4658501.777	451643.469	413.698

TABLE 5. COORDINATES OF POINTS (Φ, Λ, H) MEASURED IN THE TIRANA AREA (ETRF2000, EPOCH2021.5)

Point No.	Catalogue No.	φ_{GRS80} *(dd.mmssssss)*	λ_{GRS80} *(dd.mmssssss)*	N(UTM) (m)	E(UTM) (m)	h_{GRS80} *(m)*
1	1000	41.20042123	19.49366521	4576554.990	401835.713	177.1826
2	8884	41.21476314	19.48571265	4579756.784	400960.544	215.243

3	8879	41.22161222	19.50509873	4580599.753	403617.604	342.7391
4	10027	41.19120288	19.51258525	4574911.843	404352.729	268.6779
5	10037	41.17120855	19.5350246	4571169.550	407662.706	351.9794
6	8886	41.20390470	19.42346694	4577768.539	392043.246	267.9903
7	8814	41.21385236	19.46261848	4579524.660	397449.672	136.1983
8	8884	41.21476249	19.48571236	4579756.584	400960.474	215.546
9	8922	41.37274472	20.01555257	4608515.453	419369.782	324.88
10	8962	41.29270702	20.26248679	4593399.933	453274.305	871.428

TABLE 6. COORDINATES OF POINTS (Φ, Λ, H) MEASURED IN THE KUKËS-PESHKOPI AREA

(ETRF2000, EPOCH2021.777)

Point No.	Catalogue No.	φ_{GRS80} *(dd.mmssssss)*	λ_{GRS80} *(dd.mmssssss)*	N(UTM) (m)	E(UTM) (m)	h_{GRS80} *(m)*
1	65106	42.02292099	20.22005952	4654571.978	447596.463	869.624
2	7719	41.58167456	20.23482109	4646767.706	450015.691	819.813
3	7733	41.53288717	20.1926822	4637934.238	443929.738	669.522
4	7734	41.55294012	20.21382178	4641628.290	446985.351	583.533
5	7737	41.53384292	20.21579048	4638202.429	447413.491	1144.176
6	7756	41.49196705	20.20044801	4630241.891	444737.974	912.250
7	7760	41.47490996	20.22137399	4627426.163	447699.410	887.960
8	7770	41.44374641	20.23238213	4621504.406	449274.831	817.818
9	7771	41.43580008	20.20032361	4620321.695	444632.474	556.490
10	7781	41.42500931	20.22502804	4618198.606	448476.306	592.972
11	7782	41.42217782	20.20363187	4617348.310	445374.084	502.141
12	7784	41.40509803	20.20573127	4614544.426	445838.114	557.267
13	7785	41.41244900	20.22236531	4615563.063	447841.794	544.573
14	8835	41.34094302	19.46120220	4602686.786	397449.838	799.953
15	8836	41.33492833	19.43366496	4602117.622	393842.246	308.562
16	8899	41.34045815	19.59156193	4602301.592	415596.132	477.140
17	88105	41.37320238	19.59151338	4608699.195	415659.948	340.523
18	8903	41.35133251	20.28153169	4604061.964	455900.730	614.967
19	8921	41.37288672	20.10152014	4608438.782	430932.727	1068.836

20	8922	41.37274471	20.01555250	4608515.439	419369.764	325.000
21	8927	41.37124013	20.26198684	4607751.081	453251.612	752.754
22	8929	41.35421878	20.02560716	4605253.683	420735.033	378.156
23	8937	41.35093003	20.26426158	4603951.317	453753.608	608.840

3.2 Comparison between coordinates of different kinds

In the Tables 7, 8, 9, 10, 11 given the transformed 2-D coordinates (N,E) referred ETRF2000, Epoch2021.5 into ALB1986 provided through 3 transformation models: (1) ALBACO developed by IGUF, (2) 4-P Helmert and (3) Polynomial, as well as the corresponding quadratic mean deviations for the areas: (a) Berat, (b) Tepelena, (c) Shkodra, (d) Tirana and (e) Kukes-Peshkopi.

TABLE 7. TRANSFORMED 2-D COORDINATES (N,E) REFERRED ETRF2000, EPOCH2021.5 INTO ALB1986 FOR THE BERAT

Point No.	N(ALB1986)	E(ALB1986)	ALBACO		4-P Helmert		Polynomial	
			$N(ALB1986)_1$	$E(ALB1986)_1$	$N(ALB1986)_2$	$E(ALB1986)_2$	$N(ALB1986)_3$	$E(ALB1986)_3$
1	4467615.67	413293.39	4467615.299	413293.733	4467615.403	413293.718	4467615.384	413293.7311
2	4471461.40	414693.18	4471461.193	414693.514	4471461.277	414693.529	4471461.261	414693.5371
3	4471592.21	410250.10	4471592.013	410250.338	4471592.083	410250.343	4471592.065	410250.3583
4	4474672.49	411834.13	4474672.364	411834.346	4474672.425	411834.381	4474672.408	411834.3924
5	4476783.96	415168.60	4476784.345	415169.378	4476784.394	415169.439	4476784.379	415169.4451
6	4479395.23	409148.67	4479395.000	409148.601	4479395.036	409148.665	4479395.02	409148.6792
7	4482021.35	412179.30	4482021.136	412179.388	4482021.163	412179.487	4482021.149	412179.4951
8	4482093.04	408262.22	4482092.995	408262.194	4482093.023	408262.279	4482093.007	408262.2933
9	4484101.96	416797.79	4484102.229	416798.407	4484102.23	416798.539	4484102.218	416798.5392
10	4486099.87	409139.39	4486099.889	409139.399	4486099.907	409139.522	4486099.893	409139.5329
11	4489204.29	408868.11	4489204.23	408868.34	4489204.247	408868.484	4489204.233	408868.4944
12	4490511.10	415004.18	4490511.122	415004.41	4490511.113	415004.588	4490511.101	415004.5889
13	4493363.35	411261.29	4493363.306	411261.459	4493363.32	411261.639	4493363.307	411261.6439
14	4494074.19	417021.90	4494074.264	417022.056	4494074.232	417022.268	4494074.222	417022.2637
15	4498070.39	408062.87	4498070.347	408062.953	4498070.377	408063.133	4498070.367	408063.1414
16	4501944.13	412967.19	4501944.123	412967.283	4501944.155	412967.502	4501944.146	412967.5018
17	4508777.07	410993.07	4508777.091	410993.011	4508777.169	410993.209	4508777.162	410993.2095
			$\sigma_0(N)$=0.183 m	$\sigma_0(E)$= 0.298 m	$\sigma_0(N)$= 0.164 m	$\sigma_0(E)$= 0.377 m	$\sigma_0(N)$= 0.167 m	$\sigma_0(E)$= 0.382 m

The errors of the transformed 2-D coordinates (N,E) referred ETRF2000, Epoch2021.5 into ALB1986 provided through 3- transformation models: (1) ALBACO developed by IGUF, (2) 4-P Helmert and (3) Polynomial for the Berat area are respectively:

	ALBACO		4-P Helmert		Polynomial	
	dN	dE	dN	dE	dN	dE
0÷10.0 *cm*	59.0%	41.5	53.0	12.0	59.0	12.0
÷ 20.0 *cm*	82.5%	59.0	82.5	29.5	82.5	29.5
÷ 30.0 *cm*	88.5%	82.5	11.5	59.5	94.1	76.5
> 30.0 *cm*	11.5%	17.5	5.9	41.5	5.9	23.5

TABLE 8. TRANSFORMED 2-D COORDINATES (N,E) REFERRED ETRF2000, EPOCH2021.5 INTO ALB1986 FOR TEPELENA

Point No.	N(ALB1986)	E(ALB1986)	ALBACO		4-P Helmert		Polynomial	
			$N(ALB1986)_1$	$E(ALB1986)_1$	$N(ALB1986)_2$	$E(ALB1986)_2$	$N(ALB1986)_3$	$E(ALB1986)_3$
1	4495217.390	391434.690	4495217.393	391434.684	4495217.426	391434.727	4495217.406	391434.7611
2	4453415.221	446148.201	4453415.216	446148.197	4453415.244	446148.104	4453415.227	446148.0689
3	4426479.240	440223.050	4426479.053	440224.876	4426479.035	440224.653	4426479.012	440224.6433
4	4401057.500	437559.480	4401058.524	437559.503	4401058.426	437559.045	4401058.398	437559.056
			σ_0=0.520 m	σ_0= 0.913 m	σ_0= 0.475 m	σ_0= 0.832 m	σ_0= 0.463 m	σ_0= 0.828 m

The errors of the transformed 2-D coordinates (N,E) referred ETRF2000, Epoch2021.5 into ALB1986 provided through 3- transformation models: (1) ALBACO developed by IGUF, (2) 4-P Helmert and (3) Polynomial for the Tepelena are respectively:

	ALBACO		4-P Helmert		Polynomial	
	dN	dE	dN	dE	dN	dE
0÷10.0 *cm*	50%	75	50	50	50	50
÷ 20.0 *cm*	75%	75	75	50	75	75
÷ 30.0 *cm*	75%	75	75	50	75	75
> 30.0 *cm*	25%	25	25	50	25	25

TABLE 9. TRANSFORMED 2-D COORDINATES (N,E) REFERRED ETRF2000, EPOCH2021.5 INTO ALB1986 FOR THE SHKODRA

Point No.	N(ALB1986)	E(ALB1986)	ALBACO		4-P Helmert		Polynomial	
			$N(ALB1986)_1$	$E(ALB1986)_1$	$N(ALB1986)_2$	$E(ALB1986)_2$	$N(ALB1986)_3$	$E(ALB1986)_3$
1	4653436.22	366124.59	4653436.307	366124.252	4653436.267	366124.046	4653436.316	366124.1107
2	4654212.26	369178.36	4654212.371	369178.051	4654212.296	369177.861	4654212.344	369177.922
3	4658380.12	381252.12	4658380.455	381252.149	4658380.573	381252.008	4658380.618	381252.0524
4	4654008.41	379148	4654009.316	379148.103	4654009.357	379147.931	4654009.4	379147.9776
5	4660497.63	451755.24	4660497.639	451755.244	4660497.834	451755.298	4660497.848	451755.2297
			σ_0=0.437 m	σ_0= 0.210 m	σ_0= 0.479 m	σ_0= 0.336 m	σ_0= 0.508 m	σ_0= 0.292 m

The errors of the transformed 2-D coordinates (N,E) referred ETRF2000, Epoch2021.5 into ALB1986 provided through 3- transformation models: (1) ALBACO developed by IGUF, (2) 4-P Helmert and (3) Polynomial for the Shkodra area are respectively:

	ALBACO	4-P Helmert	Polynomial

	dN	dE	dN	dE	dN	dE
0÷10.0 *cm*	60%	60	40	60	40	60
÷ 20.0 *cm*	60%	80	60	60	60	60
÷ 30.0 *cm*	80%	100	60	60	60	60
> 30.0 *cm*	20%	00	40	40	40	40

TABLE 10. TRANSFORMED 2-D COORDINATES (N,E) REFERRED ETRF2000, EPOCH2021.5 INTO ALB1986 FOR THE TIRANA

Point No.	N(ALB1986)	E(ALB1986)	ALBACO		4-P Helmert		Polynomial	
			$N(ALB1986)_1$	$E(ALB1986)_1$	$N(ALB1986)_2$	$E(ALB1986)_2$	$N(ALB1986)_3$	$E(ALB1986)_3$
1	4578517.411	401926.891	4578517.663	401926.991	4578517.579	401927.166	4578517.588	401927.1683
2	4581720.58	401051.4	4581720.78	401051.471	4581720.682	401051.64	4581720.691	401051.644
3	4582563.88	403709.59	4582564.096	403709.623	4582563.994	403709.786	4582564.004	403709.7858
4	4576873.5	404444.95	4576873.849	404445.06	4576873.76	404445.209	4576873.768	404445.2084
5	4573129.81	407756.25	4573130.041	407756.438	4573129.937	407756.538	4573129.943	407756.5317
6	4579731.49	392130.47	4579731.732	392130.533	4579731.627	392130.698	4579731.637	392130.7154
7	4581488.43	397539.02	4581488.569	397539.17	4581488.464	397539.333	4581488.474	397539.3428
8	4581720.58	401051.4	4581720.58	401051.401	4581720.482	401051.57	4581720.491	401051.574
9	4610491.16	419468.25	4610491.165	419468.254	4610491.096	419468.409	4610491.11	419468.3851
10	4595369.64	453386.46	4595369.645	453386.477	4595369.389	453386.78	4595369.392	453386.6989
			σ_0=0.201 m	σ_0= 0.095 m	σ_0= 0.152 m	σ_0= 0.251 m	σ_0= 0.156 m	σ_0= 0.243 m

The errors of the transformed 2-D coordinates (N,E) referred ETRF2000, Epoch2021.5 into ALB1986 provided through 3- transformation models: (1) ALBACO developed by IGUF, (2) 4-P Helmert and (3) Polynomial for the Tirana area are respectively:

	ALBACO		4-P Helmert		Polynomial	
	dN	dE	dN	dE	dN	dE
0÷10.0 *cm*	30%	80	70	00	50	00
÷ 20.0 *cm*	60%	100	80	40	80	30
÷ 30.0 *cm*	90%	00	100	100	100	100
> 30.0 *cm*	10%	00	00	00	00	00

TABLE 11. TRANSFORMED 2-D COORDINATES (N,E) REFERRED ETRF2000, EPOCH2021.5 INTO ALB1986 FOR THE KUKËS-PESHKOPI

Point No.	N(ALB1986)	E(ALB1986)	ALBACO		4-P Helmert		Polynomial	
			$N(ALB1986)_1$	$E(ALB1986)_1$	$N(ALB1986)_2$	$E(ALB1986)_2$	$N(ALB1986)_3$	$E(ALB1986)_3$
1	4656566.350	447706.500	4656566.272	447706.613	4656566.431	447706.638	4656566.445	447706.5749
2	4648758.740	450126.700	4648758.885	450126.749	4648758.969	450126.852	4648758.981	450126.7828
3	4639921.770	444038.170	4639921.765	444038.226	4639921.894	444038.409	4639921.907	444038.3489
4	4643617.390	447095.820	4643617.352	447095.109	4643617.454	447095.272	4643617.467	447095.2071
5	4640190.990	447523.390	4640190.103	447523.371	4640190.193	447523.586	4640190.205	447523.5195
6	4632226.300	444846.740	4632226.306	444846.725	4632226.403	444846.973	4632226.415	444846.9099
7	4629409.370	447809.250	4629409.458	447809.345	4629409.524	447809.618	4629409.534	447809.5495
8	4623485.430	449385.310	4623485.43	449385.31	4623485.347	449385.681	4623485.355	449385.6088
9	4622302.220	444741.080	4622302.209	444741.096	4622302.154	444741.427	4622302.164	444741.3624

10	4620178.280	448586.360	4620178.371	448586.403	4620178.196	448586.829	4620178.205	448586.7574
11	4619327.610	445482.420	4619327.689	445482.962	4619327.554	445483.339	4619327.563	445483.2728
12	4616522.160	445947.200	4616522.707	445947.158	4616522.524	445947.558	4616522.532	445947.4904
13	4617541.730	447951.580	4617541.783	447951.622	4617541.577	447952.057	4617541.585	447951.9861
14	4604660.340	397539.510	4604660.273	397539.554	4604660.054	397539.507	4604660.072	397539.5168
15	4604090.880	393930.390	4604090.832	393930.447	4604090.659	393930.44	4604090.678	393930.456
16	4604274.700	415693.160	4604274.841	415693.103	4604274.697	415693.215	4604274.711	415693.1968
17	4610674.870	415756.970	4610675.016	415756.933	4610674.914	415757.059	4610674.930	415757.0413
18	4606036.040	456013.870	4606036.083	456013.849	4606035.776	456014.282	4606035.780	456014.1963
19	4610414.420	431036.000	4610414.476	431035.906	4610414.39	431036.078	4610414.401	431036.0357
20	4610491.160	419468.250	4610491.162	419468.237	4610491.082	419468.391	4610491.096	419468.3671
21	4609726.510	453363.720	4609726.710	453363.617	4609726.401	453364.083	4609726.406	453364.0019
22	4607228.120	420834.020	4607228.091	420834.06	4607227.993	420834.217	4607228.006	420834.1904
23	4605925.280	453865.890	4605925.382	453865.849	4605925.084	453866.283	4605925.089	453866.2007
			σ_0=0.233 m	σ_0= 0.194 m	σ_0= 0.229 m	σ_0= 0.351 m	σ_0= 0.226 m	σ_0= 0.309 m

The errors of the transformed 2-D coordinates (N,E) referred ETRF2000, Epoch2021.5 into ALB1986 provided through 3- transformation models: (1) ALBACO developed by IGUF, (2) 4-P Helmert and (3) Polynomial for the Kukes-Peshkopi are respectively:

	ALBACO		4-P Helmert		Polynomial	
	dN	dE	dN	dE	dN	dE

0÷10.0 *cm*	74%	91.5	56.5	21.7	56.5	34.8
÷ 20.0 *cm*	91.5%	8.5	91.5	43.5	91.5	56.5
÷ 30.0 *cm*	91.5%	8.5	95.7	56.5	95.7	91.5
> 30.0 *cm*	8.5%	8.5	4.3	43.5	4.3	8.5

4. CONCLUSION

1. Based on the mean square deviations of the three coordinates transformation models, we conclude that the ALBACO model developed by MGIF and the 4-P Helmert model proposed by the Department of Geodesy give almost the same results.
2. The errors of the transformed 2-D coordinates (N,E) referred ETRF2000, Epoch2021.5 into ALB1986 of test points in the areas (a) Berat, (b) Tepelena, (c) Shkoder, (d) Tirana and (e) Kukës-Peshkopi have resulted: up to 20 cm (with 80% confidence level), while up to 40 cm (with 95% confidence level).
3. Three models of the transformed 2-D coordinates (N,E) referred ETRF2000, Epoch2021.5 into ALB1986, which are not officially approved recommended to be used for the topographic mapping of the territory of Albania up to a scale of 1: 5000.
4. Three models of the transformed 2-D coordinates (N,E) referred ETRF2000, Epoch2021.5 into ALB1986 can be improved if we will perform additional measurements in existing points of the horizontal control network referred ALB1986.

ACKNOWLEDGEMENTS

The authors did not receive funds, grants, or other support from any organization for the submitted work. This research is part of the continuous qualification of the Academic Staff. All the material is owned by the authors and/or no permissions are required.

REFERENCES

B. Nurçe, (2013) Thesis: The development of H and V references of Albania.

EUREF Publication No. 8, (1999) Report on the Symposium of the IAG Sub-commission for Europe (EUREF), ISSN 0340-7691, ISBN 3-7696-9622-0, p.106-113.

Geodesy and Geophysics Department, Geodetic Surveys Division, (October 1994) GPS Geodetic Control Network Survey in Albania, Publication GGB-94-038.

R. Maseroli, (January 2010) Relazione sui lavori geodetici eseguiti sul territorio albanese per la realizzazione della rete geodetica satellitare.

T. Greening and G. Barnes, (April 1998) Establishment of a Geodetic Infrastructure and an Integrated Property Surveying and Mapping Methodology for Albania.

THE MOST APPROPRIATE CARTOGRAPHIC PROJECTION FOR ALBANIA'S CONDITIONS

Dr. Sc. Bilbil Nurçe

Polytechnic University of Tirana, Faculty of Civil Engineering, Department of Geodesy

E-Mail: billnurce@gmail.com, bilbil.nurce@fin.edu.al, ORCID: 0000-0001-7179-618X

Abstract

Since 1868 onwards, different institutes (Military Geographical Institute of Vienna, Austria; Military Geographical Institute of Florence, Italy; CNIGA-IK Moscow Institute; former Military Topographic Institute of Albania) have been built different geodetic bases for supporting of the mapping of the Albanian territory in different scales (1: 75000/ 50000/ 25000/ 10000/ 5000) in different projections. Especially, since 1948, all cartographic and numerical information with great practical and study value based on the classical Albanian coordinate reference ALB86. After the 1990's, cartographic information (Orthophotos, vector maps, cadastral maps, etc.) were based on global (ITRFxx) or European (ETRFyy) references. In different countries the large-scale topographic maps in the different projections for various engineering projects recommended. Aim of this study is to analyze and show the most appropriate cartographic projection for Albania's conditions.

Keywords: Cartographic projection, ellipsoid, distortion scale factor, TM/UTM/TMzn projection.

1. INTRODUCTION

In order to present a 3-dimensional object on a plane, (ie on paper) we must project the object by means of a geometric body which can lie on the plane. As is mentioned earlier, the Albanian coordinate reference based on the Krassowsky-1940 ellipsoid, Gauss-Krüger transverse conformal cylindrical projection (TM), central meridian $\lambda_0 = 21^o$, Distortion scale factor at the Central Meridian $k_0 = 1$ (Fig. 1).

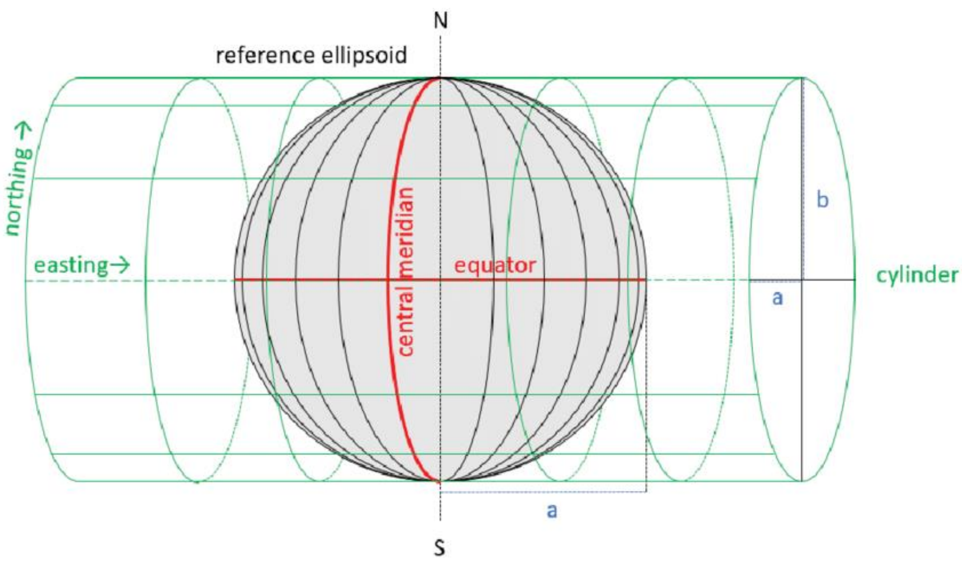

Figure 1. *Gauss-Krüger transverse conformal cylindrical projection*

(https://www.researchgate.net/profile/Fabian-Gross, December 2020)

Projections used to accurately present the most important characteristics of the topographic terrain or a certain phenomenon. Map projections have the following features (Shehu, 1989):

1) Conformal projections preserve the similarity of objects during projection.

2) Equivalent projections keep surfaces undistorted and the same degree of distortion, all directions.

3) Equidistant projections where distances preserve magnitudes.

4) Azimuthal projections that preserve some of the arcs of great circles undeformed.

Several Cartographic projections are used to create topographic maps. In order to have a projection as appropriate as possible for topographic maps, the following requirements must be taken into account:

- The condition of conformity (similarity), ie the projection must be conformal.
- The condition of the position/orientation of the territory.
- Allowed size of distortions to support topographic plans of large scales (1 : 5 000 to 1 : 1000).
- The accuracy of calculation of distortions (on point, on distance, on surface).

The allowed value of distortions is the most important indicator of choosing the most appropriate projection for mapping a territory, as well as the distortions should be within the allowed values in accordance with the graphic (theorical) accuracy of the topographic maps (plans) of the largest scale. Stated differently, projection distortions should not impair the accuracy of field measurements that determine the position of points. In order to fulfill these two important requirements, it is maneuvered with the choice of two projection parameters on which the value of the distortions depends:

- Selection of the central meridian of the rectangular coordinate area projected (λ_0),
- Selection of the distortion scale factor at the Central Meridian (k_0).

The selection and final determination of the above parameters is carried out by computational attempts, until the minimum of distortions is reached for the largest mapping scale, which is usually accepted 1:1 000. According to the allowed graphic accuracy (0.2 *mm*), the distortions of the point positions are as follows: 0.2 *m*, 0.5 *m* and 1 *m* respectively for the scales 1 : 1 000, 1 : 2 500 and 1 : 5 000.

According to the recommendations of the INSPIRE directive (DIRECTIVE 2007/2/E), the accuracy in the planimetric position at the contour points on the cadastral plans should not exceed m_p= 0.4 *m*.

Projection distortions (σ_P) must be at least 10 times smaller than the allowed accuracy in the position of contour points, ie they must not exceed the value:

$\sigma_P = m_P/10 = 0.4/10 = 0.04$ *m*

and, the distortion of a length L = 1000 *m* should not exceed the size:

$$m_L = \sigma_P \text{ x } \sqrt{2} = 0.04 \, x \, 1.414 = 0.056 \text{ } mm \text{ or } 56 \text{ } ppm.$$

2. MATERIALS AND METHODS

The central meridian $\lambda_0 = 21°$ (of classical reference ALB1986) is positioned in the easternmost extreme of Albania, leaving over 99.7% of the country's territory to its west, while the central meridian $\lambda_0 = 20°$ (of modern reference) divides it almost in half. In the case of the central meridian 21°, the coastal area has the largest projection distortions. The distortions of this surface affect the accuracy of the topographic plans of large scales, which are necessary for the development of the touristic, economic infrastructure and the cadastral system. We emphasize that in the period 1927-1939, MGIF has chosen $\lambda_0 = 20^o$ as the central meridian of the projection for the Albanian territory to support the mapping of the country even on large scales (1:5 000, 1:2 000, 1:1 000).

So, that the projection distortions do not exceed the graphic accuracy of large scales, it is necessary to re-define the existing projection parameters, re-selecting the central meridian, the scale factor of distortion in this meridian, as well as the ellipsoid. In the following, the distortions at the point positions, length and surface referred the central meridians (λ_0 = 21^0, and λ_0 = 20^0), the scale factors of distortion in the central meridian (k_0 =1, and k_0 = 0.99996) and the ellipsoids (Krassowsky-1940 and GRS80) are calculated.

2.1 Calculation of the scale factor distortion (k) in the points projection

Based on Mathematical Geodesy (Skuka, 2018), the *point distortion* (*k*) calculated according to the geodesic coordinates (φ,λ) and (x,y) of the projection. In terms of the geodetic coordinates (φ,λ), the point scale factor k is given by:

$$k = k_0 + \frac{l^2}{2}cos^2\varphi(1+\eta^2) + \frac{l^4}{24}cos^4\varphi(5-4t^2+14\eta^2+28t^2\eta^2) + \frac{l^6}{720}cos^6\varphi(61-148t^2+16t^4)$$

(1)

where, $l = \lambda - \lambda_0$, $t = tg(\varphi)$, $\eta = e'^2 cos(\varphi)$, k_0 is scale factor in the central meridian.

The point distortions are calculated for the most extreme borders of the Albania territory:

Point Number	Point Name	**φ** *(dd.mmss)*	**λ** *(dd.mmss)*
1	Kapshtice	40˚.40’ 00”	21˚.03’ 25”
2	Konispoli (S)	39˚.38’ 40”	20˚.11’ 40”
3	Sazani	40˚.30’ 10”	19˚.15’ 50”
4	Shishtavec (NE)	41˚.58’ 10”	20˚.37’ 30”
5	Vermosh (N)	42˚.39’ 40”	19˚.43’ 25”
6	Shkoder	42˚.10’ 45”	19˚.17’ 00”

In the following, the point distortions referred the central meridians λ_0 =21^0 , k_0 =1 (ALB-1986 reference), λ_0 =20^0, k_0 =1, k_0 =0.99996 (new proposal), and the ellipsoids (Krassowsky-1940 and GRS80) are calculated. The numerical results of the calculations are presented in Tables 1, 2, 3:

Table 1. Distortions at the projected point referred (ellipsoid Krassowsky, TM; λ_0 =21˚; k_0 =1)

Point Number	Point Name	*k*	*k (ppm)*
1	Kapshtice (SE)	1.000000284	0.284
2	Konispoli (S)	1.000058608	58.608
3	Sazani (SW)	1.000265484	265.484
4	Shishtavec (NE)	1.000011841	11.841
5	Vermosh (N)	1.000134205	134.205
6	Shkoder (NW)	1.000246541	246.541

Table 2. Distortions at the projected point referred (Krassowsky, TM; λ_0 =20˚; k_0 =1),

(GRS80, TM; λ_0 =20˚; k_0 =1), (GRS80, TM; λ_0 = 20˚; k_0 =0.99996)

Point Number	Point Name	k	k (*ppm*)
1	Kapshtice (SE)	1.000097905	97.905
2	Konispoli (S)	1.000003415	3.415
3	Sazani (SW)	1.000047720	47.720
4	Shishtavec (NE)	1.000032891	32.891
5	Vermosh (N)	1.000006292	6.292
6	Shkoder (NW)	1.000042962	42.962

Table 3. Distortions at the projected point referred (Krassowsky, TM; $\lambda_0 = 20^{\circ}$; $k_0 = 0.99996$)

Point Number	Point Name	k	k (*ppm)*
1	Kapshtice (SE)	1.000057905	57.905
2	Konispoli (S)	0.999963415	-36.585
3	Sazani (SW)	1.000007720	7.720
4	Shishtavec (NE)	0.999992891	-7.109
5	Vermosh (N)	0.999966292	-33.708
6	Shkoder (NW)	1.000002962	2.962

RESULTS

Changing 1) the Central Meridian (CM) from 21° to 20° and 2) the distortion scale factor from $k_0 = 1$ to $k_0 = 0.99996$ gives the following effects on the distortions of the projected points:

Distortions of Kapshtica (S-E extreme) and Shishtavec (N-E extreme) increase respectively from 0 *ppm* to 98 *ppm*, as well as from 12 *ppm* to 33 *ppm*, while the distortions of Sazani (S-W extreme) and Shkodra (N-W extreme) decrease 6-*times*, distortions of Konispoli (S extreme) decrease 17-*times* and distortions of Vermosh (N extreme) decrease 21-*times*.

(Krassowsky, TM; $\lambda_0 = 21^{\circ}$; $k_0 = 1$) → (GRS80, TM; $\lambda_0 = 20^{\circ}$; $k_0 = 1$)			
Point Number	Point Name	Distortion scale factor (*times*)	Gradient
1	Kapshtice (SE)	-	-
2	Konispoli (S)	-17	↓
3	Sazani (SW)	-6	↓
4	Shishtavec (NE)	3	↑
5	Vermosh (N)	-21	↓
6	Shkoder (NW)	-6	↓

2.2 Calculation of the scale factor distortion (k) in the projected lengths

The *projected length distortion* is calculated according to the following equation:

$$L_{projected} = L_{physical} \cdot (1 + (\tilde{Y}^2/R^2_m)) \qquad (2)$$

where, Ỹ is the length (*km*) from the central meridian, calculated to the following equation:

$$\bar{y} = N\cos\varphi \cdot l + \frac{l^3}{6} N\cos^3\varphi \cdot (-1+t^2-\eta^2) + \frac{l^5}{120} N\cos^5\varphi \cdot (5-18t^2+t^4-14\eta^2-58t^2\eta^2) + \frac{l^7}{5040} N\cos^7\varphi \cdot (-61+479t^2-179t^4+t^6) \qquad (3)$$

and, R_m is average radius of curvature (*km*), at the given point.

In the following, the length distortions referred the central meridians $\lambda_0 = 21^0$, $k_0 = 1$ (ALB1986 reference), $\lambda_0 = 20^0$, $k_0 = 1$, $k_0 = 0.99996$ (new proposal), and the ellipsoids (Krassowsky-1940 and GRS80) are calculated, while the changes (physical length-projected length) are presented in the corresponding Tables 4,5.

Table 4. *Changes (physical length-projected length) referred (ellpsoid Krassowsky, TM; $\lambda_0 = 21^\circ$; $k_0 = 1$)*

Point Number	Point Name	500	1000	1500	2000	5000	10000
		(m)	*(m)*	*(m)*	*(m)*	*(m)*	*(m)*
1	Kapshtice (SE)	0.000	-0.001	-0.001	-0.001	-0.003	-0.006
2	Konispoli (S)	-0.059	-0.118	-0.177	-0.235	-0.588	-1.177
3	Sazani (SW)	-0.266	-0.533	-0.799	-1.066	-2.664	-5.328
4	Shishtavec (NE)	-0.012	-0.024	-0.036	-0.048	-0.119	-0.238
5	Vermosh (N)	-0.135	-0.269	-0.404	-0.539	-1.347	-2.693
6	Shkoder (NW)	-0.247	-0.495	-0.742	-0.989	-2.474	-4.947

Table 5. Changes (physical length-projected length) referred

(Krassowsky, TM; $\lambda_0 = 20^\circ$; $k_0 = 1$), (Krassowsky, TM; $\lambda_0 = 20^\circ$; $k_0 = 0.99996$), (GRS80, TM; $\lambda_0 = 20^\circ$; $k_0 = 0.99996$), (GRS80, TM; $\lambda_0 = 20^\circ$; $k_0 = 1$)

Point Number	Point Name	500	1000	1500	2000	5000	10000
		(m)	*(m)*	*(m)*	*(m)*	*(m)*	*(m)*
1	Kapshtice (SE)	-0.098	-0.197	-0.295	-0.393	-0.983	-1.965
2	Konispoli (S)	-0.003	-0.007	-0.010	-0.014	-0.034	-0.069
3	Sazani (SW)	-0.048	-0.096	-0.144	-0.192	-0.479	-0.958
4	Shishtavec (NE)	-0.033	-0.066	-0.099	-0.132	-0.330	-0.660
5	Vermosh (N)	-0.006	-0.013	-0.019	-0.025	-0.063	-0.126

6	Shkoder (NW)	-0.043	-0.086	-0.129	-0.172	-0.431	-0.862

RESULTS

Changing 1) the Central Meridian (CM) from 21° to 20° and 2) the distortion scale factor from k0 =1 to k0 =0.99996 gives the following effects on the distortions of the projected lengths:

Distortions of Kapshtica (S-E extreme) and Shishtavec (N-E extreme) increase respectively 3-times, while the distortions of Sazani (S-W extreme) and Shkodra (N-W extreme) decrease 6-*times*, distortions of Konispoli (S extreme) decrease 17-*times* and distortions of Vermosh (N extreme) decrease 21-*times*.

2.3 Calculation of the scale factor distortion (k) in the projected surfaces

The *projected surface distortion* is calculated according to the following equation:

$$A_{projected} = A_{physical} \cdot (1 + (\tilde{Y}^2/2 \cdot R^2_m)) \qquad (4)$$

In the following, the projected surface distortions referred the central meridians $\lambda_0 = 21^0$, $k_0 = 1$ (ALB1986 reference), $\lambda_0 = 20^0$, $k_0 = 1$, $k_0 = 0.99996$ (new proposal), and the ellipsoids (Krassowsky-1940 and GRS80) are calculated, while the changes (physical surface – projected surface) are presented in the corresponding Tables 6, 7.

Table 6. *Changes (physical surface-projected surface) referred (ellpsoid Krassowsky, TM; λ_0 =21˚; k_0 =1)*

Point Number	Point Name	1000	2500	5000	10000	50000	100000
		(m^2)	*(m^2)*	*(m^2)*	*(m^2)*	*(m^2)*	*(m^2)*
1	Kapshtice (SE)	0.000	-0.001	-0.001	-0.003	-0.014	-0.029
2	Konispoli (S)	-0.059	-0.147	-0.294	-0.588	-2.942	-5.883
3	Sazani (SW)	-0.266	-0.666	-1.332	-2.664	-13.321	-26.641
4	Shishtavec (NE)	-0.012	-0.030	-0.059	-0.119	-0.594	-1.188
5	Vermosh (N)	-0.135	-0.337	-0.673	-1.347	-6.733	-13.466
6	Shkoder (NW)	-0.247	-0.618	-1.237	-2.474	-12.368	-24.736

Table 7. Changes (physical surface-projected surface) referred (Krassowsky, TM; λ_0=20˚; k_0=1), (Krassowsky, TM; λ_0=20˚; k_0=0.99996), (GRS80, TM; λ_0=20˚; k_0 =0.99996), (GRS80, TM; λ_0=20˚; k_0=1)

Point Number	Point Name	1000	2500	5000	10000	50000	100000
		(m^2)	*(m^2)*	*(m^2)*	*(m^2)*	*(m^2)*	*(m^2)*
1	Kapshtice (SE)	-0.098	-0.246	-0.491	-0.983	-4.913	-9.827
2	Konispoli (S)	-0.003	-0.009	-0.017	-0.034	-0.171	-0.343
3	Sazani (SW)	-0.048	-0.120	-0.240	-0.479	-2.395	-4.790
4	Shishtavec (NE)	-0.033	-0.083	-0.165	-0.330	-1.651	-3.301

5	Vermosh (N)	-0.006	-0.016	-0.032	-0.063	-0.316	-0.631
6	Shkoder (NW)	-0.043	-0.108	-0.216	-0.431	-2.156	-4.312

RESULTS

Changing 1) the Central Meridian (CM) from 21° to 20° and 2) the distortion scale factor from k_0 =1 to k_0 =0.99996 gives the following effects on the distortions of the projected surfaces:

Distortions of Shishtavec (N-E extreme) increase 3-*times*, while the distortions of Sazani (S-W extreme) and Shkodra (N-W extreme) decrease 6-*times*, distortions of Konispoli (S extreme) decrease 17-*times* and distortions of Vermosh (N extreme) decrease 21-*times*.

(Krassowsky, TM; $\lambda_0 = 21^\circ$; k_0 =1) → (GRS80, TM; $\lambda_0 = 20^\circ$; k_0 =1)			
Point Number	Point Name	Distortion scale factor (*times*)	Gradient
1	Kapshtice (SE)	-	-
2	Konispoli (S)	17	↓
3	Sazani (SW)	6	↓
4	Shishtavec (NE)	3	↑
5	Vermosh (N)	21	↓
6	Shkoder (NW)	6	↓

4. CONCLUSION

5. From the above calculated values of the distortions it can be seen that changing the Central Meridian (CM) from 21° to 20° and the distortion scale factor from k_0 =1 to k_0 =0.99996 gives the ***reduction of the projected points/ lengths/ surfaces distortions***, that are within the graphic (therorical) accuracies of topographic plans of large scales up to 1:1 000.
6. The ***new projection*** ($\lambda_0 = 20°$, k_0=0.99996) proposed, becomes a secant/cut-off projection compared to the old projection, which is tangential.

The ***new false origin of the coordinates*** is proposed to be as follows:

Northern False orthogonal origin (FN): 0.000 *m*,

Eastern False orthogonal origin (FE): 200 000.000 *m*

7. The ***final definition of the new coordinate coordinate reference*** is proposed to be as follows:

Ellipsoid:	GRS80,
Northern ellipsoidal origin (φ_0):	$\varphi_0 = 0°$,
Eastern ellipsoidal origin (λ_0):	$\lambda_0 = 20°$,
Projection:	Transversal i Merkatorit zonal (TMzn),
Northern False orthogonal origin (FN):	0.000 *m*,
Eastern False orthogonal origin (FE):	200 000.000 *m*,

Distortion scale factor in Central Meridian: $k_0 = 0.99996$.

8. The ***new projection ($\lambda_0 = 21^\circ$, $k_0 = 1$) is recommended as a coordinate reference for the mapping of our territory for scales 1:5,000 and larger***, while the old projection may remain in use for mapping at scales of 1:10,000 and smaller.

ACKNOWLEDGEMENTS

The author did not receive funds, grants, or other support from any organization for the submitted work. This research is part of the continuous qualification of the Academic Staff. Bilbil Nurçe thanks his daughter Ina, for her insightful comments and suggestions. All the material is owned by the authors and/or no permissions are required.

REFERENCES

A. Shehu, (1989) Mathematical Cartography.

Claude Boucher and Zuheir Altamimi, Version 8: (02.10.2008) Memo: Specification for reference frame fixing in the analysis of a EUREF GPS campaign.

DIRECTIVE 2007/2/EC (INSPIRE: https://inspire.ec.europa.eu/quick-overview-implementers/57528.

G. B. Lauf, (1983) Geodesy and Map Projections, TAFE Publications, Collingwood.

https://en.wikipedia.org/wiki/Transverse_Mercator_projection

M. Hotine, (1969) Mathematical Geodesy, ESSA Monograph 2, United States Department of Commerce, Washington, D.C.

Q. Skuka, (2018) Mathematical Geodesy.

ASSUMPTION CONTROL IN PARAMETRIC AND NON-PARAMETRIC DATA AND AN APPLICATION IN R

Gülşah Keklik

Çukurova University, Faculty of Agriculture, Department of Animal Science, Division of Biometry and Genetics, Adana, Türkiye

gulsahkeklk@gmail.com, ORCID: 0000-0002-1775-2773

Abstract

The validity of the assumptions about the tests should be controlled by looking at the explanatory statistics of the analyzed data to choose the tests to be applied while performing the statistical analysis, that is, to determine which of the parametric or non-parametric tests will be used. Parametric tests are applied by providing some assumptions about the parameters of the population from which the sample is drawn. The most important of these assumptions are; It can be stated that the populations from which the samples are drawn show normal distribution, the populations from which the samples are drawn have the same variances, the observations in the samples are independent of each other, and the dependent variables are quantitative (scalar) at least on the interval scale. In cases where at least one of the assumptions about parametric tests can not be met, non-parametric tests are used. Several procedures need to be done to understand whether the assumptions about parametric and non-parametric statistical methods are valid. These; examining descriptive statistics, making a visual assessment, and statistical tests.

In this study, the above-mentioned processes will be introduced to control the assumptions of parametric and non-parametric data, and the application will be made on a data set in R, which is a powerful, free and open-source software environment for statistical calculation and graph-based analysis, and the analysis results will be evaluated.

Keywords: Parametric, Non-parametric, Assumption control, Statistical calculation, R

1. INTRODUCTION

Although it is necessary to examine the explanatory statistics of the analyzed data and to control the assumptions to determine whether parametric or non-parametric tests will be applied in statistical analyzes, assumption control is ignored in most of the studies (Yu, 2013). These assumptions are: The populations from which the samples are drawn should show normal distribution, the populations from which the samples are drawn should have the same variances, the units/observations in the samples should be independent of each other, the dependent variables should be quantitative variables at least on the interval scale. Non-parametric statistics are statistical methods and techniques applied when one or more assumptions about parametric tests can not be met. Non-parametric tests do not require the distribution of variables or measurement scales, as they are studied sequentially, not with the original observation values themselves. Of the above assumptions, normality is one of the most important in deciding whether to use parametric or non-parametric tests in statistical analysis. For normally distributed variables, there is no right or left skewness as the observations are symmetrically distributed around the mean. Nonparametric methods are easier, simpler, and faster than parametric methods. They are more powerful than parametric methods in cases where assumptions can not be met (Bradley, 1960). Here are the steps to understand whether the assumptions about parametric and non-parametric statistical methods are valid: visual assessment, examining descriptive statistics, and statistical tests.

2. MATERIALS AND METHODS

To control the assumptions of parametric and non-parametric data, statistical calculations and evaluations were made through applications on a randomly generated parametric and non-parametric data set in R, a powerful, free, and open-source software environment. These applications are; data visualization (through Histogram, Box-Plot, and Q-Q Graphs), descriptive statistics, and statistical tests. For normality testing, the “shapiro.test” function in the basic “stats” package is used in R. The “ad.test “ function in the “nortest” package and the Anderson-Darling test gives similar results when applied to the same data. One of the tests used for this purpose is the Levene test. It is run with the “leveneTest” function in the “car” package (Fox & Weisberg, 2018) in R. By using the “bartlett.test” in the “stats” package in R, the homogeneity of variances can be checked using the Bartlett K-square test. Lastly, the “durbinWatsonTest” from the car package was run for a linear regression model in R.

3. RESULTS

The table below contains two birth weight data from two different groups.

Table 1. Data for Birth Weight_1 and Birth Weight_2

Birth Weight_1	Group	Birth Weight_2	Group
4.2	A	3.0	A
3.3	A	2.5	A
3.0	A	2.8	A
2.4	A	4.7	A
3.7	A	2.7	A
2.9	A	3.9	A
3.8	A	13.3	A
4.0	A	4.0	A
3.6	A	12.1	A
3.2	A	14.3	A
2.9	B	10.8	B
3.1	B	8.1	B
2.6	B	7.3	B
3.2	B	5.2	B
3.8	B	6.9	B
4.1	B	2.7	B
3.5	B	3.1	B
2.2	B	2.2	B
3.6	B	4.3	B
3.4	B	3.4	B

3.1. Visual assessment

Histogram, Box-Plot, and Q-Q charts are among the charts used in data visualization.

3.1.1. Histogram

Below are histogram graphs representing two separate data sets. Looking at the first of these graphs, it is seen that it has a normal distribution. In the second histogram graph, it is seen that this distribution is not normal.

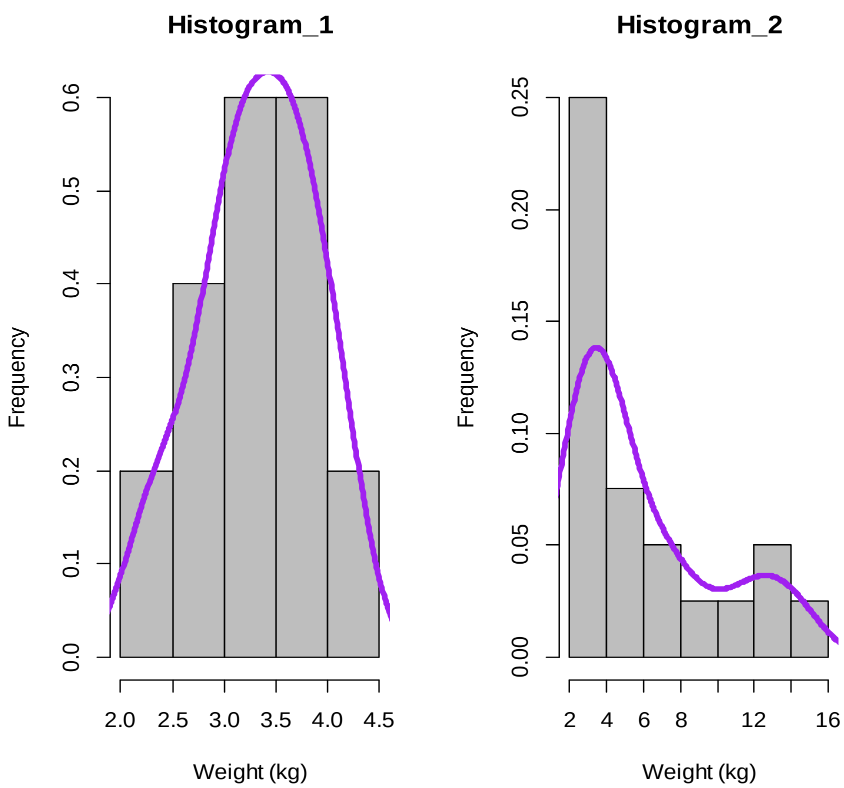

Figure 1. Histogram graphs of two different experiments

3.1.2. Box-Plot Graph

In a normally distributed box-whisker plot, the line in the middle of the box should be in the middle of the box. In the experiment on the left, it is seen that the placement of the box and the line in the middle are close to normal. In the experiment on the right, it is clearly seen that there is a departure from the normal distribution, as observed in the histogram graph before. The line is in the middle of the box and the box is closer to the left.

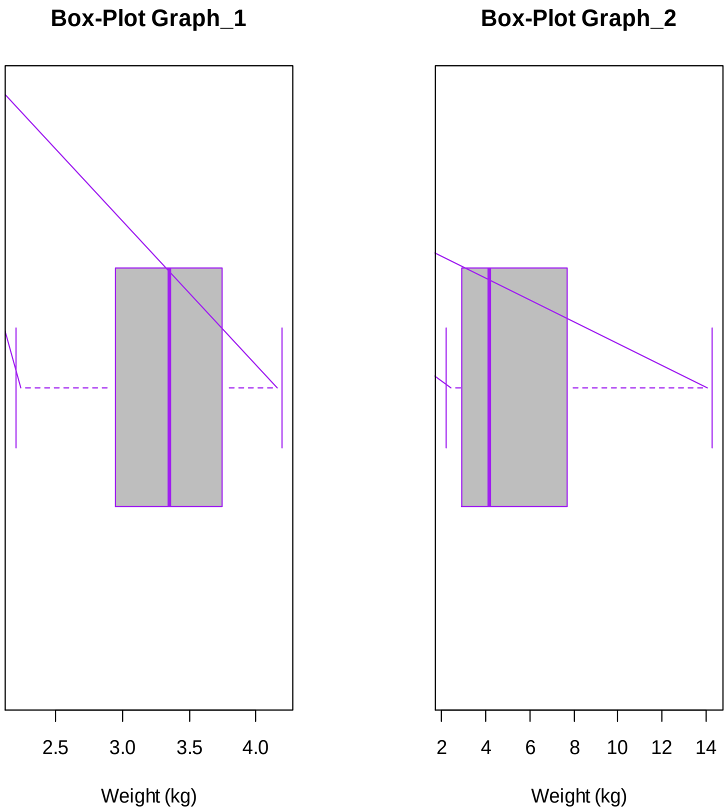

Figure 2. Box-Plot graphs of two different experiments

3.1.3. Q-Q Graph

The fact that the observed values are on the line extending along the diagonal and close to the line is an indication of a normal distribution. In the Q-Q graph of the Birth Weight_1 data on the left, the sample-theoretical quantile pairs are almost on the purple regression line; only one observation at the upper end is observed to be distant. This situation is accepted as a normal or at least a normal distribution of the variable. In the Q-Q graph on the right, it is seen that both the purple regression line can not be located along the diagonal and many quantile pairs are far from the line in the lower, middle and upper parts. This shows that the distribution of the birth weight variable of the Birth Weight_2 data is not normal.

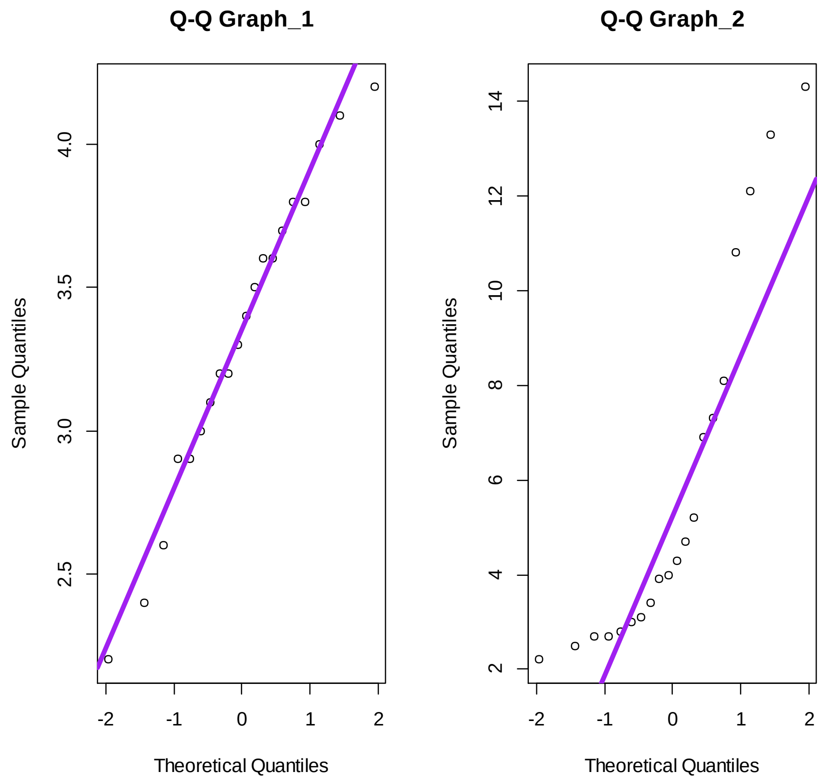

Figure 3. Q-Q graphs of two different experiments

3.2. Examining descriptive statistics

Descriptive statistics provide sufficient information about normality. In a normal distribution, the arithmetic means, median, and peak values should be equal or very close to each other. While the descriptive statistics results in Table 2 and Table 4 can be interpreted as an indicator of normal distribution, the results in Table 3 and Table 5 can be interpreted as an indicator of non-normal distribution.

Table 2: Descriptive statistics results for Birth Weight_1 data

Min.	1st Qu.	Median	Mean	3rd Qu.	Max.
2.20	2.98	3.35	3.33	3.73	4.20

Table 3: Descriptive statistics results for Birth Weight_2 data

Min.	1st Qu.	Median	Mean	3rd Qu.	Max.
2.20	2.95	4.1	5.87	7.50	14.30

Table 4: Detailed descriptive statistics results for Birth Weight_1 data

Vars	N	Mean	SD	Median	Trimmed	Mad	Min	Max	Range	Skew	Kurtosis	SE
1	20	3.33	0.55	3.35	3.35	0.59	2.2	4.2	2	-0.31	-0.86	0.12

Table 5: Detailed descriptive statistics results for Birth Weight_2 data

Vars	N	Mean	SD	Median	Trimmed	Mad	Min	Max	Range	Skew	Kurtosis	SE
1	20	5.86	3.88	4.15	5.31	2.15	2.2	14.3	12.1	0.97	-0.55	0.87

3.3. Statistical Tests

3.3.1. Normality Tests

Normality tests are tests applied to check whether the variables are normally distributed. While many of these tests use sample mean and variance, some also use statistics such as kurtosis and skewness coefficient (Cebeci, 2019).

3.3.1.1. Shapiro-Wilk Normality Test

According to the following results, while the distribution in the Birth Weight_1 data was normal (p=0.8582), it was not normal in the Birth Weight_2 data (p=0.001834).

Table 6: Shapiro-Wilk normality test results for Birth Weight_1 data

Shapiro-Wilk normality test	
W	P-value
0.97518	0.8582

Table 7: Shapiro-Wilk normality test results for Birth Weight_2 data

Shapiro-Wilk normality test	
W	P-value
0.82139	0.001834

3.3.1.2. Anderson-Darling Normality Test

According to the following results, while the distribution in the Birth Weight_1 data was normal (p=0.9349), it was not normal in the Birth Weight_2 data (p=0.0008565).

Table 8: Anderson-Darling normality test results for Birth Weight_1 data

Anderson-Darling normality test	
A	P-value
0.16204	0.9349

Table 9: Anderson-Darling normality test results for Birth Weight_2 data

Anderson-Darling normality test	
A	P-value
1.41	0.0008565

3.3.2. Controlling the Homogeneity of Variances

For the application of parametric statistical methods, the variances of the dependent variable should be homogeneous according to the groups.

3.3.2.1. Levene's Test for Homogeneity of Variance

According to the results below, it was observed that the distribution in the Birth Weight_1 data (p=0.9435) and the distribution in the Birth Weight_2 data were homogeneous (p=0.4493). However, in the results here, it is seen that the distribution in the Birth Weight_2 data fluctuates compared to the Birth Weight_1 data.

Table 10: Levene's Test for homogeneity of variance results for Birth Weight_1 data

Levene's Test for homogeneity of variance (center = median)		
Df	F value	Pr(>F)
1	0.0052	0.9435

Table 11: Levene's Test for homogeneity of variance results for Birth Weight_2 data

Levene's Test for homogeneity of variance (center = median)		
Df	F value	Pr(>F)
1	0.5983	0.4493

3.3.2.2. Bartlett Test for Homogeneity of Variance

According to the results below, it was observed that the distribution in the Birth Weight_1 data (p=0.9362) and the distribution in the Birth Weight_2 data were homogeneous (p=0.1179). However, in the results here, it is seen that the distribution in the Birth Weight_2 data fluctuates compared to the Birth Weight_1 data.

Table 12: Bartlett Test for homogeneity of variance results for Birth Weight_1 data

Bartlett Test for homogeneity of variance (center = median)		
Df	Bartlett's K-squared	P-value
1	0.0064125	0.9362

Table 13: Bartlett Test for homogeneity of variance results for Birth Weight_2 data

Bartlett Test for homogeneity of variance (center = median)		
Df	Bartlett's K-squared	P-value
1	2.4456	0.1179

3.3.3. Controlling the Independence

Each observation in the sample groups should be independent of the others, that is, not related. Many statistical tests can be used in the analysis of the independence or randomness of the sample units. The Durbin-Watson test (DWT) is one of them.

3.3.3.1. Durbin-Watson Test (DWT)

In the Birth Weight_1 data, it is seen that the autocorrelation of the residues is positive and far from moderate (0.06451442) but insignificant (p=0.4) and therefore the units in the sample groups are independent of each other. In Birth Weight_2 data, autocorrelation was found to be positive and close to moderate (0.4390335) and significant (p=0.014). Through these results, it is seen that the units in the sample groups are dependent on each other in the Birth Weight_2 trial data.

Table 14: Durbin-Watson Test results for Birth Weight_1 data

Durbin-Watson Test for controlling the independence			
lag	Autocorrelation	D-W Statistic	P-value
1	0.06451442	1.756041	0.4
Alternative hypothesis: rho != 0			

Table 15: Durbin-Watson Test results for Birth Weight_2 data

Durbin-Watson Test for controlling the independence			
lag	Autocorrelation	D-W Statistic	P-value
1	0.4390335	1.068267	0.014
Alternative hypothesis: rho != 0			

4. DISCUSSION

In some studies, the problem of not checking the assumptions of the data is encountered. Statistical analyzes are made without applying parametric assumptions to non-parametric data, and as a result, errors occur in the research results. The results of these studies are misinterpreted and scientific errors occur. All these problems need to be resolved and some actions need to be taken. In order to prevent scientific errors, researchers should be aware of and correct the faulty parts in the produced studies. For this reason, it is important to know the parametric test assumptions, to control the assumptions, and to know and apply non-parametric tests, which are the equivalent of parametric tests.

5. CONCLUSION

This study is important for researchers to complete their statistical analyzes with or without errors and to be able to interpret them. In future studies, attention should be paid to whether or not the assumptions control is provided, and if the assumptions are not met, the problem should be solved with some methods. This awareness should be given to researchers starting from undergraduate statistics courses, and mistakes in postgraduate and postgraduate studies should be controlled.

REFERENCES

Bradley, J. V. (1960). Distribution-free statistical tests. 60(661), United States Air Force.

Cebeci, Z. (2019). R ile Parametrik Olmayan İstatistik Analiz. Abaküs Kitap, Ankara, Türkiye.

Fox, J. Weisberg, S. (2018). An R Companion to Applied Regression. Sage Publications.

Yu, C. H. (2013). Research and Evaluation of Web-Based Instruction. (Access Date: 19.11.2022)

COMPARISON OF STATISTICAL SOFTWARE PROGRAMS USED IN GRADUATE THESES IN THE FIELD OF SCIENCE IN THE LAST 10 YEARS

Gülşah Keklik

Çukurova University, Faculty of Agriculture, Department of Animal Science, Division of Biometry and Genetics, Adana, Türkiye

gulsahkeklk@gmail.com, ORCID: 0000-0002-1775-2773

Abstract

It is important to determine which statistical software program will be used in statistical research in theses in the field of Science. Invented by Ross Ihaka and Robert Gentleman of the University of Auckland, New Zealand, R was officially announced in 1997 as a free and open-source software environment and programming language for statistical computing and graphical drawing. R, which can also be used for advanced statistical and mathematical studies through various packages and functions, also provides benefits to researchers who want to develop their statistical software. Python, one of the popular programming languages published by Guido van Rossum in 1991, is technically a language that is compiled first and then interpreted through compiled code. With Python, it is possible to work in various scientific fields including big data and complex mathematical operations, as well as in fields such as Artificial Intelligence, Machine Learning, and Image Processing. SPSS, which has been officially named IBM SPSS Statistics since August 2010, is a software program for statistical analysis, the first version of which was released in 1968. As an indicator of the popularity of programming languages, according to the TIOBE Programming Community index, which is updated monthly, in October 2022, Python and R were in the top 20 in the ranking, while SPSS could not enter this list.

Within the scope of the purpose of this study, a comparison was made between R and Phyton and SPSS, which are statistical software programs used in graduate theses prepared in the field of Science in the last 10 years, obtained from the Council of Higher Education National Thesis Center. Despite the existence of open-source programming languages, the persistent use of SPSS, which is one of the very expensive programming languages, and the reasons for this are discussed.

Keywords: Programming language, R, Phyton, SPSS, Council of Higher Education National Thesis Center

1. INTRODUCTION

One of the issues to be considered during statistics education is to teach appropriate statistical package programs. Although student versions are offered at low cost, students can not use this software when they graduate. Companies, on the other hand, do not favor these programs (Team, 2017). The R for Windows package program is a publicly licensed program that is distributed free of charge over the internet. The program may be freely distributed and used under license; therefore, scientists with any programming knowledge can make changes and improvements to this code (Dalgaard and Fox, 2002). R for Windows package program users; It offers an efficient data processing and storage facility, a set of commands for array and matrix calculations, a collection of advanced techniques for data analysis, and graphical features (Clarke and Cooke, 1983). Python is a popular programming language created by Guido van Rossum in 1991. It is used in areas such as web development, software development, and system scripting. Python runs on an interpreter system, meaning it executes as soon as the code is written and runs pretty fast. Python can be approached in an object-oriented way or in a functional way (Van Rossum, 1991). One of the key features of all modern interpreted languages is that they are extensible.

When creating a Python-based script, legacy code can be integrated and extended with new functionality (Halterman, 2011). Most researchers know that much more of their time is spent in the various stages of data collection and preparation, rather than building models and producing reports. SPSS is one of the paid software programs that are often used to perform data management tasks (Levesque, 2007). According to the TIOBE Programming Community index, which is an indicator of the popularity of programming languages, Python and R are at the top of the rankings, while SPSS can not enter this list. This takes it away from making it one of the world's programming languages.

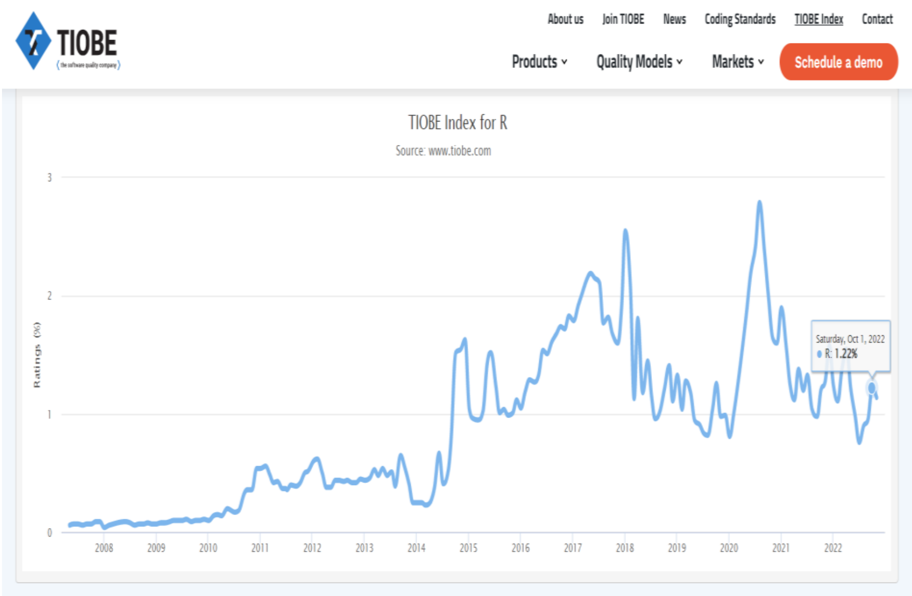

Figure 1. TIOBE Index for R

(https://www.tiobe.com/tiobe-index)

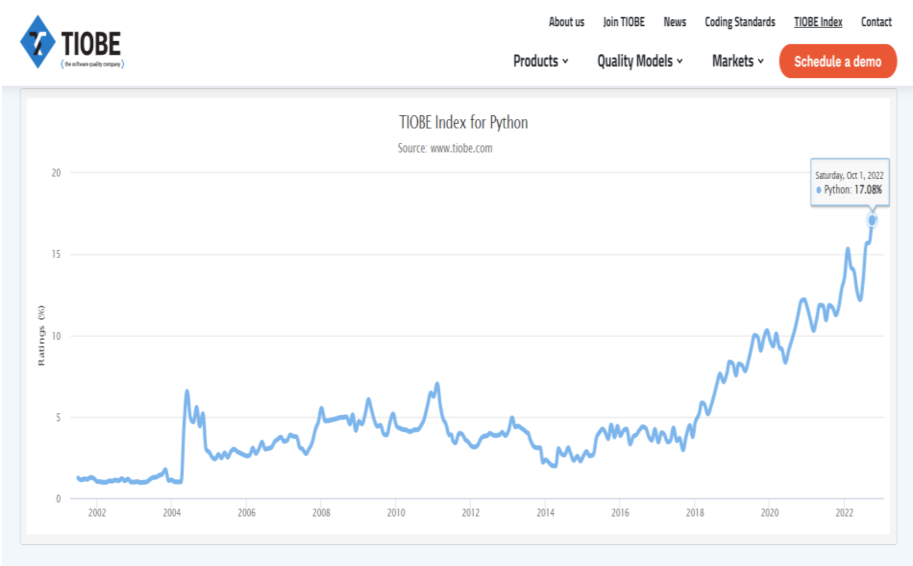

Figure 2. TIOBE Index for Python

(https://www.tiobe.com/tiobe-index)

2. MATERIALS AND METHODS

In this study, the number of authorized/unauthorized master's/Ph.D. theses written in the field of Science between the years 2012-2022 were determined by taking into account the data in the Council of Higher Education National Thesis Center. The results obtained by detailed scanning were found by writing SPSS, R, and Python in the abstract part, respectively.

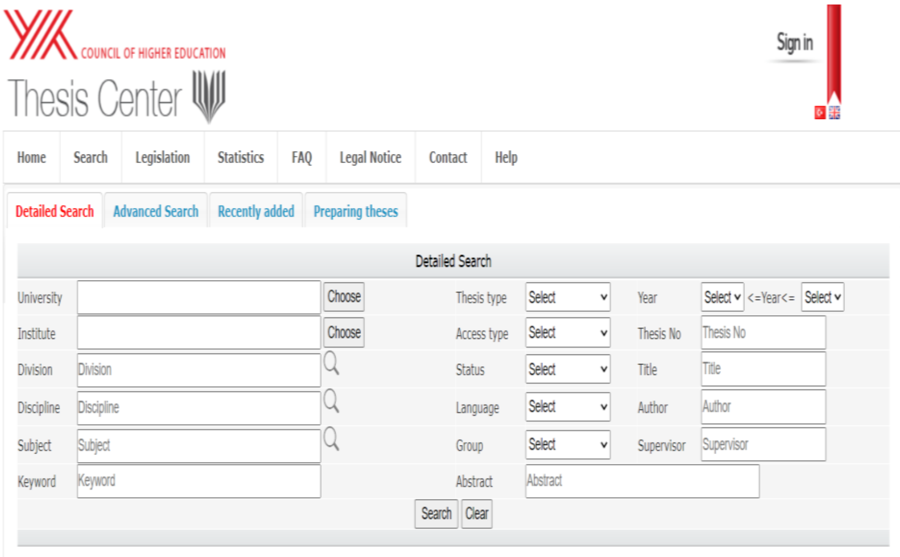

Figure 3. Council of Higher Education National Thesis Center (https://tez.yok.gov.tr/UlusalTezMerkezi/tarama.jsp)

3. RESULTS

The graphs below were created in line with the data in the Council of Higher Education National Thesis Center.

3.1. Master's Theses

In the light of the data in Table 1 and Table 2; It is seen that SPSS, one of the statistical software programs, was preferred by the author of 1406 of the 114431 master's theses (authorized + unauthorized) written in the field of Science between 2012-2022. While it was seen that Python was preferred by 507 authors in the same years, no information about R was found.

Table 1. The number of authorized master's theses written in the field of Science between 2012-2022

Statistics software program	Access Authorization	Thesis type	Group	Number
SPSS	Authorized	Master	Science	1397
R	Authorized	Master	Science	Not found
Python	Authorized	Master	Science	501

Table 2. Number of unauthorized master's theses written in the field of Science between 2012-2022

Statistics software program	Access Authorization	Thesis type	Group	Number
SPSS	Unauthorized	Master	Science	9
R	Unauthorized	Master	Science	Not found
Python	Unauthorized	Master	Science	6

3.2. Ph.D. Theses

In the light of the data in Table 3 and Table 4; It is seen that SPSS, one of the statistical software programs, was preferred by the authors of 211 out of 25891 Ph.D. theses (authorized + unauthorized) written in the field of Science between 2012-2022. While it was seen that Python was preferred by 53 authors in the same years, no information about R was found.

Table 3. Number of authorized Ph.D. theses written in the field of Science between 2012-2022

Statistics software program	Access Authorization	Thesis type	Group	Number
SPSS	Authorized	Ph.D.	Science	209
R	Authorized	Ph.D.	Science	Not found
Python	Authorized	Ph.D.	Science	52

Table 4. Number of unauthorized Ph.D. theses written in the field of Science between 2012-2022

Statistics software program	Access Authorization	Thesis type	Group	Number
SPSS	Unauthorized	Ph.D.	Science	2
R	Unauthorized	Ph.D.	Science	Not found
Python	Unauthorized	Ph.D.	Science	1

In the table below, the numbers showing the distribution of theses written in the field of Science between 2012-2022 according to their types are given.

Table 5. Distribution of theses written in the field of Science between 2012-2022 according to their types

Thesis type	Number of theses (authorized + unauthorized)
Master	114431
Ph.D.	25891

4. DISCUSSION

One of the important issues while writing master's and Ph.D. theses is the determination of statistical software programs and statistical analysis methods. There are many paid/free software programs for this. Despite the existence of open-source software programs, many people still prefer paid software today. There are of course many reasons for this. When using programs such as R and Python, knowing how to write code and run command lines correctly requires considerable effort. Many researchers find it easier to choose the tests they want by clicking the options in the menu instead of doing this. In R and Python, it is more difficult to get output from the program due to problems caused by a slight lack of punctuation or errors in the commands. For this reason, researchers take advantage of the programs purchased by some companies and universities or they want to purchase these software programs for a certain period by paying large amounts. However, R and Python software programs allow the user to write programs according to the details of the technique and provide the opportunity to work on advanced analysis techniques. In addition, they are user-friendly software programs in terms of the number of open methods and the development of their packages. SPSS, on the other hand, is one of the most common software purchased and used in this way. In this study, the comparison of statistical software programs SPSS, R, and Python was made based on postgraduate theses. Although it is paid, it has been observed that SPSS is preferred much more than the other two software.

5. CONCLUSION

As a result of this work, researchers should be encouraged to use open-source and free software programs instead of buying paid programs. For this reason, it is important for master's and Ph.D. thesis advisors to explain the content of related software programs to their students, to prepare the infrastructure of their studies accordingly, and to support their students in various ways during the thesis writing process. At this point, students need to train and develop themselves. It should be aimed that the research results prepared as a result of the use of coding-based programs reach worldwide standards. One of the efforts to create software awareness in our country is the courses that are desired to be given by faculty members or good software developers to increase the quality of postgraduate theses. Some of the courses in this field can also be accessed free of charge on the internet. Another suggestion can be offered to enable users to encounter R and Python at an earlier age by starting to provide training at the undergraduate level. Eventually, it should be our priority to develop a behavior style according to what today's world requires and to achieve world standards in our academic studies.

REFERENCES

Clarke, G. M. and Cooke, D. (1983). “A Basic Course in Statistics.” Second Edition, Edward Arnold, London.

Dalgaard, P. (2002). Introductory Statistics with R, Springer-Verlag New York, Inc,

Halterman, R. L. (2011). Learning to Program with Python, Python Software Foundation, 283.

https://tez.yok.gov.tr/UlusalTezMerkezi/tarama.jsp (Access Date: 15.11.2022)

https://www.tiobe.com/tiobe-index/ (Access Date: 15.11.2022)

Levesque, R. (2007). SPSS Programming and Data Management. A guide for SPSS and SAS Users.

Team, R. C. (2017). The Comprehensive R Archive Network.

Van Rossum, G. (1991). Python.

STATISTICAL LITERACY

Gülşah Keklik

Çukurova University, Faculty of Agriculture, Department of Animal Science, Division of Biometry and Genetics, Adana, Türkiye

gulsahkeklk@gmail.com, ORCID: 0000-0002-1775-2773

Abstract

Katherine K. Wallman defined statistical literacy as the ability to understand and critically evaluate statistical results that affect our daily lives and to appreciate the contribution statistical thinking can make to public and private, professional and personal decisions. Being able to read and make sense of the statistics encountered in the news, media, and surveys is of great importance in terms of adapting to the changing world in today's information society. A society consisting of people who can not read and evaluate statistics and can not interpret the graphics they see is not considered a fully developed society. Statistical literacy users, who can access and filter complex data of information, always need to improve their statistical skills. For this purpose, ease of expression and statistical literacy skills should be provided at a level that people from every profession can understand.

This study covers the importance of people of all ages and occupations having statistical literacy skills and efforts to develop different methods and strategies to increase these skills, taking into account strategic priorities.

Keywords: Statistical literacy, Statistical skill, Statistics

1. INTRODUCTION

In recent years, the importance of developing statistically literate citizenship has increased. As the world is increasingly dependent on statistical data, instant access to statistical information is gained through communication technologies in the modern world. A statistically literate citizen will be able to understand this information and reach a decision in light of this information (Rumsey, 2002). Carmichael (2010) defined the dictionary definition of statistical literacy as the capacity to interpret statistical messages and communicate these messages in writing or orally. Statistical literacy, like reading literacy, focuses on making decisions using statistics. Statistical literacy, which includes skills such as reading, writing, and speaking, includes two reading skills, understanding and commenting (Schield, 1999).

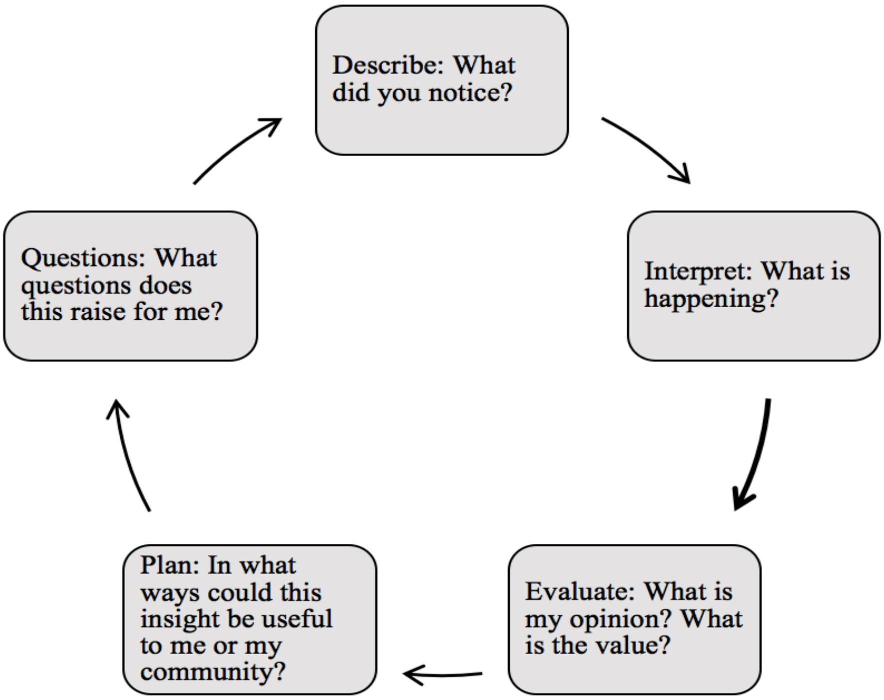

Figure 1. The questioning cycle

(https://www.statisticsteacher.org/2020/11/12/data-interrogations-critical-statistical-literacy/)

In general, Hayden (2004) defined statistical literacy as the skills a person needs to deal with probability and statistics issues that arise in daily life. According to Schield (2001), statistical literacy is "examination, interpreting, analyzing and evaluating (and detecting errors that occur there)." According to Garfield (1999), understanding statistical language; relates to words, symbols, and terms. Interpreting charts and tables, reading statistics, and interpreting them meaningfully in press and questionnaires. Chance (2002) approached this process from a global perspective, which includes understanding variability and the statistical process as a whole, taking into account existing definitions. The definition of Gal (2004) is stated as follows.

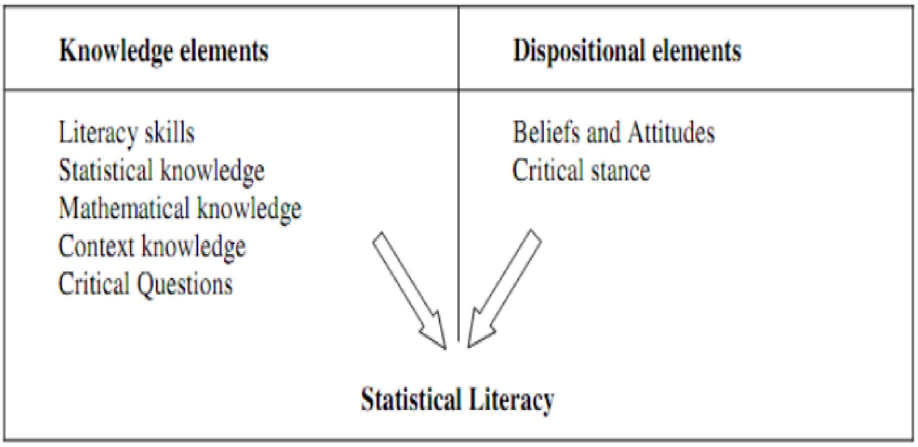

Figure 2. Gal's (2004) definition of statistical literacy

Researchers and educators have often recommended the development of statistics teaching methods. These are the methods in which scientific methods are applied, especially with authentic statistical experiences (Bryce, 2005). Statistical literacy can serve societies in many ways. Adults need to be aware of trends (crime rates, population growth, etc.) of social and personal importance. Increasing demands for employees to understand statistical information on the quality of operations (Packer, 1997) and statistical literacy are needed in many businesses for employees to understand this data (Bowen and Lawler, 1992). According to Gal (2000), making statistics is not the same as understanding statistics. It is important to understand the steps used to calculate the standard deviation, but being able to calculate it easily does not mean having the ability to understand the standard deviation. Statistics formulas are a simple mathematical shortcut for creating a statistic, but students tend to forget these formulas easily after they pass their exams (Moore, 1998).

Yorke (2006) defined employability as a contribution to the self, society, and economy that enables graduates in higher education to find a job and achieve success in their occupation. It is important to increase student's awareness of the employability of statistical literacy and to bring them closer to the courses related to quantitative information, and studies on quantitative and qualitative research methods show that most students come to the university with fixed ideas and have negative aspects in quantitative methods (Murtonen, 2005).

1.1. Statistical Thinking

Statistical thinking includes having the ability to see the whole process, understanding the relationship between variables, having the ability to research data, and producing new research questions other than those asked in research (Chance, 2002). Pfannkuch and Wild (2004) proposed five key ideas for statistical thinking: data recognition, digitization, evaluation of diversity, and integration in a statistical and contextual sense by reasoning with statistical models. They also stated that it is necessary to synthesize statistical and contextual information for statistical thinking and defined this competence as the integration of statistical and contextual. Sanchez (2007) proposed two different statistical literacy models, in which the complexity of statistical literacy and its relation to other disciplines vary between models. In this model, L stands for statistical literacy, R stands for statistical reasoning, and T stands for statistical thinking.

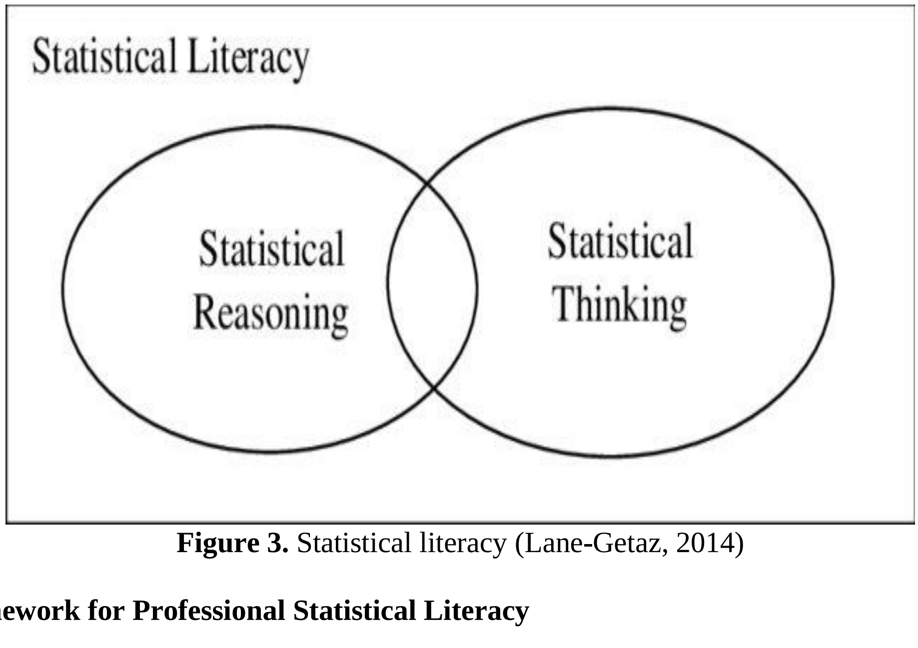

Figure 3. Statistical literacy (Lane-Getaz, 2014)

1.2. A Framework for Professional Statistical Literacy

The Professional Statistical Literacy Framework supplies focus on the statistical literacy necessary to interpret data in tables, graphs, and other forms. Three levels are proposed for the interpretation of the data, and although successful performance at the higher levels is based on that at the lower levels, the hierarchy here aims to show an order of instruction. Read values at the lowest level of the frame include being able to read directly accessible items in the data. An experienced graphic reader starts by reading the title first. To tell stories about data by quickly checking variable names and value ranges, the graph reader needs to take it to a higher level.

The level of comparison values can be used when comparing data values, looking for trends, identifying skewed data in the form of a boxplot, etc. applied level. Making statistically valid conclusions about data requires more than a comparison. At the highest level of data interpretation, and analysis of the dataset, consideration is given to the dataset as a whole, not individual components. It is important to determine whether the differences between data sets are statistically significant.

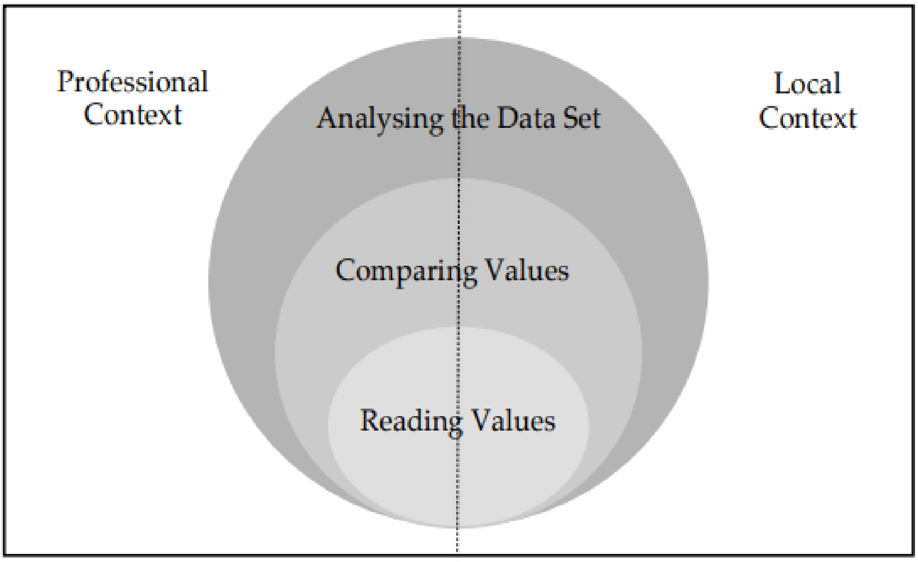

Figure 4. A framework for professional statistical literacy (Pierce and Chick, 2011)

2. DISCUSSION AND CONCLUSION

Statistical literacy is much more than computation. It is very important to understand and evaluate the tables encountered in daily life and to conclude these tables. It should be ensured that statistical literacy can be done at a basic level through the processes of making sense of data, using statistical databases, and creating visualizations. Increasing statistical knowledge and skills, contributing to positive attitudes and behaviors towards statistics, and individuals working in various institutions and organizations should be taught new techniques with the help of courses. Accepting to face problems will make important contributions to increasing the level of literacy. For this purpose, statistical literacy skills with ease of expression that can be understood by people from all occupational groups and all age levels should be gained. Statistics should be taught in the school curriculum to teach reading and comprehension skills at very young ages. It should be ensured that the students studying at the university take statistics courses regardless of faculties and departments, and at least some basic skills should be acquired and successfully applied in their future life. Large-scale statistical presentations should be made by organizing meetings and seminars in institutions and organizations providing professional services. In the developing and changing digital world societies, it is important to use technology correctly for this purpose and to develop applications and present them to the service of individuals in society. Gaining statistical literacy and awareness skills by learning statistics correctly will enable us to create a common form of communication.

REFERENCES

Bowen, D. E., & Lawler, E. E. (1992). The empowerment of service workers: What, why, how and when. Sloan Management Review, 31-39.

Bryce, G. R. (2005). Developing tomorrow's statisticians. Journal of Statistics Education, 13(1).

Carmichael, C. S. (2010). The development of middle school children’s interest in statistical literacy (Doctoral dissertation, University of Tasmania).

Chance, B. L. (2002). Components of statistical thinking and implications for instruction and assessment. Journal of Statistics Education, 10(3).

Gal, I. (2000). Adult Numeracy Development: Theory, Research, Practice. Series on Literacy: Research, Policy, and Practice. Hampton Press, Inc., 23 Broadway, Cresskill, NJ 07626.

Gal, I. (2004). Statistical literacy. In The challenge of developing statistical literacy, reasoning and thinking, 47-78, Springer, Dordrecht.

Garfield, J. (1999). Thinking about statistical reasoning, thinking, and literacy. First Annual Roundtable on Statistical Thinking, Reasoning and Literacy (STRL-1).

Hayden, R. (2004). Planning a statistical literacy program at the college level: Musings and a bibliography, In ASA Proceedings of the Section on Statistical Education, 2685-2692.

https://www.statisticsteacher.org/2020/11/12/data-interrogations-critical-statistical-literacy/ (Access Date: 19.11.2022)

Lane-Getaz, S. J. (2014). What students learn and don't learn about inferential reasoning in their introductory statistics courses. In Joint Statistical Meetings (JSM) Proceedings, Statistical Consulting Section. Alexandria, VA: American Statistical Association. Retrieved from https://www.amstat.org/membersonly/proceedings/2014/data/assets/pdf/311030_8660 (Vol. 8).

Moore, D. S. (1998). Shaping Statistics for Success in the 21st Century: A Panel Discussion. Kansas State University Technical Report II-98-1.

Murtonen, M. (2005). University students' research orientations: Do negative attitudes exist toward quantitative methods?, Scandinavian Journal of Educational Research, 49(3), 263-280.

Packer, A. (1997). Mathematical Competencies That Employers Expect. Why numbers count: Quantitative literacy for tomorrow’s America, 137-154.

Pfannkuch, M., & Wild, C. (2004). Towards an Understanding of Statistical Thinking. In the Challenge of Developing Statistical Literacy, Reasoning and Thinking, 17-46, Springer, Dordrecht.

Pierce, R. U., & Chick, H. L. (2011). Reacting to quantitative data: Teachers' perceptions of student achievement reports. In 23rd Biennial Conference of The Australian Association of Mathematics Teachers Inc. and the 34th Annual Conference of the Mathematics Education Research Group of Australasia Inc. (AAMT-MERGA Conference), 1, 631-639.

Rumsey, D. J. (2002). Statistical literacy as a goal for introductory statistics courses. Journal of statistics education, 10(3).

Sanchez, J. (2007). Building statistical literacy assessment tools with the IASE/ISLP. International Association for Statistical Education (IASE)/International Statistics Institute (ISI) Satellite.

Schield, M. (1999). Statistical literacy: Thinking critically about statistics. Of Significance, 1(1), 15-20.

Schield, M. (2001, August). Statistical literacy: Reading tables of rates and percentages. In ASA Proceedings of Statistical Education Section.

Yorke, M. (2006). Employability in higher education: what it is-what it is not, Vol. 1, York: Higher Education Academy.

TARIMDA HASAT VE HASAT SONRASI GIDA KAYIPLARININ ÖNLENMESİ

Coşkun Yıldırım

Tabit Yönetim Danışmanlığı ve Tarımsal Teknoloji Ltd. Şti.

coskun.yildirim@tabit.com.tr

Necmi Cemal Özdemir

Kocaeli Üniversitesi, Mühendislik Fakültesi, Elektrik Mühendisliği

necmi.ozdemir@kocaeli.edu.tr

Türkan Nur Metin

Tabit Yönetim Danışmanlığı ve Tarımsal Teknoloji Ltd. Şti.

turkan.metin@tabit.com.tr, ORCID: 0000-0002-3753-8790

Sevdam Yıldırım

Tabit Yönetim Danışmanlığı ve Tarımsal Teknoloji Ltd. Şti.

yildirimsevdam@gmail.com

Özet

Bu çalışma, tarımda hasat ve hasat sonrası yaşanan gıda kayıplarına çözüm bulması için tasarlanmıştır. Üretilen tarımsal ürünlerde yaşanan ürün kayıplarının yarısına yakın oranda hasat ve hasat sonrası tedarik zincirinde yapılan hatalardan kaynaklandığı belirlenirken, üretilen ürünlerin alışıla gelmiş standartlara uymaması ve perakende alıcılar tarafından tercih edilmemesi değerinin çok daha altında fiyatlara satılmasına üreticinin üretim maliyetlerinin çok daha altında kazanç elde etmesine sebep olmaktadır. Bunun yanı sıra ani piyasa daralmalarından kaynaklanan, pazarda satış şansı bulamayan ürünlerin tedarik zincirinde değerlendirilemeyip gıda hammaddelerinde kayıpların yaşanmasına sebep olmaktadır.

Tam bu noktada yapay zekâ destekli gıda kurtarma yazılımı ile çözüme ulaştırılmaktadır. Pazarda yer bulamayan gıda ürünlerinin gıda ve kozmetik ürünlerine uygun üretim yapabilmesi için gıda üretim tesislerinin âtıl kapasitelerini anlık olarak takip edebilmekte, işletmelere yönelik süreçleri tanımlayarak, en uygun ürün formu için alternatifler hazırlayabilmektedir. Aynı zamanda üretim aşamasında yaşanması muhtemel risklerin önlenmesi açısından gıda üretim tesislerinin tüm süreçlerini takip ederek, iş ortaklığı süreçlerini kolaylaştıracaktır.

Tüm aşamaların takip edilerek, muhtemel risklerin belirlenmesi pazarda yer bulamayan ürünlerin gıda tedarik zincirinde çöpe dönüşmeden değerlendirilip değer zincirinde yer edinmesine imkân tanır. Böylelikle ürünlerin katma değerleri arttırılarak, gıda atıklarının azaltılmasına, gıdaya erişimi kolaylaştırarak gıda enflasyonunu düşürmektedir. Her şeyden önemlisi Dünya kaynaklarımızın boşa harcanmasının önüne geçilerek, bu kaynakların sürdürülebilirliğini arttırmaktadır.

Anahtar Kelimeler: Tarım teknolojileri, yapay zekâ, gıda kayıpları, tedarik zinciri, katma değer

PREVENTION OF HARVEST AND POST-HARVEST FOOD LOSSES IN AGRICULTURE

Abstract

This study is designed to find solutions to harvest and post-harvest food losses in agriculture. While it has been determined that nearly half of the product losses experienced in the agricultural products produced are caused by the mistakes made in the harvest and post-harvest supply chain, the fact that the products produced do not comply with the usual standards and are not preferred by retail buyers cause the producer to earn a profit much lower than the production costs. In addition, the products that cannot be sold in the market due to sudden market contractions cannot be evaluated in the supply chain, causing losses in food raw materials.

At this point, it is solved with artificial intelligence supported food recovery software. It can instantly monitor the idle capacities of food production facilities so that food products that cannot find a place in the market can produce suitable for food and cosmetic products, can define processes for businesses and prepare alternatives for the most suitable product form. At the same time, it will facilitate business partnership processes by following all processes of food production facilities in terms of preventing possible risks during the production phase.

By following all stages, identifying possible risks allows products that cannot find a place in the market to be evaluated in the food supply chain before they turn into garbage and to take a place in the value chain. Thus, it reduces food inflation by increasing the added value of products, reducing food waste, facilitating access to food. Most importantly, it prevents the waste of our world resources and increases the sustainability of these resources.

Keywords: Agricultural technologies, artificial intelligence, food losses, supply chain, added-value

1. GİRİŞ

Günümüzde insan varlığının devamlılığının ön koşulu besin ve içme suyu kaynaklarına erişimdir. Ancak artan nüfus ve çevresel kirletici faktörler gıda ve su üzerinde önemli bir baskı aracı yaratmaktadır. Bu nedenle gıda ve su süreçlerinin yönetiminin etkin şekilde yürütülmesi önemli bir gereksinim halini almıştır. FAO'ya göre gıda süreçlerinde % 14 oranında gıda kaybı ve israfını olduğunu belirtmiştir. Bu nedenle gıda kaybı ve israfı gıda güvenliği, ekonomi ve çevre için ciddi bir tehdit olarak kabul edilmektedir (Abiad ve Meho, 2018). İnsan tüketimi için üretilen tüm gıdaların yaklaşık üçte biri (1,3 milyar ton yenilebilir gıda) her yıl tüm tedarik zincirinde kaybolmakta ve israf edilmektedir (Gustavsson ve ark., 2011). Bir bütün olarak toplum tarafından ödenen israfın sosyal ve çevresel maliyetlerine bakılmaksızın, bu gıda kaybı ve israfı miktarının parasal değerinin yaklaşık 936 milyar ABD Doları olduğu tahmin edilmektedir (FAO, 2009). Kayıp ve israf miktarı, dünya nüfusunun sekizde birini yetersiz beslenmeden kurtarmak (Gustavsson ve ark., 2011) ve 2050 yılına kadar mevcut talebin yaklaşık %150-170'ine ulaşabilecek olan artan gıda talebini karşılamak için küresel zorluğu ele almak için yeterli olarak görülmektedir (FAO, 2014).

Gıda kayıp ve israf miktarı, gelir düzeyi, kentleşme ve ekonomik büyümeden etkilenmekte, bu nedenle ülkeler arasında değişiklik göstermektedir (Chalak ve ark., 2016). Daha az gelişmiş ülkelerde, gıda kaybı ve israfı küresel kayıp ve israfın yaklaşık % 44'ünü oluşturan hasat sonrası ve işleme aşamasında meydana gelmektedir (Gustavsson ve ark., 2011; Lipinski ve ark., 2013). Bunun nedeni kötü uygulamalar, teknik ve teknolojik yetersizlikler, işgücü ve finansal kısıtlamalar, nakliye ve depolama için uygun altyapı eksikliği olduğu belirtilmektedir (Gustavsson ve ark., 2011).

Avrupa, Kuzey Amerika ve Okyanusya ülkeleri dâhil olmak üzere gelişmiş ülkeler ve sanayileşmiş Japonya, Güney Kore ve Çin ülkeleri dünya gıda kayıp ve israfının % 56'sını üretmektedir (Lipinski ve ark., 2013). Bunun, gelişmiş ülkelerdeki gıda kayıpları ve israfı %40'ı, çoğunlukla tüketici davranışları, değerleri ve tutumları (Bond ve ark., 2013) tarafından yönlendirilen tüketim aşamasında meydana gelir (FAO, 2009). Gıda israfının büyük bir kısmı, kötü planlama ve toplu satın alma ile ilişkili olabilecek aşırı alışverişin bir sonucu olarak hazırlama, pişirme veya servis işlemlerinden sonra ve son kullanma tarihinden önce tüketilmemesinden kaynaklanmaktadır (Bond ve ark., 2013; Priefer ve ark., 2016). Sanayileşmiş ülkelerdeki yaklaşık 222 milyon ton olan gıda atığı miktarı, gıda sıkıntısı çeken Sahra Altı Afrika ülkelerindeki toplam net üretime (230 milyon ton) neredeyse eşit olduğu belirtilmiştir (Gustavsson ve ark., 2011). Gıda kayıp ve israfı, insan tüketimi için gıdanın mevcudiyetini azalttığı için beslenme güvensizliği açısından kritik bir endişe kaynağıdır. Gıda kayıp ve israfının ayrıca ciddi çevresel, ekonomik, yoksulluk ve doğal kaynak etkileri önemli etkileri bulunmaktadır (Bond ve ark., 2013). Gıda kaybı sonucu oluşan atıklar depolama alanlarına atıldığında, gıda kayıplarının önemli bir kısmı sera gazına (GHG) ve karbondioksitten 25 kat daha fazla küresel ısınma potansiyeline sahip metana dönüştürülmektedir (Parry ve ark., 2007). Gıda kayıpları, daha yüksek bir metan verimi ile o

alanda biyojenik sekestrasyona herhangi bir katkı sağlamadan, diğer depolama alanlarından daha hızlı ayrışmaktadır (Levis ve Barlaz, 2011).
Rutten (2013)'e göre, gıda kayıp ve tarım sektöründe harcanan yatırımı temsil eder ve toprak, iş gücü, su, gübre ve enerji gibi girdi yönlerinde önemli verimsizlikler yaratmaktadır. Birkaç çalışma, gelişmiş ülkelerdeki gıda kayıp ve israf miktarlarını azaltma girişimlerinin gelişmekte olan ülkelerde gıda fiyatlarını azaltabileceğini (Rutten, 2013), tedarik zincirlerinde verimliliği artırabileceğini ve gıda yetersizliği çekenleri beslemek için kullanılabilecek kaynakları koruyabileceğini göstermiştir (Buzby ve ark., 2013). Bu tür çalışmalarla yapılan değişiklikler, savunmasız haneler için besleyici gıdalara erişimin iyileştirilmesine yol açabilecektir (Gustavsson ve ark., 2011). 2000'li yıllarla birlikte gelişen teknoloji ve tarımda karar verici destek yazılımların kullanılmaya başlanması ve benzeri araştırmaların yayınlarındaki artış önemli bir fayda sağlayacağını göstermektedir. Bu nedenle bu çalışmada gıda tedarik zincirinin aşamalarında veya bir bütün olarak gıda kayıp ve israfının ana etkenleri incelemiş ve karar destek verici bir mekanizma olarak geliştirilen yazılım projesi tanıtılmıştır.

1.1. Gıda Kaybı ve İsrafı

Gıda kayıpları, tedarik zincirinin özellikle insan tüketimi için yenilebilir gıdaya yol açan kısmı boyunca yenilebilir gıda kütlesindeki azalmayı ifade etmektedir. Gıda kayıpları, gıda tedarik zincirinde ürün hasadı, hasat sonrası ve işleme aşamalarında meydana gelmektedir (Parfitt ve diğerleri, 2010). Gıda zincirinin sonunda (perakende ve nihai tüketim) meydana gelen gıda kayıpları ise perakendecilerin ve tüketicilerin davranışlarıyla ilgili olarak "gıda israfı" olarak tanımlanmaktadır (Parfitt ve diğerleri, 2010). "Gıda" israfı veya kaybı, yem ve yenilebilir olmayan ürün parçaları hariç, yalnızca insan tüketimine yönelik ürünler için ölçülmektedir. Tanım gereği, gıda kayıpları veya israfı, gıda zincirlerinin "insan tüketimine giden yenilebilir ürünlere" yol açan kısmında kaybolan veya israf edilen gıda kütleleridir (FAO, 2011). Bu nedenle, başlangıçta insan tüketimine yönelik olan ancak tesadüfen insan besin zincirinden çıkan yiyecekler, daha sonra gıda dışı bir kullanıma (yem, biyoenerji vb. gibi) yönlendirilse bile gıda kaybı veya israfı olarak kabul edilmektedir. Bu yaklaşım, "planlı" gıda dışı kullanımları, burada kayıplar altında muhasebeleştirilen "plansız" gıda dışı kullanımlardan tamamen ayırmaktadır.

1.2. Gıda Kaybı ve İsrafının Miktarı

Birleşmiş Milletler ve Gıda ve Tarım Örgütü'ne (FAO) göre, dünya çapında üretilen gıdanın yaklaşık % 14'ü hasat ve perakende satış arasında kaybolmakta, perakende ve tüketim düzeyinde de önemli miktarlarda israf edildiği de belirtilmiştir (Abiad ve Meho, 2018). UNEP'e göre, dünya hali hazırda gezegendeki herkesi beslemeye yetecek kadar gıda üretildiğini belirtmiş ve yakın tarihli Gıda İsrafı Endeksi Raporu'na göre toplamda gıdanın % 17'sinden fazlasının israf edildiği ortaya konmuştur (Zhongming ve ark., 2021) FAO (2014)'e göre, gıda israfının küresel hacminin 1,6 milyar ton "birincil ürün eşdeğerleri" olduğu tahmin edilmektedir. Bunun yenilebilir kısmı için toplam gıda israfı 1,3 milyar ton olarak belirtilmektedir (FAO, 2014).

1.3. Gıda Kaybı ve İsrafının Çevresel Etkileri

Gıdadaki bu israfın gıda tüketimi ve maliyet kayıplarının yanı sıra çevre üzerinde ciddi bir etkisi olduğu belirtilmektedir. Gıda israfının karbon ayak izinin yılda atmosfere salınan 3,3 milyar ton CO_2 eşdeğeri sera gazı olduğu tahmin edilmektedir. Kaybolan veya israf edilen gıdaları üretmek için her yıl kullanılan toplam su hacmi 250 km^3'tür (Cattaneo ve ark., 2021). Bunun yanı sıra her yıl 1,4 milyar hektar arazi (dünyanın tarım alanının % 28'i) kaybolan veya israf edilen gıdayı üretmek için kullanılmaktadır (FAO, 2014). Tarım, Uluslararası Doğayı Koruma Birliği (IUCN) tarafından izlenen risk altındaki bitki ve hayvan türlerine yönelik tehditlerin çoğundan da sorumlu tutulmaktadır (Harfoot ve ark., 2021). Tüm gıda israfının düşük bir yüzdesi kompost hale getirilmekte ya da çoğu çöplüklerde belediye katı atığının büyük bir bölümünü oluşturmaktadır. Düzenli depolama alanlarından kaynaklanan metan emisyonları aynı zamanda atık sektöründen kaynaklanan en büyük sera gazı emisyonu kaynaklarından birini de temsil oluşturmaktadır (Schott ve ark. 2016).

1.4. Karar Destek Mekanizmasına İhtiyaç

Türkiye İsrafı Önleme Vakfı (TİÖV)'nın 2017 yılında yayınladığı bir rapora göre Türkiye'de bir yılda yetişen 49 milyon ton meyve ve sebzenin %25-40'nın heba olduğunu, hasat ve hasat sonrası uygulamaların yetersizliğinden kaynaklanan miktar ve kalite kaybının parasal karşılığı olarak 214 milyar Türk Lirası kaydedildiğini belirtilmiştir. Gıda maddeleri hasat sonrası depolamak zahmetli ve yüksek maliyetlidir. Hasat zamanı gelen ürünleri hasat etmeden bekletmek ise mümkün değildir. Hasat zamanı dalında bekleyemeyen ürünleri hızla değerlendirmek ise bir çiftçinin kendi başına çözüme ulaştırabileceği bir sorun olarak görünmemektedir. Aynı şekilde plansız bir şekilde ortaya çıkmış bir gıda hammaddesi fırsatını değerlendirecek kaynakları planlamak da gıda profesyonellerinin tercih ettiği bir yöntem değildir. Bunlar; üretici ciddi emek, zaman ve maddi kayıplara neden olmaktadır. Ürünler hasat edilmez ise dökülmeye başlamakta ve tarlanın gelecek yılları içinde önemli bir zarar oluşturmaktadır. Piyasalardaki ani daralmalar nedeniyle talebin azalması, standartları sağlayamadığı için perakendecilerin tercih etmediği ürünler, çoğu zaman hasat maliyetlerini karşılayamadığı için hasat edilmeden bahçede bırakılmasının yanı sıra, farklı alıcılara düşük fiyatlarla satılmasına neden olmaktadır. Bunun yanı sıra üreticiler genellikle böyle durumda kararsız kalmakta ve alınan kararlarda genellikle zarardan kar etme mantığı gütmektedir. Bu nedenle üreticilerin hasat ve hasat sonrası süreçlerde tedarik zincirinin bilgilerini taşıyan ve üreticinin kararlarına destek sunacak bir mekanizmaya ihtiyaç duymaktadır.

2.1. Projenin Konusu ve Amacı

Projenin konusu kullanımı kolay bilgisayar yazılımları ve sistemleri ile kısa vadede riskleri önceden tahmin edilebilen, uzun vadede yaş sebze ve meyve karlılığı ve verimliliği artıracak, bitkisel üretimde kazanç getirecek bir çözümü kırsal alanda yaygınlaştırmayı sağlamaktır. Bu kapsamda üretilen hızlıca bozulabilecek gıda hammaddesi ürünlerin özellikle yaş sebze ve meyve piyasaların daralması ve/veya başka bir nedenle alıcı bulamaması halinde kayıp yaşanmasını önleyebilecek, tarımsal ürünlerin atığa dönüşmeden gıda ürününe dönüştürülmesini sağlayacak, üretici ve gıda tedarikçilerini bir araya getirecek, yapay zeka destekli bir yazılım geliştirilmesi hedeflenmiştir. Proje uygulaması ile spot gıda sektöründe mal alan satan ürettiren Gıda ticareti yapanlara (brokerlere) doğrudan hizmet verirken, gıda hammaddesine dönüştürülebilecek tarımsal ürünü olan çiftçilere ve üretim tesislerinde atıl kapasitesi bulunan gıda üretim işletmelerine (fabrikalar, atölyeler, kooperatif işlikleri ve tarımsal birlik tesisleri) dolaylı olarak hizmet vermeyi amaçlamaktadır.

2.2. Projenin Yazılımı Tasarımı

Hasat dönemine gelmiş ürünlerin hangi gıda ya da kozmetik ürünler için hammadde olacağını; hangi tesislerin bu ürünleri işlemek için âtıl kapasitelerinin bulunduğunu; bu tesislerde işlenecek bu ürünlerin hasat, taşıma, hammaddenin işlenmesi, ambalajlanması gibi gerekli süreçlerinin kaç paraya mal olabileceğini; bu süreçlerin risk faktörlerini alternatifli bir şekilde üye olan Spot Gıda Brokerlerine dakikalar içinde toparlayabilecek ve Spot Gıda Brokerinin alacağı karara göre tüm tarafları otomatik olarak bilgilendirecek bir karar destek yazılımıdır. Karar destek yazılımının işletme diyagramı Şekil 1'de sunulmuştur.

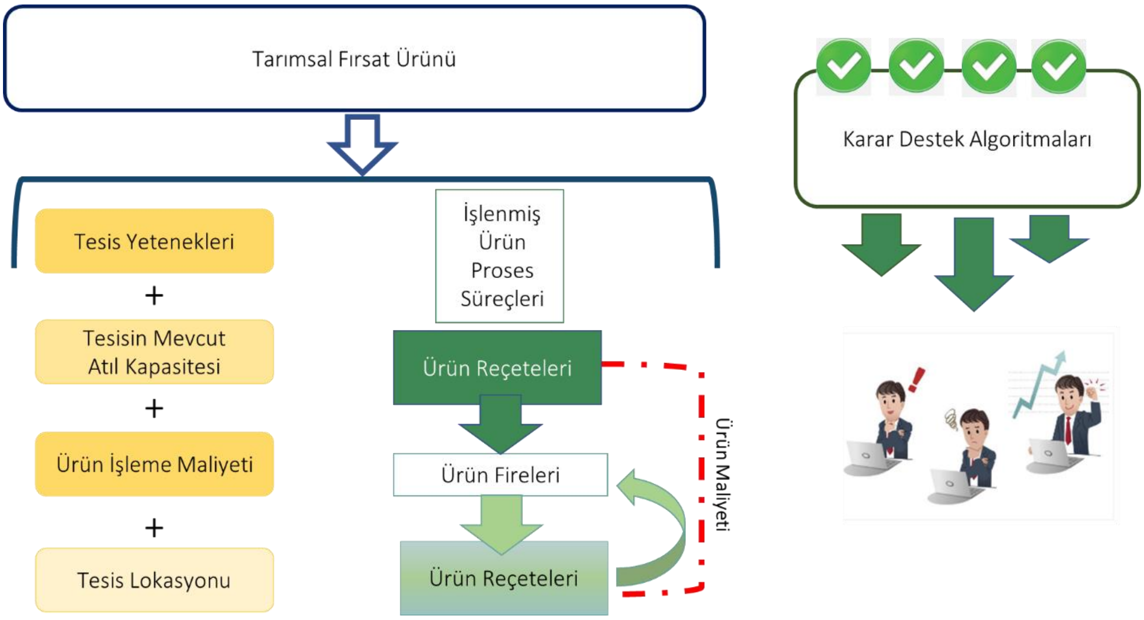

Şekil 1. Proje Yazılımı İşletme Diyagramı

Proje yazılımı, hasat döneminde fiyatı düşen, hasat edilmeden tarlada bırakılması düşünülen ürünlerin sisteme kayıt edilmesi sonrasında dakikalar içinde maliyet odaklı üretilebilecek ürünler, bu ürünlerin-üretim yerleri, nakliye fiyatlaması gibi değişik parametrelerde onlarca alternatif bulunan bir rapor oluşturacaktır. Bu raporun içeriğinde; ürünün özellikleri, amaca yönelik sertifika ve standardizasyona sahip bölgedeki tesislerin bir listesi ve süreç içerisindeki tüm maliyet başlıkları yer alacaktır. Gıda tedarikçisinin ürünü nasıl ve nerede işleyebileceği konusunda karar vermesine olanak sağlamasını hedeflediğimiz sistemde, süreçlerin her bölümünde uzman desteği ve gıda üretim danışmanlığı hizmetlerinin verilmesi öngörülmüştür. Bu sayede tüm taraflar yapılacak ticarette kendilerini maksimum güvende hissedebilmeleri hedeflenmektedir. Bu verilere sahip olan gıda brokerleri oluşturulan güvenli tedarik zinciri içinde üretim kararlarını verebilecek ve avantajlı fiyatlarla gıda üretimi yaptırabilecektir. Bunun doğal sonucu olarak hasat ve hasat sonrasında yaşanan kayıplar gıda ürününe dönüştürülürken, çeşitli nedenlerle (çoğunlukla yeterli sermayesi olmayan) atıl kapasitesi olan işletmeler, daha fazla üretim yapabileceklerdir. Bu durum işletmeler açısından verimlilik karlılık ve istihdam getirileceği düşünülmektedir.

2.3. Yazılım Çalışma Prensipleri ve Değer Zinciri

Projemiz yazılımı makine öğrenmesi temelli bir süreç kurgulamaktadır. Gelen sipariş veya fazla gıda sisteme veya çağrı merkezi kanalıyla alınmaktadır. Makine öğrenmesi süreçleri ürünün fayda parametrelerini ürün parametreleri ile eşleştirerek en optimal öneriyi sunar daha sonra sistem bir fiyat teklifi üreterek iletişim birimine aktarmaktadır. Gerekli sistem onayı ile birlikte gıdanın ihtiyaç duyulan alanlarda veya talep edilen alanlara yönlendirmekte, böylece tedarikçi veya üretici stok yetersizliğine nedeniyle veya ürünlerin bozulma durumuna göre ürünlerini zarar etmeden elden çıkarması sağlanmaktadır. Bu sistem zaman ve maliyet tasarrufu sağlayarak gıdanın atığa dönüşmesini engelleyeceği öngörülmüştür. Sistem ürün ve tesis kapasitesi dâhil olmak üzere bir matematiksel model çerçevesinde birçok parametreyi kullanmaktadır. Bu reçete ürünün işleme şartlarından bozulma sürecine kadar çoklu bilgi sunarak kayıp oranını azaltarak kazanç oranını artırmakta ve değer artışı sağlamaktadır.

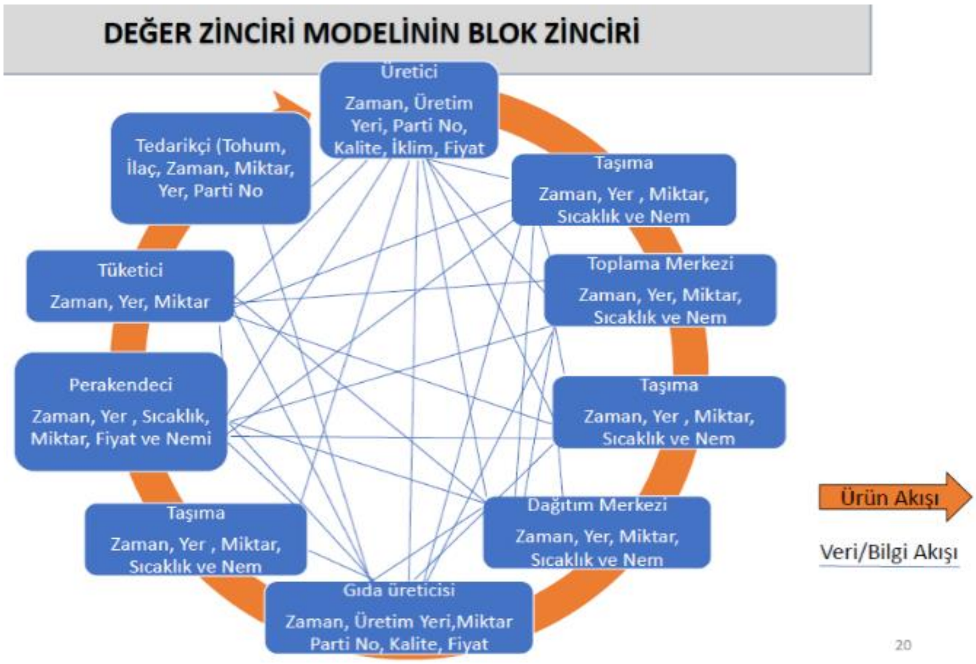

Şekil 2. Yazılım değer zincir modelinin blok zinciri.

Yazılım ortamının özellikle bir paylaşım platformu olarak kullanılması gıda tedarikçileri ile ürün üreten paydaşların kurumsal kaynak planlama süreçlerine destek olmakla birlikte küçük ve orta büyüklükte üreticiler için maliyet anlamında avantaj sağlamaktadır. Şekil 2'de görüldüğü gibi değer zinciri odaklı yaklaşımı ile bilgi akışı doğru ve tek elden sağlanarak şeffaflık gıda sistemindeki sorunlar ve birçok veri izlenebilmekte ve hızlı müdahalesi gerçekleşmektedir. Yazılım çalışmasında değer zincirinin modelinin blok zinciri Şekil 2'de sunulmaktadır.

2.3. Yazılımın Yenilikçi Yönü ve Teknolojik Düzeyi

Tedarik zincirinin her halkasının, oluşabilecek durumları önceden tahmin edebilen, hızlı karar aldırabilen alternatif bilgi ve donanıma sahip, risk ve sürprizlerden uzak, bir süreç yönetimine sahip olan bir iş ortağına sahip olmak istediği belirlenmiştir. Zamana karşı yarışmayı gerektiren yaş sebze meyve tedarik süreçlerini tamamen teknoloji tabanlı yönetebilecek bir Gıda Kurtarma Proje Yazılımı, coğrafyalar arasında çok hızlı hareket edebilme kabiliyetine sahiptir. Bölgesel bir aracının satmak istediği bir ürün için irtibatta olduğu birkaç üretim tesisi bulunuyorken, proje için tasarlanan yazılım yüzlerce tesisin uygun olan kapasiteleri, o tesislerde ürünün hangi forma dönüştürülebileceği, nakliye dâhil tüm giderlerin ne kadar olacağı gibi hesaplamalar dakikalar içinde yapabilecektir. Bu proje sayesinde, çok hızlı şekilde karar alabileceği bilgilere sahip olan spot gıda brokerinin üretime başlaması sağlanırken, üreticinin emekle ürettiği ürünlerin zayi olması önlenebilecektir.

Proje kapsamındaki girişim, spot gıda sektöründe mal alan, satan, ürettiren gıda ticareti yapanlara doğrudan hizmet verirken, gıda hammaddesine dönüştürülebilecek tarımsal ürünü olan çiftçilere ve üretim tesislerinde atıl kapasitesi bulunan gıda üretim işletmelerine (fabrikalar, atölyeler, kooperatif işlikleri ve tarımsal birlik tesisleri) dolaylı olarak hizmet vermeyi amaçlanmıştır. Spot gıda brokerlarını spot gıdanın işleneceği amaca uygun sertifikaya sahip gıda işleme tesislerine kolayca erişim sağlayarak, tüm süreç boyunca ihtiyaca yönelik hizmet alabilecektir. Çiftçiler/Üreticilerin ürünlerini tedarikçileriyle buluşturacak sistemimizde, spot gıda alıcıları sunulan seçenekler arasından ihtiyacına yönelik seçimi yapabilecek ve spot gıda fırsatlarını hızlı bir şekilde değerlendirilebilecektir. Danışmanlık sistemini farklı kılan, dakikalar içinde olası tüm senaryoları değerlendirebilen bir karar destek yazılımı ve çoklu dil yapısı ile birçok ülkede hizmet verebilecek yapıya kavuşabilecek olanaklar barındırmaktadır.

Projede tasarlanan yapay zekâ destekli proje yazılımı ile karar verme mekanizmasına dayanan hataların minimuma indirilmesi, geliştirilen kapalı devre (finansal güvenlik) gıda brokerliği pazar yeri ile çok geniş coğrafyalarda ürünlerin talep görmesi amaçlanmıştır. Proje yazılımı, tarımsal tedarik zincirindeki tüm paydaşları bir araya getirerek daha bilinçli karar vermelerine gereksiz evrak işlerini ortadan kaldırmalarına, tedarik zinciri verimsizliğini ve riskini azaltmalarına, karlılığı arttırmaya olanak tanıyan bir yazılım platformu olma özelliğine sahip olup ve birçok özelliği ile girişimimizle kesişen kümesi bulunmaktadır. Ancak proje yazılımı, atığa dönüşmek üzere olan tarımsal ürünlerin karar destek sistemi ve danışmanlık yönlendirmeleri ile gıda ve kozmetik ürüne dönüştürülmesine odaklanması açısından farklılıklar barındırmaktadır.

3. SONUÇ

Gıda tedarik zincirindeki tüm halkaların, sektörel farklılıklara rağmen geleneksel yöntemlerle hareket ettiği ve değişen dinamiklere uyum sağlamakta oldukça zorlandığı bilinmektedir. Bunun sonucu olarak 20 yıl ve üzeri ismini koruyabilen gıda firması sayısı oldukça azdır. Üstelik bu durum iç piyasada sıkıntı yaratırken, dış piyasada da tedarikçi prestijimizi düşürmektedir. Gıda üretim firmaları yerel aracılar üzerinden hammadde tedariki yapmaktadır. Yerel aracılar ise çiftçilere fiyat teklif etmektedir, ancak bu teklifler genellikle piyasa fiyatının çok altında değerlerde gerçekleşmektedir. Gıda üreticileri, aracılar için maksimum karlılıkta bir üretim zinciri olarak görünse de, tarımsal üreticinin ezildiği sistem, tedarik zincirinin en önemli halkalarının birbirine güvensizliği sonucunu doğurmaktadır. Güvensizlik içinde kalan üretici hem ekonomik kaygılar hem de güvensiz ortam nedeniyle üretimden vazgeçmektedir. Bunun yanı sıra her yıl gıda kayıp ve israfı bu durumun en önemli tetikleyici olmaktadır. Tedarik zincirinin her halkasının, oluşabilecek durumları önceden tahmin edebilen hızlı karar aldırabilen alternatif bilgi ve donanıma sahip, risk ve sürprizlerden uzak, bir süreç yönetimine sahip olan bir karar destek mekanizmasına ihtiyacı olduğu belirlenmiştir.

Tüm bu tespitler, kurulacak işin özellikle ilk yıllarında gereksiz ve yıpratıcı rekabet koşullarından uzakta, kendi büyümesi ve gelişmesi için olağanüstü fırsatlar olarak değerlendirilmektedir. Bu proje kapsamındaki girişim, gıda tedarik zincirinin tüm halkalarını kapsayıcı niteliktedir. Hasat ve hasat sonrası kayıpların değerlendirilerek önlenmesine odaklandığından, yazılım kapsamında arz fazlası olan ürün ve sezon odaklı bir iş modeli geliştirilmesi planlanmıştır. Türkiye'nin farklı illerinde birçok gıda üretim tesisi yöneticisi ile yapılan ön görüşmelerde Türkiye'deki gıda işleme tesislerinin her yıl ortalama minimum %25 atıl kapasiteyle çalıştığı bilgisine erişilmiştir. Bu sonuç literatürdeki çalışmalarla da paralellik taşımaktadır (FAO, 2014; TİÖV, 2017). Gıda tesislerinin depolama, ambalajlama ve taşıma sırasında kalite kaybına uğrayan ürünleri imha etmek yerine ürünleri gıda sanayide kullanılabilir hale getirmek için tesislerin üretim sürecini değiştirmeyecek her türlü imalatı fason olarak yapma konusunu değerlendirebilecekleri bilgisine ulaşılmıştır. Bu proje yazılımı ile birlikte üreticilere, tedarikçilere eş zamanlı bilgi alışverişi sağlanacak, ek istihdam kaynağı yaratırken işletmelerinin karlılıkları artırılacaktır.

Üretilen gıda hammaddesi ürünlerin, özellikle yaş sebze ve meyvelerin- piyasaların daralması ve/veya başka bir nedenle alıcı bulamaması halinde kayıp yaşanmasını önleyebilecek teknoloji destekli spot gıda üretim danışmanlığı sağlayacak bir yazılım geliştirilmesi her yıl Türkiye'de üretilen 52 milyon ton yaş sebze meyvenin yaklaşık %25-30 unun hasat sırasında ya da sonrası kayba uğramasını engelleyeceği düşünülmektedir.

KAYNAKLAR

ABIAD, M. G., ve MEHO, L. I. (2018). Food loss and food waste research in the Arab world: A systematic review. *Food security, 10*(2), 311-322.

BOND, M., MEACHAM, T., BHUNNOO, R., ve BENTON, T. (2013). *Food waste within global food systems*. Swindon, UK: Global Food Security.

BUZBY, J. C., ve HYMAN, J. (2012). Total and per capita value of food loss in the United States. *Food policy*, *37*(5), 561-570.

CATTANEO, A., FEDERIGHI, G., ve VAZ, S. (2021). The environmental impact of reducing food loss and waste: A critical assessment. *Food Policy*, *98*, 101890.

CHALAK, A., ABOU-DAHER, C., CHAABAN, J., ve ABİAD, M. G. (2016). The global economic and regulatory determinants of household food waste generation: A cross-country analysis. *Waste management*, *48*, 418-422.

FAO. (2014) Food Wastage Footprint: Full-Cost Accounting, Final Report; FAO: Rome, Italy.

FAO. (2009). How to Feed the World in 2050. Popul. Dev. Rev., 35, 837–839.

GUSTAVSSON, J., CEDERBERG, C., SONESSON, U., VAN OTTERDİJK, R., ve MEYBECK, A. (2011). Global food losses and food waste. FAO and Swedish Institute for Food and Biotechnology (SIK), Gothenburg, Sweden.

HARFOOT, M. B., JOHNSTON, A., BALMFORD, A., BURGESS, N. D., BUTCHART, S. H., DİAS, M. P., ve GELDMANN, J. (2021). Using the IUCN Red List to map threats to terrestrial vertebrates at global scale. *Nature ecology ve evolution*, *5*(11), 1510-1519.

LEVİS, J. W., ve BARLAZ, M. A. (2011). What is the most environmentally beneficial way to treat commercial food waste?. *Environmental science ve technology*, *45*(17), 7438-7444.

LİPİNSKİ, B., HANSON, C., WAİTE, R., SEARCHİNGER, T., ve LOMAX, J. (2013). Reducing food loss and waste. UNEP Working Paper, WSI.

PARRY, M. L., CANZİANİ, O., PALUTİKOF, J., VAN DER LİNDEN, P., ve HANSON, C. (2007). *Climate change 2007-impacts, adaptation and vulnerability: Working group II contribution to the fourth assessment report of the IPCC* (Vol. 4). Cambridge University Press.

PRİEFER, C., JÖRİSSEN, J., ve BRÄUTİGAM, K. R. (2016). Food waste prevention in Europe–A cause-driven approach to identify the most relevant leverage points for action. *Resources, Conservation and Recycling*, *109*, 155-165.

RUTTEN, M. M. (2013). The economic impacts of (reducing) food waste and losses: A graphical exposition. WASS Working Paper.

SCHOTT, A. B. S., WENZEL, H., ve LA COUR JANSEN, J. (2016). Identification of decisive factors for greenhouse gas emissions in comparative life cycle assessments of food waste management–an analytical review. *Journal of Cleaner Production*, *119*, 13-24.

TİÖV. (2020). İsraf Raporu 2020. http://www.israf.org/sayfa/Turkiyede-Sayilarla-Israf/250 (Erişim Tarihi: 30.11.2022)

ZHONGMİNG, Z., LİNONG, L., XİAONA, Y., WANGQİANG, Z., ve WEİ, L. (2021). UNEP Food Waste Index Report 2021.

İKİ ALANLI ENTERKONNEKTE GÜÇ SİSTEMİNİN KARGA ARAMA ALGORİTMASI İLE SEKONDER FREKANS KONTROLÖR TASARIMI

Araş. Gör. Cenk ANDİÇ

İstanbul Teknik Üniversitesi / Elektrik-Elektronik Fakültesi / Elektrik Mühendisliği Bölümü

E-Posta: andic18@itu.edu.tr, ORCID: 0000-0003-1123-899X

Özet

Bu çalışma, iki bölgeli bir güç sisteminde Sekonder Frekans Kontrolü (SFK) için yeni bir yaklaşım sunmaktadır. SFK güç sistemlerinin frekans kararlılığının sağlanabilmesi için önemli bir kontrol işlemidir ve ayrıca otomatik üretim birimi olarak da bilinmektedir. Güç sistemlerinde SFK'nın yapılabilmesi için çeşitli kontrolör yöntemleri kullanılmaktadır. Bu çalışmada ise SFK için oransal - integral (PI) kontrolör tipi kullanılmaktadır ve PI kontrolörün kazanç parametreleri olan K_p ve K_i optimal değerlerini belirlemek için bir meta-sezgisel yöntem olan Karga Arama Algoritması (KAA) önerilmektedir. Önerilen KAA, termik üretim birimleri içeren iki alanlı enterkonnekte bir güç sisteminde test edilmiştir. Simülasyonun 3. saniyesinde 0.1 birim değerlik bir yük değişimi uygulanmıştır ve kontrolörün bu yük değişimine karşı frekansı sabit tutabilme performansı incelenmiştir. Elde edilen sonuçlar geleneksel yöntem olarak bilinen Genetik Algoritma ve Ziegler-Nichols sonuçları ile karşılaştırılmıştır. Sonuçlar, önerilen KAA'nın diğer yöntemlere göre daha kısa oturma süresine ve daha az aşma değerine sahip olduğunu göstermektedir.

Anahtar Kelimeler: Sekonder Frekans Kontrolü, PI Kontrolör, Karga Arama Algoritması.

SECONDER FREQUENCY CONTROLLER DESIGN OF A TWO-AREA SYSTEM VIA CROW SEARCH ALGORITHM

Abstract

This paper presents a novel approach for Secondary Frequency Control (SFC) in a two-area power system. The SFC is an important control process to ensure frequency stability of power systems and also known as an automatic generation control. Various controller methods are used for the SFC in power systems. In this study, Proportional - Integral (PI) controller type is used for the SFC and a novel meta-heuristic method, the Crow Search Algorithm (CSA) is proposed to determine the optimal values of Kp and Ki, which are the gain parameters of the PI controller. The proposed CSA has been tested in a two-area interconnected power system with a thermal generator units. In the 3rd second of the simulation, a load change of 0.1 per unit was applied in Area-2 and the frequency stabilization performance of the controller against this load disturbance was examined. The obtained results were compared with the Genetic Algorithm and Ziegler-Nichols results known as the traditional method. The results show that the proposed CSA method has a shorter settling time and less overshoot than other methods.

Keywords: Seconder Frequency Controller, PI Controller, Crow Search Algorithm.

1. GİRİŞ

Güç sistemlerinde elektrik enerjisi kalitesi için sistemin frekans ve gerilim değeri kabul görülen sınır aralığında olması gereklidir. Sistemin frekans ve gerilim değeri ise sistemdeki yüklerin dinamik bir yapıya sahip olmasından dolayı etkilenmektedir. Sistemdeki üretim birimlerinin üretmiş oldukları güç miktarları ya da talep edilen yük değerindeki değişimler sistemin aktif güç dengesini bozacaktır ve sistem frekansının nominal değerinden sapmasına neden olacaktır. Bu sebeple, sistemin bir bozucu etki sonrasında frekans ve gerilim kararlılığını koruyabilmek için kontrolörlere ihtiyaç duyulmaktadır.

Sistem frekansının nominal frekans değerinden sapması sonucu bir alan kontrol hatası oluşmaktadır ve bu hata değerinin sıfırlanması için sekonder frekans kontrolü işlemi yapılmaktadır. Sekonder frekans kontrolü için çeşitli kontrolör yöntemleri kullanılmaktadır. Örneğin basit bir yapıya sahip olan PI ya da PID kontrolörler kullanılmaktadır. PI ya da PID kontrolörlerin kazanç parametrelerinin optimal değerlerini belirlemek için Ziegler-Nichols (ZN) gibi geleneksel yöntemler kullanılmaktadır (Mallesham ve ark., 2011). Ancak sistemin büyümesi ve karmaşık bir hal almasıyla birlikte bu yöntemlerin optimal değerleri bulması zorlaşmaktadır (Canol ve ark., 2022). Bu durumda, sezgisel yöntemlere dayalı yöntemler geliştirilmektedir (Andic, 2022). Genetik Algoritma (GA) kullanılarak PI kontrolörün parametresi ayarlaması yapılmıştır (Abdel-Magid ve ark., 1995). Parçacık Sürüsü Optimizasyon (PSO) yöntemi kullanılarak PI kontrolörün parametreleri ayarlanmıştır (Shayeghi ve ark., 2008). Yeni sezgisel yöntemlerden biri olan Bal Porsuğu Algoritması (BPA) (Andic ve ark., 2022) ile PI kontrolörün parametreleri ayarlanmıştır.

Bu çalışmada ise iki alanlı enterkonnekte güç sistemlerinde sekonder frekans kontrolü için doğadan esinlenilmiş yeni bir meta-sezgisel yöntem olan Karga Arama Algoritma (KAA) tabanlı PI kontrolör önerilmektedir. Önerilen KAA-tabanlı PI kontrolörün yük değişim cevapları, GA ve ZN ile karşılaştırılmıştır.

2. SEKONDER FREKANS KONTROLÜ

Güç sistemlerinde senkron jeneratörün uç gerilim değeri ile reaktif güç değeri ve frekans değeri ile aktif güç değeri arasında bir ilişki vardır (Andic ve ark., 2022). Bu durumda, sistemdeki aktif güç talebinin değişim göstermesi sistemin frekansını değiştirmektedir. Sistemin frekans kararlılığını koruyabilmek için kontrolöre ihtiyaç duyulmaktadır. Herhangi bir yük değişimi sonrası sistemin frekansını koruyabilmek için primer frekans kontrolü, sekonder frekans kontrolü veya tersiyer frekans kontrolü işlemleri uygulanmaktadır. Primer frekans kontrolde talep edilen güç değeri ve üretilen güç değerleri birbirlerine eşitlenirken, frekansta üretim birimlerinin frekans düşülerine bağlı olarak bir miktar kayma olmaktadır. Sekonder frekans kontrolü ise, primer frekans kontrolünde oluşan bu frekans kayma hatasını düzelmektedir. Sekonder frekans kontrolü, sistemin frekansını düzeltebilmek için enterkonnekte sistemde yer alan alanlardaki üretim ve tüketimi dengeye getirmeye çalışmaktadır. Sekonder frekans kontrolünde, primer frekans kontrolüne ek olarak Alan Kontrol Hatası (Area Control Error – ACE) sinyali oluşmaktadır. Enterkonnekte bir güç sisteminin primer ve sekonder frekans kontrolü Şekil 1'de gösterilmiştir.

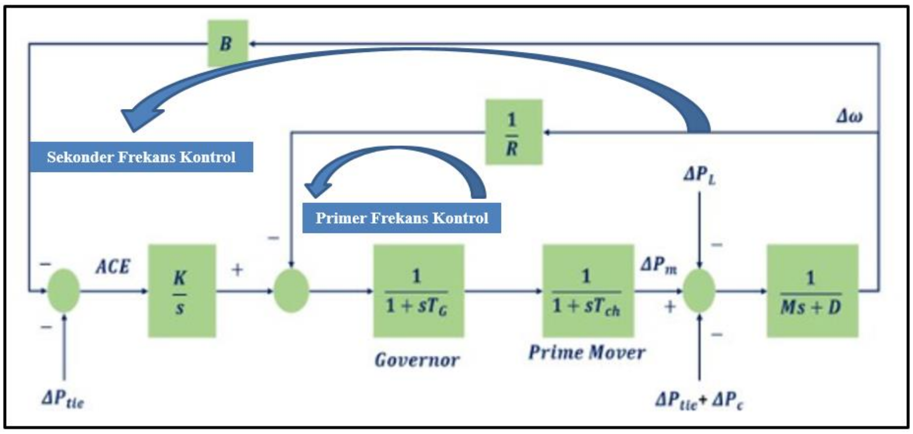

Şekil 1. Primer ve sekonder frekans kontrolü.

Sekonder frekans kontrolü işleminde, frekansın nominal değerinden farklı bir değer alması sonucu oluşan ACE sinyalini sıfırlamak istenilmektedir. ACE sinyalinin denklemi aşağıdaki gibidir:

$$ACE = \Delta P_{12} + B.\Delta f \tag{1}$$

burada, ΔP_{12} enterkonnekte güç sisteminde Alan-1 ve Alan-2 arasındaki güç akışı değişimini temsil etmektedir, B generatörlerin frekans yönelim faktörüdür birimi MW/Hz'dir ve Δf yük değişimi sonucunda frekanstaki değişimi göstermektedir.

Bu çalışmada, frekans değişimi sonucu oluşan ACE sinyalini sıfırlamak için PI kontrolör kullanılmıştır.

3. KARGA ARAMA ALGORİTMASI

Doğadan esinlenen yeni bir meta-sezgisel yöntem olan Karga Arama Algoritması (KAA) Askarzadeh tarafından 2016 yılında önerilmiştir (Askarzadeh, 2016). KAA, kargaların yiyecek arama davranışlarından esinlenilmiş bir algoritmadır. Kargalar çok zeki bir kuş türüdür ve yiyecek aramaları ve saklamaları dikkatleri üzerine çekmiştir. Kargalar sürüler halinde yaşayan canlılardır. Kargalar buldukları yiyeceklerin fazlasını yuvalarında depolamaktadır. Kargalar birbirlerini takip eden, izleyen canlılardır ve yiyecek arama davranışlarını taklit etmekte hatta yiyecek-hırsızlığı yapmaktadır. Kargalar birbirlerini takip ederken takip edildiklerini fark edip etmediklerini belirleyen bir farkındalık olasılığı parametresi vardır. Bu parametre algoritmanın küresel arama kabiliyetini öne çıkarmaktadır (Andic ve ark., 2020). Kargaların arama uzayında yeni bir çözüm ararken yerel arama kabiliyetlerini ilgilendiren bir diğer parametre ise uçuş mesafesidir. Uçuş mesafesi parametresi ve farkındalık olasılığı parametresi sayesinde karga arama algoritması keşif ve sömürü adımlarını başarıyla gerçekleştirebilmektedir (Andic ve ark., 2022). Bu çalışmada ise enterkonnekte güç sisteminde sekonder frekans kontrolü için kullanılan PI kontrolörün kazanç parametrelerinin belirlemek için KAA önerilmektedir.

4. TEST SİSTEMİ

Önerilen KAA-tabanlı sekonder frekans kontrolör tasarımı iki alanlı enterkonnekte bir güç sistemi üzerinde test edilmiştir. İki alanlı enterkonnekte güç sisteminde her iki alanda da termik üretim birimi bulunmaktadır. Önerilen test sistemi MATLAB / Simulink benzetim programı üzerinde modellenmiştir. Modellenen sistem Şekil 3'te gösterilmektedir.

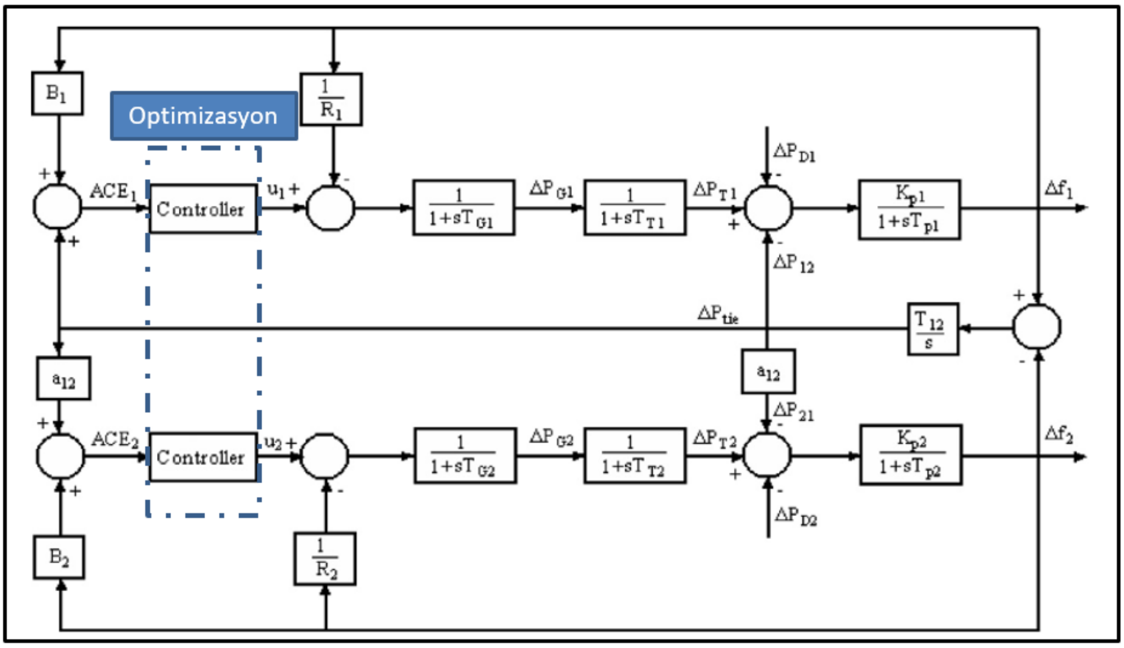

Şekil 3. İki alanlı enterkonnekte güç sisteminin modellenmesi.

Şekil 3'te, Alan-1'de termik üretim birimine ait generatör – türbin ve güç sisteminin transfer fonksiyon modellemesi sırasıyla belirtilmiştir. Alan-1'de uygulanacak herhangi bir yük değişimi ΔP_{D1} olarak gösterilmiştir ve alanlar arası yük değişimi ise ΔP_{12}olarak gösterilmiştir. Yük değişimi sonucu oluşan frekans değişimi ise kontrolör yardımı ile kontrol edilmektedir. Bu çalışmada PI kontrolör kullanılmıştır ve PI kontrolörün kazanç parametreleri olan K_p ve K_i parametrelerinin optimal değerlerini belirlemek için yeni bir meta-sezgisel yöntem olan Karga Arama Algoritması kullanılmıştır. Karga arama algoritması, arama uzayında PI kontrolör kazanç parametrelerinin optimal değerini ararken uyması gereken alt ve üst sınır aralığı vardır. Bu aralıklar aşağıdaki denklemde gösterilmiştir.

$$K_{P,min} \leq K_P \leq K_{P,max} \quad (2)$$

$$K_{I,min} \leq K_I \leq K_{I,max} \quad (3)$$

5. SİMÜLASYON SONUÇLARI

Şekil 3'te gösterilen test sisteminde, simülasyonun 3. saniyesinde Alan-1'de 0.1 pu'luk bir yük değişimi yapılmıştır. Bu değişimine karşı sistemin frekans değeri salınım göstermektedir ve kontrolör yardımıyla bu oluşan frekans salınımının en kısa sürede oturması istenilmektedir. Bu çalışmada kullanılan PI kontrolörün kazanç parametrelerinin optimal değerlerini belirlemek için Karga Arama Algoritması 30 kez koşturulmuştur. KAA'nın parametreleri ise şöyledir; karga sürüsü sayısı = 50, karga sayısı (arama uzayındaki çözüm adaylarını temsil etmektedir ve bu problemde optimal değerleri bulunulmak istenilen 4 değişken vardır) = 4, uçuş mesafesi = 2, farkındalık olasılığı = 0.3, değişkenlerim alt sınır değeri = -2.0, değişkenlerin üst sınır değeri = 2.0, maksimum iterasyon sayısı = 10.
Önerilen KAA'nın optimizasyon işleminden sonra bulmuş olduğu PI kontrolör kazanç parametre değerleri Tablo 1'de diğer yöntem sonuçları ile birlikte karşılaştırmalı olarak verilmiştir.

Tablo 1. PI kontrolörün optimal kazanç parametre sonuçları.

PI Kontrolörün Parametreleri	Yöntemler		
	Ziegler-Nichols	Genetik Algoritma	**Karga Arama Algoritması**
K_{P1}	-1.5755	-0.3958	-0.0966
K_{I1}	-0.2674	-0.0449	-0.0160
K_{P2}	-1.4288	-2.0000	-1.9962
K_{I2}	-0.6148	-0.9565	-0.9208
Maliyet Fonksiyonu (ITAE)	8.3242	5.1645	4.8502

Tablo 1'e göre önerilen KAA ile elde edilen PI kontrolör kazanç parametre değerleri -0.0966, -0.0160, -1.9962 ve -0.9208'dir ve görüldüğü üzere başta belirtilen alt ve üst sınır aralığına uymaktadır. Önerilen yöntemin performansını değerlendirebilmek için çeşitli yöntemler kullanılmaktadır. Bu çalışmada ise ITAE değeri dikkate alınmıştır ve bu değer sistemin maliyet fonksiyonunu temsil etmektedir ve minimize edilmesi istenilmektedir. Tablo 1'e göre, önerilen KAA-Tabanlı PI kontrolör sistemin parametrelerini en iyi şekilde optimize ederek en az ITAE değerine ulaşılmasını sağlamıştır.

Önerilen KAA-Tabanlı PI kontrolör, iki alanlı enterkonnekte güç sistemi üzerinde test edilmiştir ve simülasyonun 3. saniyesinde Alan-1'de 0.1 pu'luk bir yük değişimi uygulanmıştır. Böyle bir senaryo durumunda Alan-1'de oluşan frekans değişimi Şekil 4'te gösterilmiştir.

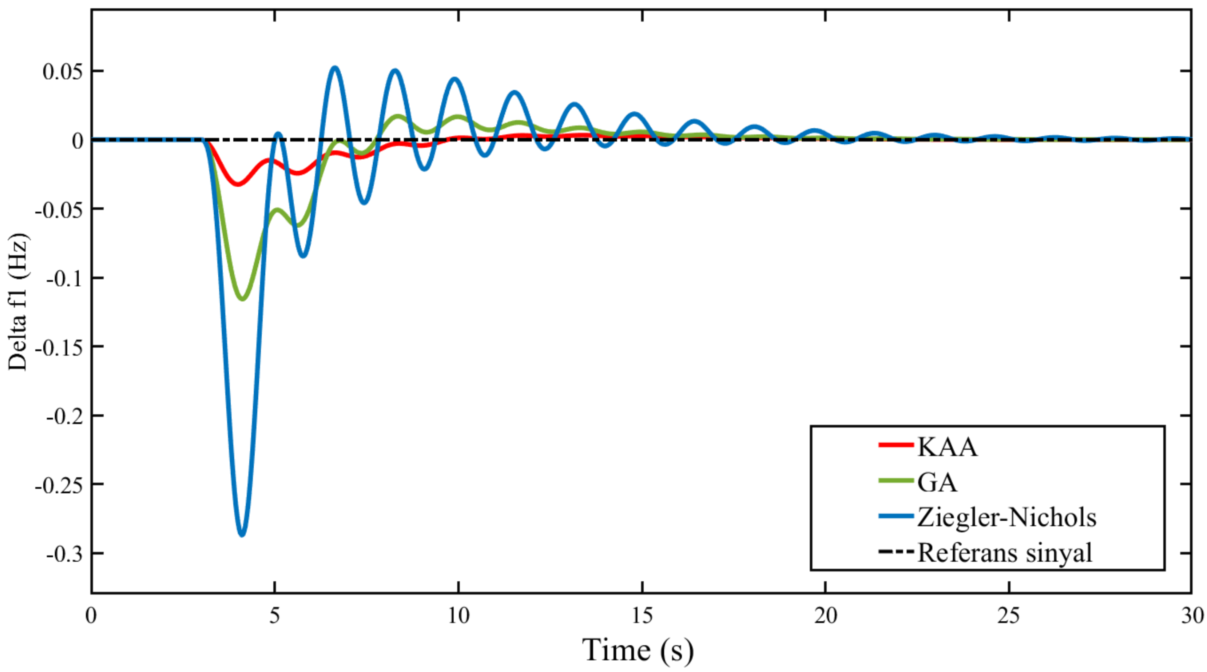

Şekil 4. Alan-1'deki frekans değişimi.

Şekil 4'de, yük değişimi sonrası Alan-1'deki frekans değişimi gösterilmiştir ve frekansın en az genliğe sahip olması ve en kısa sürede yük değişimi öncesindeki başlangıç durumuna dönebilmesi istenilmektedir. Şekil 4'de görüldüğü üzere, frekansın en az aşma değerine ve en kısa sürede oturduğu durum önerilen KAA-tabanlı PI kontrolör durumudur. Şekil 5'te ise Alan-2'deki frekans değişimi gösterilmiştir.

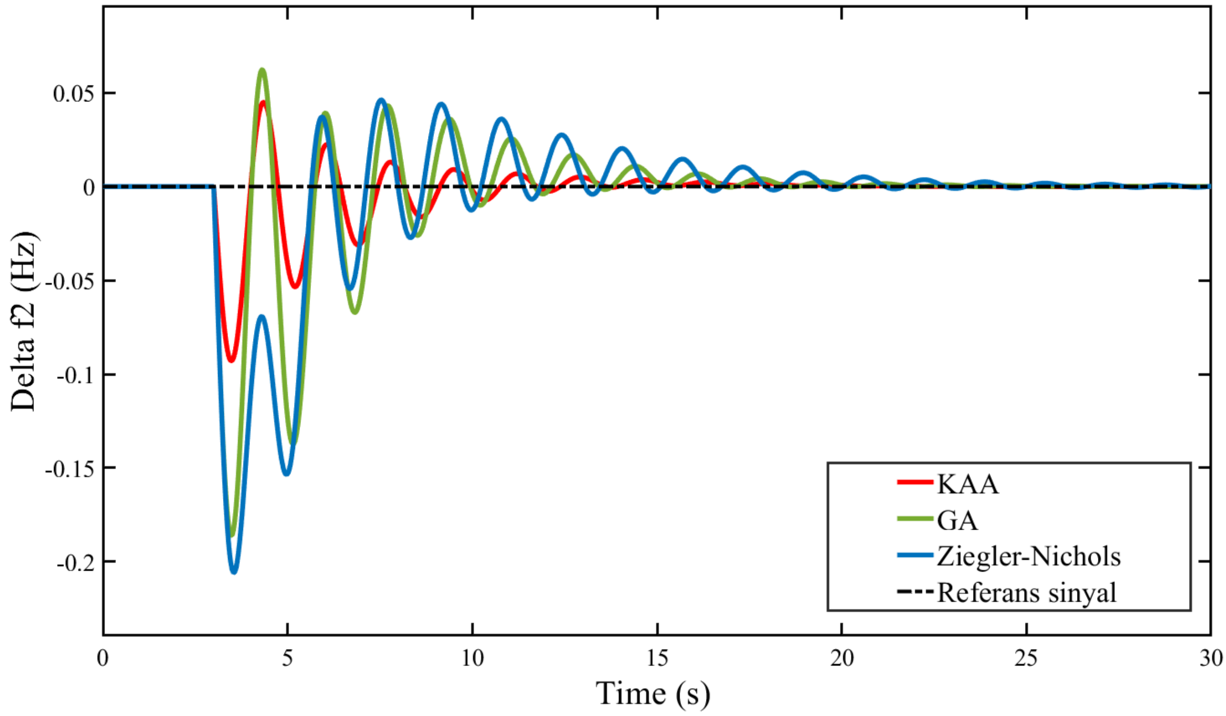

Şekil 5. Alan-2'deki frekans değişimi.

Şekil 5'te ise frekanstaki salınım önerilen KAA-tabanı kontrolör yardımıyla en kısa sürede oturduğu görülmektedir. Şekil 6'da alanlar arasındaki güç değişimi gösterilmektedir.

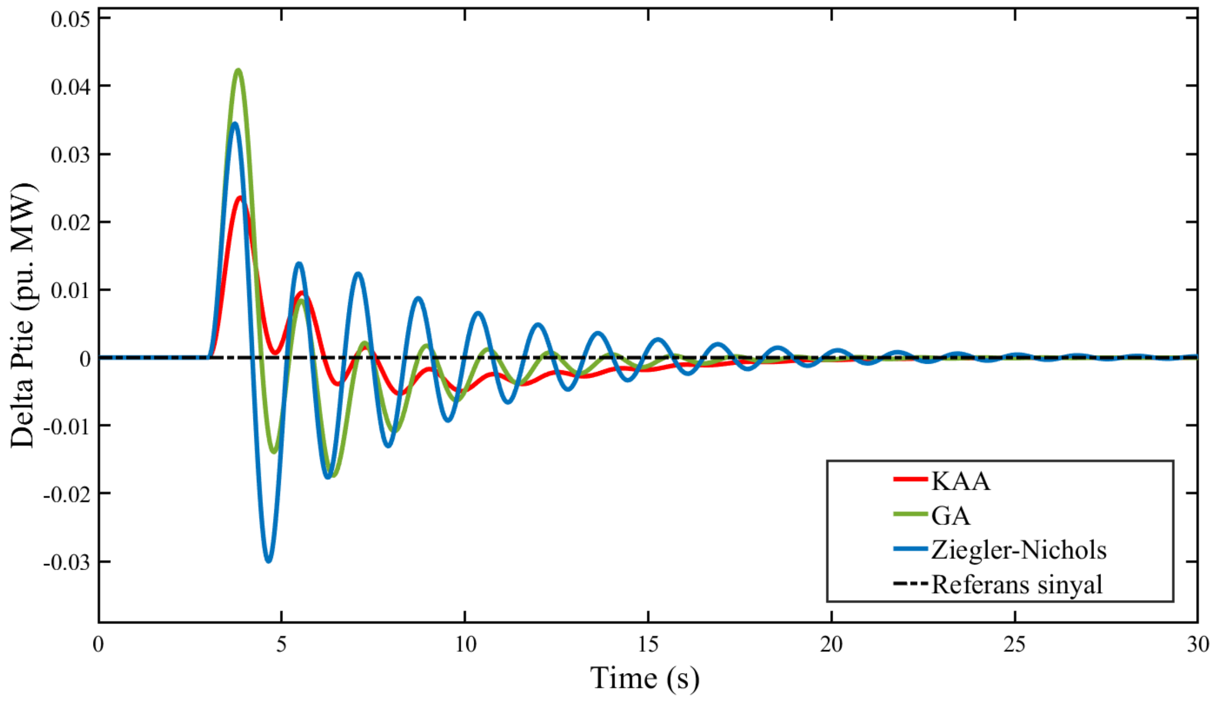

Şekil 6. Alanlar arasındaki güç değişimi.

Şekil 6'da, önerilen KAA-tabanlı kontrolörün yük değişimine karşı alanlar arasındaki güç değişimini çok etkilemende hızlı bir şekilde kontrol altına aldığı görülmektedir.

6. SONUÇLAR

Bu çalışmada iki alanlı enterkonnekte güç sisteminin sekonder frekans kontrolü KAA-tabanlı PI kontrolör önerilmiştir. Simülasyonun 3. saniyesinde Alan-1'de 0.1 pu'luk bir yük değişimi uygulanmıştır ve bu yük değişimine karşı frekansın hızlı bir şekilde nominal değerine getirilmesi istenilmektedir. Önerilen KAA-tabanlı PI kontrolör sonuçları ile Genetik Algoritma ve Ziegler-Nichols yöntem sonuçları karşılaştırılmıştır. Elde edilen sonuçlar, önerilen KAA-tabanlı kontrolörün diğer yöntemlere göre sistemin frekansını çok daha az aşma değeriyle birlikte çok daha kısa zamanda oturttuğu görülmektedir. Bu çalışma, güç sistemlerinde sekonder frekans kontrolü için önerilen KAA-tabanlı PI kontrolör yönteminin uygulanabileceğini göstermektedir.

KAYNAKLAR

Abdel-Magid, Y. L., & Dawoud, M. M. (1995). Genetic algorithms applications in load frequency control.

Andic, C., Ozturk, A., & Turkay, B. (2022). Rotor Angle Stability Analysis by Using Lyapunov's Direct Method of a SMIB Power System. In *2022 4th Global Power, Energy and Communication Conference (GPECOM)* (pp. 296-300). IEEE.

Andic, C., Ozumcan, S., Ozturk, A., & Turkay, B. (2022). Honey Badger Algorithm Based Tuning of PID Conroller for Load Frequency Control in Two-Area Power System Including Electric Vehicle Battery. In *2022 4th Global Power, Energy and Communication Conference (GPECOM)* (pp. 307-310). IEEE.

Andic, C., ÖZTÜRK, A., & Tosun, S. (2022). Dynamic Economic Dispatch with Valve-Point Effect Using Crow Search Algorithm. *Balkan Journal of Electrical and Computer Engineering*, *10*(3), 237-244.

ANDİÇ, C. (2022). YAPAY ZEKAYA TEMELLİ ENERJİ DEPOLAMA SİSTEMLERİ VE YENİLENEBİLİR ENERJİ KAYNAKLARININ ENTEGRASYONU. *TEKNOBİLİM-2022: Enerji Krizi ve Yenilenebilir Enerji*, 137.

ANDİÇ, C., ÖZTÜRK, A., & TOSUN, S. (2020). Türkiye'deki Güç Sisteminde Karga Arama Algoritması Kullanılarak Ekonomik Yük Dağıtımı. Düzce Üniversitesi Bilim ve Teknoloji Dergisi, 8(1), 428-436.

Askarzadeh, A. (2016). A novel metaheuristic method for solving constrained engineering optimization problems: crow search algorithm. *Computers & structures*, *169*, 1-12.

Canol, B., Andic, C., Purlu, M., & Turkay, B. E. (2022). Optimum Energy Management in Electric Vehicle Parking Lots Using Heuristic Methods. In *2022 4th Global Power, Energy and Communication Conference (GPECOM)* (pp. 473-477). IEEE.

Mallesham, G., Mishra, S., & Jha, A. N. (2011). Ziegler-Nichols based controller parameters tuning for load frequency control in a microgrid. In *2011 International conference on energy, automation and signal* (pp. 1-8). IEEE.

Shayeghi, H., Jalili, A., & Shayanfar, H. A. (2008). Multi-stage fuzzy load frequency control using PSO. *Energy conversion and management*, *49*(10), 2570-2580.

DISTANCE DEPENDENT PERFORMANCE OF MICROSTRIP PATCH ANTENNA FOR BREAST TUMOR DETECTION

Haluk Kırkgöz

Istanbul Technical University, Faculty of Electrical and Electronics, Department of Electronics and Communication Engineering

kirkgozh@itu.edu.tr, ORCID: 0000-0001-6870-2103

Assistant Professor Onur Kurt

Istanbul Technical University, Faculty of Electrical and Electronics, Department of Electronics and Communication Engineering

onurkurt@itu.edu.tr, ORCID: 0000-0002-4486-2257

Abstract

One of the most prevalent and dangerous diseases among women worldwide is breast cancer. The early identification of this disease is therefore crucial. However, typical methods for diagnosing breast cancer have some drawbacks. In order to overcome these disadvantages, microwave imaging methods have been developed. This study presents the design and modification of a rectangular microstrip patch antenna on an FR-4 substrate operating at 2.45 GHz in the ISM band for breast cancer detection. Both the proposed antenna and a five-layer breast phantom with and without a 5 mm-radius tumor were designed using CST software. To detect the presence of a tumor, distance dependent simulations were performed between the antenna and the breast phantom. The simulation outcomes revealed that the return loss, electric field, magnetic field, and surface current all change when a tumor is present in the breast phantom. Moreover, our results indicated that the antenna located 20 mm from the breast phantom can identify the tumor more efficiently compared to **the antenna located at** 40 mm. We also observed that the VSWR of the antenna is lower than 2, which is an acceptable limit for radiation. Due to its tumor detection capability and acceptable SAR values, our proposed antenna can be used as a sensor in biomedical applications.

Keywords: Microstrip Patch Antenna (MPA), Microwave Imaging (MWI), Breast Tumor, Breast Cancer Detection, Biomedical Applications.

1. INTRODUCTION

The diagnosis of breast cancer has been the subject of extensive research by many researchers in recent years, as breast cancer is the most common type of cancer among women (Slimi et al., 2019). Uncontrolled development of breast cells causes breast tumors. Although these developments are commonly referred to as breast tumors, not all of them are cancerous. Breast tumors can be classified into two types: benign and malignant. Malignant tumors are the only type of cancer. Malignant tumors can spread and develop rapidly, engulfing healthy cells and consuming their nutrients, blood, and space since tumor cells, like all other body cells, require blood and nutrients to survive. In addition, malignant tumors are called metastatic tumors when they spread to the rest of the body. On the other hand, benign tumors are referred to as tumors that do not infiltrate into neighboring tissues or spread to other parts of the body. Generally speaking, benign tumors are less dangerous than malignant ones. However, a benign tumor might still cause various issues in the breast by pressing on adjacent tissue (Dishali et al., 2019).

In both industrialized and developing nations, breast cancer affects women more often than other types of cancer. One in four of all tumors in women worldwide currently occurs as a result of breast cancer. In 140 of 184 countries around the globe, it is the most commonly diagnosed cancer in women. More than 2.3 million women received a breast cancer diagnosis in 2020, and 685,000 of them passed away.

According to research, a woman receives a breast cancer diagnosis every 14 seconds around the world (Breast Cancer Research Foundation, 1993). Due to a late diagnosis, women all over the world suffer from the effects of this disease. Therefore, early breast cancer tumor detection is crucial to providing the necessary, accurate, and effective treatment to increase the survival rate of women.

Tumor detection involves the use of various techniques such as X-ray mammography, ultrasound, computed tomography (CT) scan, magnetic resonance imaging (MRI) scan, biopsy, and others. These techniques are usually used at the stage where the tumor is located, and they are unable to identify malignant cells in the early stages. The drawbacks and limitations due to the side effects of these techniques, such as ionizing radiation in CT, long scan times in MRI, and contrast problems in ultrasound, have encouraged researchers to create a more efficient, inexpensive diagnostic technique to identify cancer (Al-Nahiun et al., 2021). For instance, the size of the tumor, the density of the breast tissue, and the expertise of the radiologist performing and interpreting the mammography may all affect a mammogram's ability to detect breast cancer.

In recent years, antenna technology has advanced far more quickly across all communication fields. A microstrip antenna currently plays a crucial role in the medical industry, in addition to its uses in other fields. The study of on-body antennas has applications in microwave imaging and medical diagnosis. The antenna is utilized in numerous medical applications, including cancer therapy, tumor identification, remote health monitoring, digestive monitoring, hyperthermia, and cancer treatment. It is anticipated that human body absorption and coupling will change significant antenna performance characteristics (Sukhija and Sarin, 2017). Antennas are frequently chosen for biomedical applications due to their versatile features, such as their non-ionizing nature, increased bandwidth, low profile, lightweight, flexibility, compact and lower dimensions, simple transportability, low cost, and ease of manufacture (Balanis, 2016).

It has been investigated how non-destructive microwave imaging systems based on radar can be used to diagnose cancer. A microwave imaging system for the detection of breast cancer comprises a transmitting antenna that sends electromagnetic waves to the breast and a receiving antenna that gathers the scattered waves. Information about the location, shape, size, and electrical characteristics of the tumor are all contained in scattered waves that have been received by the antenna. The received information is then analyzed with an appropriate signal processing technique. Due to the different water content between malignant cells and neighboring healthy tissues, electrical differences such as permeability and conductivity allow cancer to be identified by the antenna. Therefore, utilization of the antenna is an integral factor for microwave breast cancer detection (Mahalakshmi and Jeyakumar, 2012) (Suriya et al., 2018).

Microstrip patch antennas have been used extensively in research on the early diagnosis of breast cancer. In 2016, RamaDevi et al. designed a single-element rectangular microstrip antenna operating at 6 GHz for biomedical use in locating breast cancer tissues (RamaDevi et al., 2016). In 2016, Ali Kahwaji et al. presented a breast phantom simulation along with the design and modeling of a hexagonal microstrip antenna. By adding a hexagonal slot in the middle of the patch, it was possible to imitate an antenna with an impedance bandwidth of over 5 GHz (Kahwaji et al., 2016). In 2019, Marwa Slimi et al. introduced a CPW antenna design for microwave tumor cell identification. At 4.5 GHz, the simulation outcomes of the antenna performance in free space using CST-MWS are displayed (Slimi et al., 2019). In 2019, Sumita Shekhawat et al. proposed an antenna operating at 2.46 GHz in the frequency range (2.41-2.5 GHz) of the ISM band suitable for medical purposes (Shekhawat et al., 2019). In 2021, Donia N. Elsherif et al. also presented the design and modification of a rectangular microstrip patch antenna for breast cancer detection (Elsherif and Makkey, 2021).

In this paper, we report on the direct detection of breast tumors in breast phantoms using a microstrip patch antenna (MPA) operating in the ISM band. The Computer Simulation Technology (CST) Studio Suite is used to design and simulate the antenna and a biological breast phantom consisting of five tissue layers. The performance of the suggested antenna is assessed by contrasting changes in specific absorption rate (SAR), gain, electric field, directivity, VSWR, and reflection coefficient on a tumor-free and tumor-affected phantom positioned at different distances. According to simulation outcomes, our results reveal that the tumor can be detected in the breast phantom with our proposed antenna at different distances. Results from the antenna located 20 mm from the breast phantom containing the tumor outperform the results obtained at a distance of 40 mm.

2. MATERIALS AND METHODS

2.1 Microstrip Patch Antenna Design

The basic MPA structure consists of a rectangular patch, a feed line, a dielectric substrate, and a ground plane. Although an MPA has several benefits, such as smaller size and lower fabrication cost, its drawbacks include a limited frequency range, low power handling capability, low gain, and poor efficiency due to dielectric and conductor losses.

In this study, we designed a slotted MPA with an FR-4 substrate together with a breast phantom for tumor detection applications. The proposed MPA was simulated at a resonant frequency of 2.45 GHz under the ISM frequency band (2.4–2.5 GHz) in CST Studio Suite 2020.

Annealed copper material was used for the patch layer, feed line, and ground layer of the antenna since copper is readily available, a good conductor, relatively inexpensive, and a highly reactive material that is effective at dissipating electrical energy. The substrate layer of the antenna was made of lossy FR-4 material with dimensions of $65.4 \times 88.99 \times 1.6\ \mathrm{mm}^3$, a dielectric constant of 4.3, and a loss tangent of 0.025. The patch layer and ground layer of the antenna are each 0.035 mm thick. The total thickness of the proposed antenna is 1.67 mm.

The geometrical shape of the rectangular slotted MPA fed by a microstrip feed line is shown in Figure 1. The white color in Figure 1 represents the substrate, while the yellow color denotes the metallic parts. The inset-feeding method has been applied to the antenna, and the waveguide port for that feeding was placed at the bottom of the feeding line. With this kind of feed technique, the feeding port can be etched on the same substrate, producing a planar structure. Using the transmission-line circuit model, the design goal was to maintain a low return loss almost at the resonance frequency of 2.45 GHz (Balanis, 2016). A rectangular slot is cut in the middle of the rectangular patch, which helps to lower the reflection coefficient below -10 dB.

The width of the patch W, the effective dielectric constant ε_{reff}, the effective length L_{eff}, the extended incremental length on account of the fringing factor ΔL, the actual length of the patch L, the width of the ground plane W_g, and the length of the ground plane L_g for the proposed MPA can be calculated by the following equations:

$$W = \frac{c}{2f_0\sqrt{\frac{\varepsilon_r + 1}{2}}} \tag{1}$$

$$\varepsilon_{reff} = \frac{\varepsilon_r + 1}{2} + \frac{\varepsilon_r - 1}{2}\left(1 + 12\frac{h}{W}\right)^{-0.5} \tag{2}$$

$$L_{eff} = \frac{c}{2f_0\sqrt{\varepsilon_{reff}}} \tag{3}$$

$$\Delta L = 0.412\frac{\left(\frac{W}{h} + 0.264\right)\left(\varepsilon_{reff} + 0.3\right)}{\left(\frac{W}{h} + 0.813\right)\left(\varepsilon_{reff} - 0.258\right)} \tag{4}$$

$$L = L_{eff} - 2\Delta L \tag{5}$$

$$W_g = 2W \tag{6}$$

$$L_g = 2L \tag{7}$$

where c is the velocity of light in free space, f_0 is the operating or resonant frequency, ε_r is relative permitivity of the substrate, and h is the thickness of the substrate. As can be seen, the physical dimension of the antenna is electrically shorter than the patch of the antenna due to the fringing factor. Therefore, the fringing factor was subtracted from the effective length in order to determine the patch's actual length.

The theoretically calculated values must be adjusted in order to attain our target resonant frequency because they are insufficient to fulfill our goal for the design. Using the CST Studio Suite parametric sweep optimization tool, several of the design parameters were optimized. The suitable simulation measurements were chosen in order to check for antenna design purposes. The appropriate and optimized design parameters in the millimeter range for the suggested antenna are summarized in Table 1.

Table 1. The Proposed Antenna Dimensions in Free Space

Parameter	Value (mm)	Description
Sub_X	65.4	Substrate and Ground Dimension along X-Axis
Sub_Y	88.99	Substrate and Ground Dimension along Y-Axis
Sub_Z	1.6	Substrate Thickness along Z-Axis
Patch_X	37.26	Patch Dimension along X-Axis
Patch_Y	37.027	Patch Dimension along Y-Axis
Ins_Gap	1.537	Gap between Feeding Line and Patch
Ins_Dis	9.574	Feeding Line Insertion
Feed_W	3.036	Feeding Line Width
Cop_T	0.035	Copper Thickness along Z-Axis
Slot_X	13.6	Slot Dimension along X-Axis
Slot_Y	1.065	Slot Dimension along Y-Axis

The antenna is constructed and simulated using the CST time domain solver with hexahedral mesh in the initial step of our planned work. The next step is to use CST to construct the breast phantom with the suitable dimensions. After successfully designing the antenna and phantom model, the next step is to determine whether a breast tumor is present in the breast model. The proposed antenna is then individually tested on the phantom with and without a tumor.

2.2 Breast Phantom Modeling

Using the CST, a realistic biological multi-layer model resembling a human breast is created. For ease of modeling, each breast phantom is created as a hemisphere with a radius of 56 mm, containing the breast layers from the skin layer to the glandular tissue of the breast. There are five tissue layers in the phantom, and the electrical characteristics and thickness of each layer are specific. These layers include skin, adipose (breast fat), glandular tissue, blood, and muscle.

The Tissue Properties Database of the Foundation for Research on Information Technologies in Society (IT'IS Foundation) was used to determine the permittivity, electrical conductivity, mass density, heat capacity, and thermal conductivity of tissue layers. Table 2 lists all the electrical properties at 2.45 GHz and the physical dimensions of the different parts of the breast phantom.

After designing the phantom, a tumor with a radius of 5 mm was placed in the breast phantom. The tumor was modeled as a sphere located 30 mm below the apex of the breast phantom. Distance-dependent measurements were acquired when phantoms with and without tumors were placed 20 mm and 40 mm from the center of the antenna. The results obtained from the simulations were acquired at an operating frequency of 2.45 GHz.

Table 2. Electrical and Physical Characteristics of the Multi-Layer Breast Phantom at 2.45 GHz

	Skin	Adipose	Blood	Breast Gland	Muscle	Tumor
Permittivity	38	5.14	58.2	57.2	52.7	55
Conductivity (S/m)	1.48	0.14	2.57	2	1.76	4
Mass Density ($\mathrm{kg/m^3}$)	1109	911	1050	1041	1090	1058
Heat Capacity (J/kg/°C)	3391	2348	3617	2960	3421	-
Thermal Conductivity (W/m/°C)	0.37	0.21	0.52	0.33	0.49	-
Outer Radius (mm)	56	54	52	50	-	5
Inner Radius (mm)	54	52	50	0	-	0
Thickness (mm)	2	2	2	50	8	5

Figure 1 shows the schematic of the proposed antenna, breast phantom with and without tumor, and healthy breast model with the appropriate labeling. Layers are denoted by different colors.

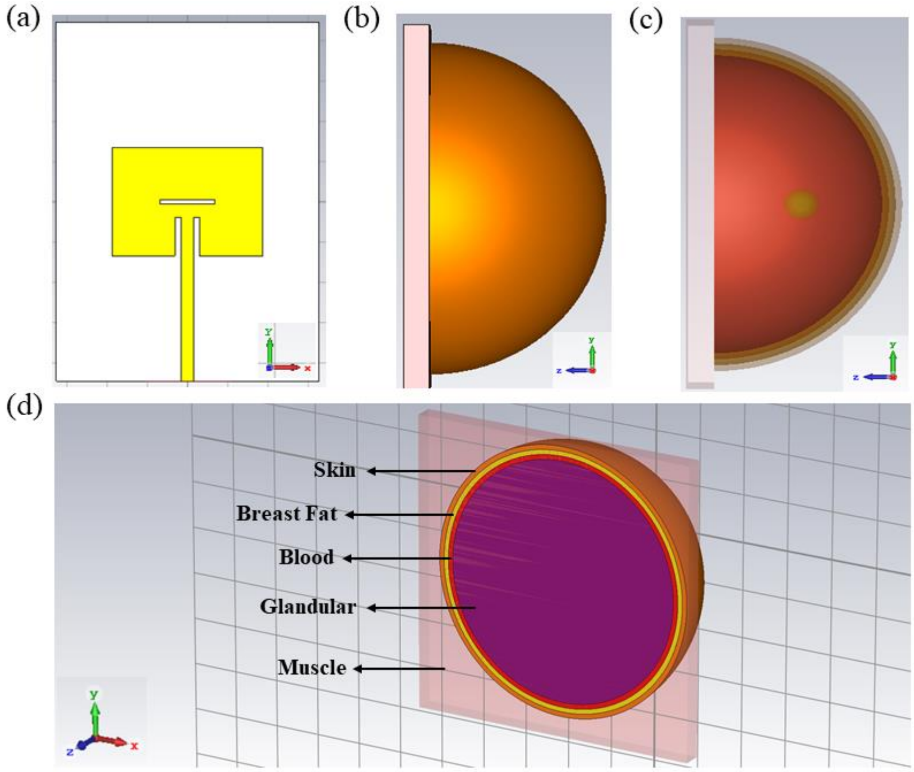

Figure 7. (a) The Geometrical Shape of the Antenna, (b) Side View of Healthy Breast Phantom, (c) Side View of Tumor-Affected Breast Phantom, and (d) Different Layers of Breast Phantom

3. RESULTS

3.1 Slotted MPA Performance Analysis in Free Space

The off-body performance characteristics of the optimized MPA were evaluated in free space. The reflection coefficient of the proposed antenna at 2.45 GHz is -28.718 dB, indicating that only 0.134% of power is reflected back from the input terminal of the antenna. The bandwidth of the antenna is 68.9 MHz from 2.4158 GHz to 2.4847 GHz. The voltage standing wave ratio (VSWR) of the antenna is very close to the optimal value of 1, which indicates a well-matched antenna, and its value is 1.0761. Directivity is equal to 6.914 dBi. The 1-D radiation pattern ($phi = 90$) has a main lobe magnitude of 6.91 dBi at 10 degrees, an angular width of 3 dB of the antenna at 82 degrees, and a side lobe level of -17.7 dB. The radiation efficiency and total efficiency of the antenna are -5.247 dB and -5.253 dB, respectively. The S_{11} parameter, VSWR, 3-D farfield radiation pattern, and electric field distribution of the designed antenna are depicted in Figure 2, while the antenna characteristics are summarized in Table 3.

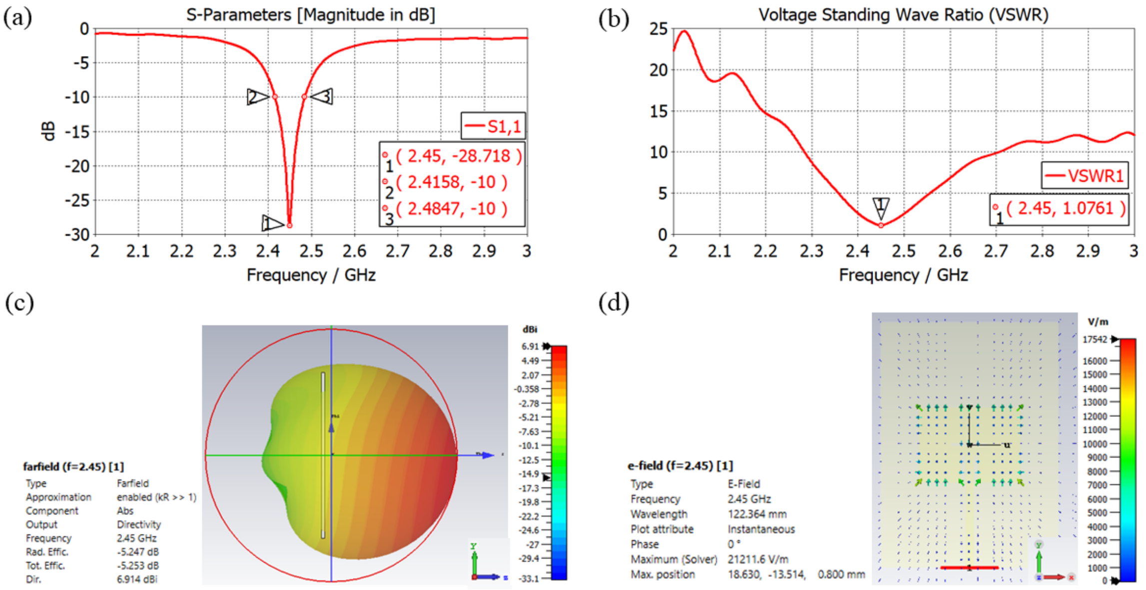

Figure 8. Performance of the Designed Antenna in Free Space. (a) Reflection Coefficient, (b) VSWR, (c) 3-D Farfield Radiation Pattern, and (d) Electric Field

Table 3. Characteristics of the Designed Antenna in Free Space

	Values
Resonant Frequency (GHz)	2.45
Reflection Coefficient (dB)	-28.718
VSWR	1.0761
10 dB Bandwidth (MHz)	68.9
Directivity (dBi)	6.914
Gain (dBi)	1.667
Main Lobe Magnitude (dBi)	6.91
Main Lobe Direction (degree)	10.0
3 dB Angular Width (degree)	82.0
Side Lobe Level (dB)	-17.7
Radiation Efficiency (dB)	-5.247
Total Efficiency (dB)	-5.253

3.2 Slotted MPA Simulation with Healthy Breast Phantom

The parameters of the antenna have been examined under on-body conditions. The tumor-free phantom was located in front of the MPA at a distance of 20 mm and 40 mm. All the data obtained from Figures 3 and 4 are summarized in Table 4.

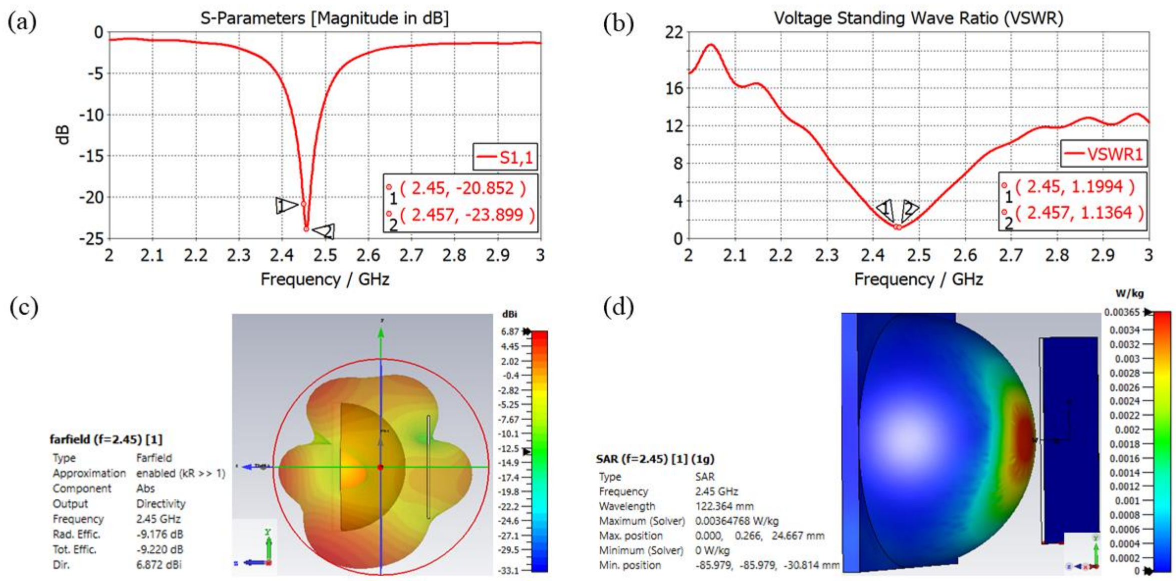

Figure 9. Performance of the Antenna at a Distance of 20 mm From Healthy Breast Phantom. (a) Reflection Coefficient, (b) VSWR, (c) 3-D Farfield Radiation Pattern, and (d) SAR Distribution

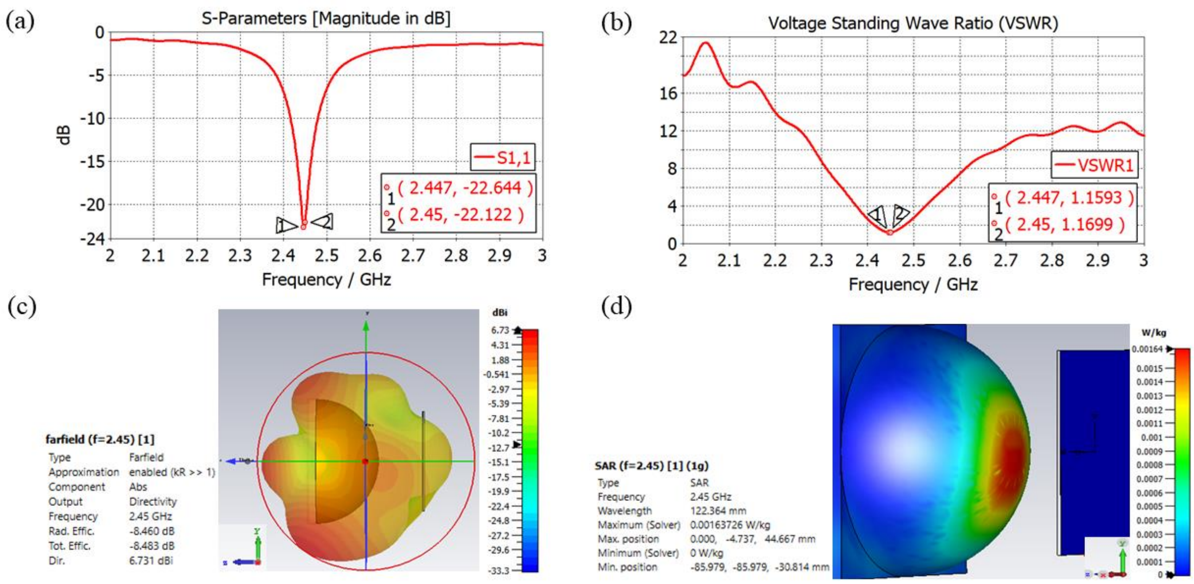

Figure 10. Performance of the Antenna at a Distance of 40 mm From Healthy Breast Phantom. (a) Reflection Coefficient, (b) VSWR, (c) 3-D Farfield Radiation Pattern, and (d) SAR Distribution

Table 4. Performance Parameters Variation of MPA with Healthy Breast Phantoms at 2.45 GHz

	Values	
Phantom-Antenna Distance	**20 mm**	**40 mm**
Resonant Frequency (GHz)	2.457	2.447
Reflection Coefficient (dB)	-20.852	-22.122
VSWR	1.1994	1.1699
Maximum Electric Field (kV/m)	18.5368	19.3491
Maximum Magnetic Field (A/m)	210.036	210.768
Maximum Surface Current (A/m)	177.01	177.427
Specific Absorption Rate (W/kg)	0.0036	0.0016

Gain (dBi)	-2.304	-1.729
Directivity (dBi)	6.872	6.731
Radiation Efficiency (dB)	-9.176	-8.460
Total Efficiency (dB)	-9.220	-8.483

3.2 Slotted MPA Simulation with Tumor-Affected Breast Phantom

The antenna characteristics, including reflection coefficient, electric field strength, surface current, magnetic field, gain, directivity, and SAR, were also obtained to detect the presence of the tumor in the breast phantom. All the data extracted from Figures 5 and 6 are summarized in Table **5**.

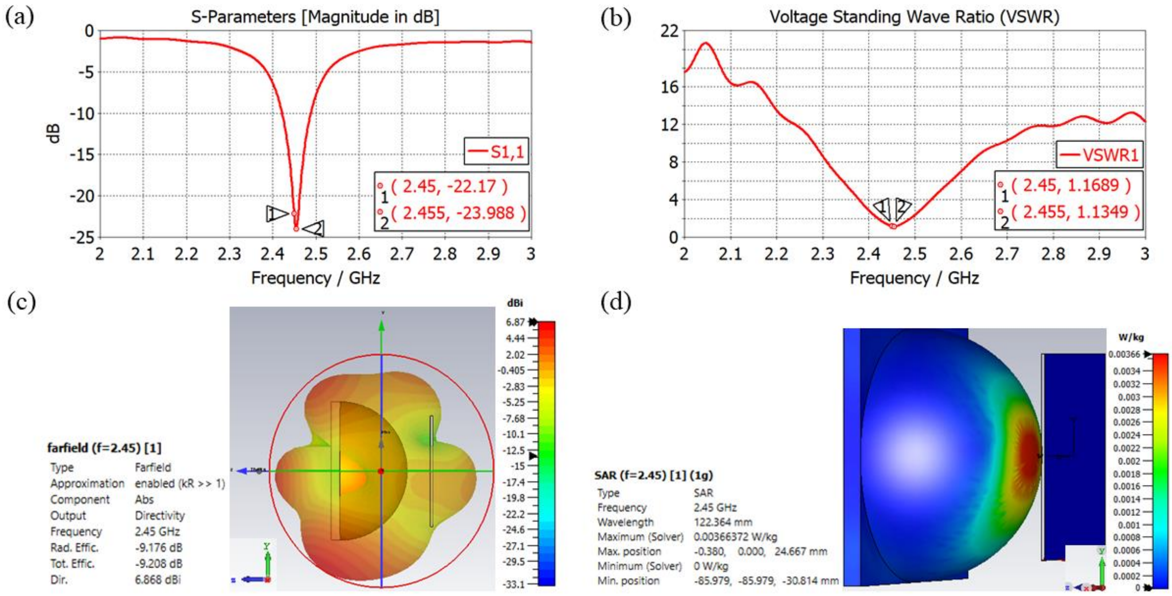

Figure 11. Performance of the Antenna at a Distance of 20 mm From Tumor-Affected Breast Phantom. (a) Reflection Coefficient, (b) VSWR, (c) 3-D Farfield Radiation Pattern, and (d) SAR Distribution

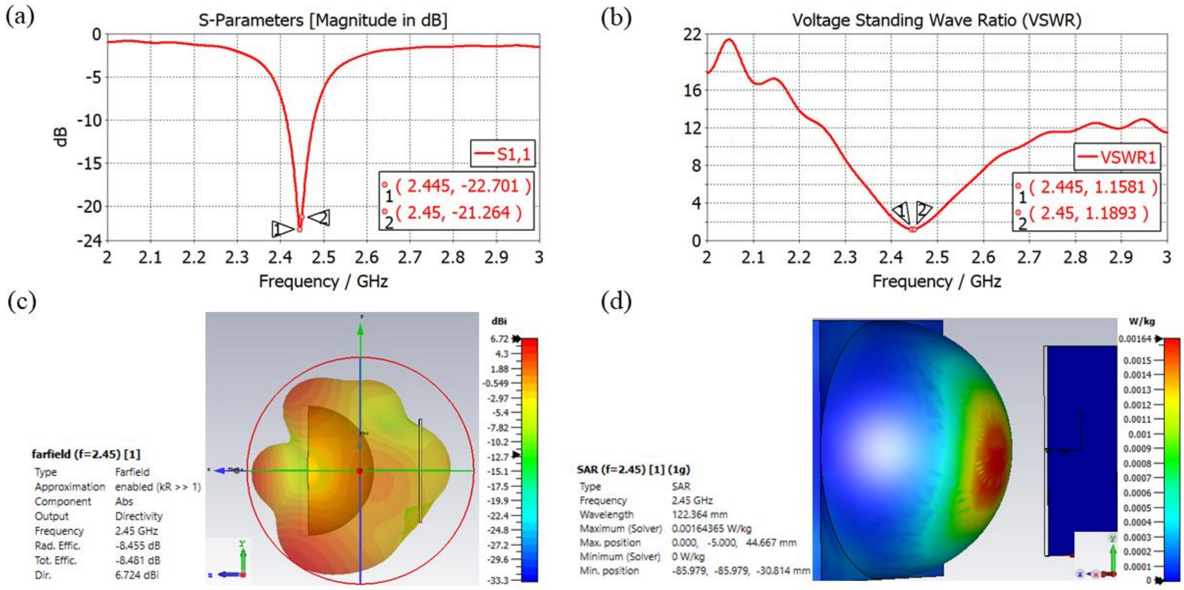

Figure 12. Performance of the Antenna at a Distance of 40 mm From Tumor-Affected Breast Phantom. (a) Reflection Coefficient, (b) VSWR, (c) 3-D Farfield Radiation Pattern, and (d) SAR Distribution

Table 5. Performance Parameters Variation of MPA with Unhealthy Breast Phantoms at 2.45 GHz

	Values	
Phantom-Antenna Distance	**20 mm**	**40 mm**
Resonant Frequency (GHz)	2.455	2.445
Reflection Coefficient (dB)	-22.17	-21.264
VSWR	1.1689	1.1893
Maximum Electric Field (kV/m)	18.736	19.508
Maximum Magnetic Field (A/m)	218.383	218.603
Maximum Surface Current (A/m)	186.561	186.551
Specific Absorption Rate (W/kg)	0.0037	0.0016
Gain (dBi)	-2.308	-1.730
Directivity (dBi)	6.868	6.724
Radiation Efficiency (dB)	-9.176	-8.455
Total Efficiency (dB)	-9.208	-8.481

4. DISCUSSION

4.1 Interpretation of Slotted MPA Simulation with Healthy Breast Phantom

The simulation results show that the return loss of the antenna at on-body decreased from 28.718 dB to 20.852 dB for a 20-mm distance and 22.122 dB for a 40-mm distance at the operating frequency of 2.45 GHz. We also observed that the resonant frequency of the antenna used for healthy breast phantom has shifted from its resonant frequency in free space. A higher VSWR was obtained for both distances when the antenna was installed on the tumor-free phantom model. However, all VSWR measurements are within acceptable limits. Its directivity gradually decreased from 6.914 dBi to 6.872 dBi for 20-mm and 6.731 dBi for 40-mm. Similarly, its gain value reduced from 1.667 dBi to -2.304 dBi for 20-mm and -1.729 dBi for 40-mm. The radiation absorbed by the phantom when the antenna starts radiating towards it must be determined before using the antenna for biological applications, such as breast cancer diagnosis, because there is a limit to how much SAR value human tissues can tolerate. The Federal Communications Commission (FCC), which refers to patient safety, states that the SAR value for 1 g of tissue should be less than 1.6 W/kg as per the American Standard (Federal Communications Commission, 2019). According to all the results obtained, we can see that the maximum SAR values for 1 g of tissue and 1 mW of power were not harmful to human health.

4.2 Interpretation of Slotted MPA Simulation with Tumor-Affected Breast Phantom

It can be seen that there is a variation in the return loss value in all results obtained from tumor-affected breast phantoms compared to healthy breast phantoms. The return loss of the antenna with the tumor-affected phantom placed at 20 mm was higher than the return loss of that at 40 mm. Therefore, it can be said that when the distance between the antenna and the phantom increases, the return loss of the antenna decreases in the unhealthy phantom case. Moreover, an inconsistent breast phantom could be inferred from a variation in the reflection coefficient value. Energy is dispersed differently as a result of this variance brought on by the tumor because normal and malignant tissue have different electrical characteristics due to the high water ingredient in the tumor. In our design, the change in reflection coefficient between a healthy and unhealthy phantom was greater for MPA at a distance of 20 mm. As a result of the antenna impedance and its feeding transmission line's mismatched impedance in these arrangements, the VSWR was quite high with respect to the value obtained for the antenna in free space, indicating that the power would not be transferred effectively. Some of the power was returned in another manner. Higher VSWR values correspond to higher impedance mismatch values. According to the results, the VSWR value increased from 1.1689 to 1.1893 when the distance between the antenna and the tumor-affected breast phantom was increased. In addition, we obtained higher VSWR at 20 mm distance for the tumor-free phantom and at 40 mm distance for the tumor-affected phantoms. Referring to Table 5, we observed that increasing the distance between the antenna and the tumor-affected phantom increased the gain of the antenna while slightly decreasing its directivity. The presence of a tumor also slightly decreased both the directivity and gain of the antenna as opposed to the tumor-free case. However, the presence of a tumor significantly increases the surface current of the antenna as compared to the antenna utilized with a healthy phantom at both distances. Our results indicate that the maximum electric field increased when the antenna was located away from the tumor-affected phantom. This makes sense since the electric field depends on the square root of the power delivered to the antenna, that is, VSWR. As for the SAR values, there was no noticeable difference in values obtained from healthy and unhealthy phantoms. However, the antenna's SAR value was observed to be slightly higher in breasts with tumors than in breasts without tumors if the fifth decimal place were taken into account of the simulated SAR values. The SAR value also decreased when the antenna-to-phantom distance was increased for both tumor-free and tumor-affected phantoms. Our proposed antenna is fully biocompatible, as it meets SAR requirements and prevents harmful heating of biological tissues.

5. CONCLUSION

In this study, a biomedical on-body slotted MPA operating at 2.45 GHz in the ISM band is presented. The proposed antenna is simulated in free space and with a 3-D breast phantom. The special characteristics of this antenna include low return loss (-28.718 dB), small dimensions, moderate bandwidth (68.9 MHz), and an acceptable VSWR profile (1.0761). A breast phantom was successfully designed and simulated for measurement of antenna parameters in both instances (with and without tumor). The embedded tumor was represented as a sphere in accordance with the different dielectric characteristics of malignant tissue, while the breast phantom was modeled as a hemisphere. The designed antenna has been tested at different positions from the phantom. Therefore, it was examined how the distance of the antenna from the phantom affects its electrical characteristics while detecting breast cancer. Various output parameters, such as the electric field, return loss, VSWR, efficiency, SAR, etc., have been achieved successfully. By measuring the difference between these parameter changes, a tumor can be determined. In terms of antenna parameters at 2.45 GHz, the simulation results at various antenna locations show that there is a difference between values with and without tumors. The presence of a tumor caused the resonance frequency to alter from 2.45 GHz to 2.455 GHz (for a 20-mm distance) and 2.445 GHz (for a 40-mm distance). The reflection coefficients without tumor are -20.852 and -22.122 dB, whereas those with tumor are -22.17 and -21.264 dB at two different distances, respectively. This indicates that a tumor causes a significant change for 20-mm distance in power reflected back because of a mismatch in the designed antenna. We also observed that the strength of the electric field increased with the presence of the tumor in the phantom at both distances. Our results show that the proposed antenna is an appropriate option for the diagnosis of breast cancer with acceptable SAR values in the simulated environment. As for the future study, different antenna geometry will be employed to improve antenna performance and further increase tumor detection sensitivity.

REFERENCES

A. Kahwaji, H. Arshad, S. Sahran, A. G. Garba, R. I. Hussain, (2016) Hexagonal microstrip antenna simulation for breast cancer detection, International Conference on Industrial Informatics and Computer Systems (CIICS), IEEE 2016, 13-15 March 2016, Sharjah, United Arab Emirates

Breast Cancer Statistics and Resources, https://www.bcrf.org/breast-cancer-statistics-and-resources/ (Access Date: 26.10.2022)

C. A. Balanis, (2016) Antenna Theory: Analysis and Design, John Wiley & Sons, February 2016, 4th Edition

D. N. Elsherif, M. Y. Makkey, (2021) Early Detection of Breast Cancer using Microstrip Patch Antenna, International Conference on Electronic Engineering (ICEEM), IEEE 2021, 03-04 July 2021, Menouf, Egypt

K. RamaDevi, A. J. Rani, A. M. Prasad, (2017) Design of Microstrip Antenna with Improved Bandwidth for Biomedical Application, Proceedings of the International Conference on Data Engineering and Communication Technology, August 2017, pp. 201-215

M. J. Dishali, K. M. Kumar, S. M. M. Nawaz, (2019) Design of Microstrip Patch Antenna for Brain Cancer Detection, Ictact Journal on Microelectronics, April 2019, Volume 05, Issue 01

M. Slimi, B. Jmai, P. Mendes, A. Gharsallah, (2019) Breast cancer detection based on CPW antenna, 19th Mediterranean Microwave Symposium (MMS), IEEE 2019, 31 October-02 November 2019, Hammamet, Tunisia

N. Mahalakshmi, V. Jeyakumar, (2012) Design and Development of Single Layer Microstrip Patch Antenna for Breast Cancer Detection, Bonfring International Journal of Research in Communication Engineering, July 2012, Volume 2, Special Issue 1

S. A. K. Al-Nahiun, F. Mahbub, R. Islam, S. B. Akash, R. R. Hasan, M. A. Rahman, (2021) Performance Analysis of Microstrip Patch Antenna for the Diagnosis of Brain Cancer & Tumor using the Fifth-Generation Frequency Band, International IOT, Electronics and Mechatronics Conference (IEMTRONICS), IEEE 2021, 21-24 April 2021, Toronto, Canada

S. Shekhawat, V. Sharma, P. K. Jain, B. R. Sharma, V. K. Saxena, D. Bhatnagar, (2019) An Off-Diagonal Feed Elliptical Patch Antenna with Ring Shaped Slot in Ground Plane for Microwave Imaging of Breast, Indian Conference on Antennas and Propogation (InCAP), IEEE 2019, 19-22 December 2019, Ahmedabad, India

S. Sukhija, R.K. Sarin, (2017) Design and performance of two-sleeve low profile antenna for bio-medical applications, Journal of Electrical Systems and Information Technology, May 2017, Volume 4, Issue 1

Specific Absorption Rate (SAR) for Cellular Telephones, https://www.fcc.gov/general/specific-absorption-rate-sar-cellular-telephones (Access Date: 04.11.2022)

Suriya, R. Nandhini, M. Leepika, S. R. Praveen, (2018) Microstrip Patch Antenna for Brain Tumour Detection, International Journal of Scientific Research and Review, 2018, Volume 7, Issue 3, pp. 63-66

COVID-19 SALGININDA ORTA ÖLÇEKLİ BİR KENTİN EV-İŞ YOLCULUKLARINDA ULAŞTIRMA TÜR SEÇİMİNDEKİ DEĞİŞİMLERİN İNCELENMESİ: TEKİRDAĞ, SÜLEYMANPAŞA ÖRNEĞİ

Şehir Plancısı Sahra Başyazgan

Yıldız Teknik Üniversitesi, Fen Bilimleri Enstitüsü, Ulaştırma Tezli YL Programı
sahra.basyazgan@std.yildiz.edu.tr, ORCID: 0000-0003-0172-9672

Dr. Öğr. Üyesi Mustafa Sinan Yardım

Yıldız Teknik Üniversitesi, İnşaat Fakültesi, İnşaat Mühendisliği Bölümü
yardim@yildiz.edu.tr, ORCID: 0000-0003-0799-9294

Özet

Covid-19 salgını, dünyanın her yerinde köklü değişimlere sebep olmuş, yeni alışkanlıkların kazanılmasına yol açmış, son dönemin en güncel konularından biridir. Gerek yapılan yolculuklar gerekse bu yolculuklardaki tür seçimleri salgın koşullarından etkilenmiştir. Bu çalışma kapsamında, orta ölçekli bir kent olan Tekirdağ ilinin Süleymanpaşa ilçesinde, ev- iş amaçlı yolculuklar bağlamında, ulaştırma tür seçimleri incelenmiş olup, bu seçimlerdeki değişimlerin salgın koşullarından etkilenip etkilenmediği araştırılmıştır. Bunun için yapılan anketlerle kullanıcılara tür seçimine dair sorular yöneltilmiştir. Salgının gelişim evrelerinden en az birinde ev-iş yolculuğu yapmış ve ulaştırma türü seçmiş bulunan 259 katılımcı analize dahil edilmiştir. Çalışma sonunda , betimleyici istatistiklerde bazı tür tercihi değişimleri gözlense de verilerin normal dağılmadığı çeşitli istatistik yöntemler kullanılarak tespit edilmiştir. Bu yüzden, analizin ilerleyen safhasında parametrik olmayan Wilcoxon İşaretli Sıralar Testi kullanılmıştır. Orta ölçekli kent Süleymanpaşa'da küçük ve büyük ölçekli kentlerin aksine, Covid-19 salgın döneminde ev-iş amaçlı yolculuklardaki ulaştırma tür seçimlerinin, salgından anlamlı bir şekilde etkilenmediği belirlenmiştir.

Anahtar Kelimeler: Covid-19 Salgını, Orta Ölçekli Kent, Ev-İş Yolculuğu, Ulaştırma Tür Seçimi, Tekirdağ, Süleymanpaşa

INVESTIGATION OF CHANGES IN TRANSPORTATION MODE CHOICE FOR HOME-WORK TRIP OF A MEDIUM-SIZED CITY DURING THE COVID-19 PANDEMIC: TEKİRDAĞ, SÜLEYMANPAŞA CASE

Abstract

The Covid-19 pandemic has caused radical changes all over the world, leading to the adoption of new habits, and is one of the most topical issues of the recent period. Both the trips made and the mode choices in these trips have been affected by the pandemic conditions. Within the scope of this study, transportation mode choices in the context of home-work trips in Süleymanpaşa district of Tekirdağ province, a medium-sized city, were examined and it was investigated whether the changes in these choices were affected by the pandemic conditions. For this purpose, users were asked questions about mode choice through surveys. A total of 259 respondents who made a commute during at least one of the development phases of the pandemic and chose a mode of transportation were included in the analysis. At the end of the study, although some changes in mode preference were observed in descriptive statistics, it was determined using various statistical methods that the data were not normally distributed. Therefore, the nonparametric Wilcoxon Signed Rank Test was used in the next stage of the analysis. In the medium-sized city of Süleymanpaşa, unlike small and large-sized cities, transportation mode choices for home-work trips during the Covid-19 pandemic period were not significantly affected by the pandemic.

Keywords: Covid-19, Medium Sized City, Home-Work Trips, Transportation Mode Choice, Tekirdağ, Süleymanpaşa

1. GİRİŞ

Covid-19 salgını dünyadaki mevcut şartlarda alışılmış olan düzeni değiştirmekle kalmamış, aynı zamanda yeni bir normal anlayışını, günlük yaşantıdaki tercihleri sorgulamayı ve hatta değiştirmeyi de beraberinde getirmiştir. Dünya nüfusunun büyük bir çoğunluğunun kentlerde yaşaması ile salgın hastalıkların yayılma riskinin de arttığı bilinen bir gerçek olduğuna göre, her ölçekten kentin kendi dinamiklerine göre ayrı bir hassasiyetle ele alınması gerekmektedir.

Salgının kentlerde ve kent sakinlerinde yaratmış olduğu değişimler birçok çalışma ile ortaya konmuştur. Shabani vd., (2022), Covid-19'un yüksek bulaşıcılığı ve özellikle yoğun saatlerde sınırlı alan ve yüksek yolcu yoğunluğu gibi toplu taşımanın bazı özelliklerini, toplu taşımada hastalığın yayılma riskini artırdığını ve ilgili sistemlere olan talebi azalttığını ifade etmiştir. Shen vd., (2020), toplu taşımanın ve yolcu terminallerinin herhangi bir salgın döneminde virüsün yayılma veya kümelenme mekanı haline dönüşebileceğini vurgulayarak, kentlinin "buluşma mekanları"nın "bulaşma mekanı"na dönüştüğünün üzerinde durmuştur. Almanya'da Berlin Hareketlilik Enstitüsü tarafından yapılan bir çalışmada da 2020 Şubat-Mart dönemindeki ulusal telefon izleme verileri kullanılarak ortalama günlük seyahat mesafesinin %47 azaldığı ortaya konmuştur (Mobility Institute Berlin, 2020). Başka bir örnek de Avustralya ve Kuzey Amerika şehirlerinde 4.500 kişinin katılımıyla gerçekleştirilmiştir. Nisan 2020'de Avustralya hükümetinin de aldığı önlemler göz önüne alındığında. Covid-19 öncesi rakamlara göre, toplu taşıma kullanımında %80'lik bir azalma olduğu tespit edilmiştir. Ayrıca burada Covid-19 öncesi ve sonrası ulaşım türü seçiminde etkili olan kriterlerinin değişimi de incelenmiştir. Montreal ve Avustralya'daki kriterlerden bazıları Covid-19 öncesi dönem ile Covid-19 dönemi arasında farklılık göstermiş, her iki çalışma sahasında da ilk sıradaki uygunluğun yerini güvenlik, ikinci sırada olan güvenliğin yerini uygunluk almıştır (Transurban, 2020). Gana'da yapılan bir araştırmaya göre de katılımcıların %50,4'lük kesimi toplu taşıma araçlarındaki koltukların birbirlerine yakın olması nedeniyle, virüsün bulaşma potansiyelinin yüksek olduğunu düşünmekte ve bu sisteme karşı derin kaygılar gütmektedir (Sogbe, 2021). Bu çerçevede bir örnek çalışma ise İsviçre Zürih'te yapılmıştır. Salgının farklı evrelerinde türel dağılım ve seyahat mesafesinin nasıl değiştiği incelenmiştir. Burada da öncekilerle benzer sonuçlar elde edilmiş; toplu taşıma kullanımının azaldığı kaydedilmiştir. Toplu taşıma kullanıcılarının azalmasının yanı sıra, ilgili çalışmada başlangıç-son matrislerinde salgın öncesi dönemde toplu taşıma kullanıcılarının salgın döneminde günlük belirli rotalarını kullanmadıkları, farklı rota arayışları içinde girdikleri de tespit edilmiştir (Marra vd., 2022).

Literatürden verilen örneklerden de görüleceği üzere, araştırmalar sürekli büyük ölçekli kentler üzerinden yapılmış ve bu kentlerdeki değişimler üzerinden salgının etkileri yorumlanmıştır. Fakat, salgının yaratmış olduğu etki büyük ölçekli kentler çerçevesinde kısıtlı değildir. Orta ölçekli ve küçük ölçekli kentler de salgından etkilenmiş ve bu etkiler literatüre kazandırılamamıştır. Bu araştırma kapsamında, salgının ev-iş yolculuklarında ulaştırma tür seçimlerin orta ölçekli bir kent bağlamında incelenmiştir. Bu çerçevede araştırma alanı olarak, Gökgür vd., (2016) ve Eurofound, (2012)'daki orta ölçekli kent kriterlerine; gerek Kanada, Brezilya, Amerika, Japonya gerekse Türkiye'deki çalışmalardakilere uyan Tekirdağ ilinin merkez ilçesi 210.574 nüfuslu Süleymanpaşa seçilmiştir (Özgür, 2005, Fulton, 2002, Seasons, 2010, Henderson, 1997).

Tekirdağ, Türkiye'nin kuzeybatısında olup Marmara Bölgesi'nde yer almaktadır. Marmara Denizi'ne kıyısı olan kent Edirne, Kırklareli, İstanbul ve Çanakkale'ye komşu olup bünyesinde üç adet liman barındırmaktadır. Bu limanlar hem ulusal hem de uluslararası birçok ticaret gemisine hizmet vermektedir. Bahsi geçen limanlardan ikisi Süleymanpaşa ilçesinde yer almakta olup, önemli mal ve hizmet akışları bu noktalardan sağlanmaktadır. Trakya Alt Bölgesi Ergene Havzası Çevre Düzeni Planı'nda da çalışma sahası olan Süleymanpaşa için hizmet merkezi kararı verilmiş, kuzeyinde yer alan Muratlı ilçesi ile demiryolu bağlantısının kurulması ile lojistik kimlik de kazandırılacağı belirtilmiştir (T.C. Çevre ve Orman Bakanlığı vd., 2009). Günümüzde demiryolu bağlantıları sağlanan ilçede bu bağlantılar üzerinden hem ulusal hem de uluslararası yoğun mal akışları gerçekleştirilmektedir.

2. MATERYAL VE METOD

Bu çalışma, Süleymanpaşa özelinde orta ölçekli bir kentin ev-iş yolculuklarında, ulaştırma tür seçimlerinin salgın koşullarından etkilenip etkilenmediğini araştırmak amacıyla yapılmıştır. Bunun için de salgın öncesi dönem, salgın dönemi ve normalleşme dönemlerinde kent sakinlerinin ev-iş yolculuklarında hangi ulaştırma türünü tercih ettiklerine dair verilere ihtiyaç duyulmuştur. İlgili veriler salgın koşullarında yaygın olarak kullanılan çevrimiçi anket yöntemi ile Mart-Mayıs 2022 tarihleri arasında kent sakinlerinden toplanmıştır. Örneklem büyüklüğü Denklem 1'de aktarılan formül ile hesaplanmış; 0,05 anlamlılık ve %95 güven düzeyi, %5 hata payı ile 383 geçerli ankete ulaşılması hedeflenmiştir. Mart 2022'de salgın koşullarının kentte ağırlaşması ve kısıtlı imkanlar nedeniyle ilgili hedefe ulaşılamamış, anlamlılık ve güven düzeyi korunmuş, hata payı ise yeniden hesaplanmıştır. %5,25 olarak hesaplanan hata payı ile 348 anket geçerli kabul edilmiştir.

$$n = \frac{Nt^2pq}{d^2(N-1)+t^2pq}$$

(1)

n: Örneklem büyüklüğü
N: Evren büyüklüğü
t: Belirli bir anlamlılık düzeyinde T Tablosuna göre bulunan teorik değer
d: Hata payı
p: İncelenen olayın gerçekleşme olasılığı
q: İncelenen olayın gerçekleşmeme olasılığı

Covid-19 salgınında ev-iş yolculuğu ulaştırma tür seçimlerini inceleyen araştırma için ise, geçerli anketlerin içerisinden bir veri kümesi oluşturulmuştur. Oluşturulan veri kümesinde değişimi gözlemleyebilmek amacıyla salgın öncesi dönem, salgın dönemi ve normalleşme dönemlerinden en az birinde ev-iş yolculuğu yapmış ve tür seçiminde bulunmuş olan kişiler analize dahil edilmiştir. Bu da 348 anket içerisinden 259 katılımcının analize dahil olduğu anlamında gelmektedir.

Ulaştırma tür seçiminde salgının etkisini görebilmek için, öncelikle, hazırlanan verilerin normal dağılıma uygun olup olmadığı araştırılmıştır. Bu kapsamda aşamalı olarak sırasıyla veri görselleştirme, tanımlayıcı istatistikler ve normallik testleri uygulanmıştır. İlk aşamada, veri görselleştirme yöntemlerinden Kutu Grafikleri (Box-Plot) ve Q-Q grafikleri kullanılmıştır. Kutu Grafiği (Box-Plot) yöntemine göre, belirli bir hat üzerinde yer alan kutuların sola doğru kaydıkları görülmektedir; halbuki normal dağılımı temsil etmesi için, ortada yer almaları gerekmektedir (Şekil 1). Son olarak, Q-Q Grafiği yöntemine göre, verilerin grafikteki doğru üzerinde yer alması gerekirken, doğrunun etrafında saçıldığı ve doğrudan uzaklaştığı saptanmıştır (Şekil 2). Özetle, veri görselleştirme yöntemleri kullanılarak yapılan normal dağılım kontrolünde her iki yöntemde de verilerin normal dağılmadığı tespit edilmiştir (Şekil 1, Şekil 2). Belirli türlerde seçimin yoğun olduğu, bu iki değerlendirme yönteminde de açık bir şekilde görülmektedir.

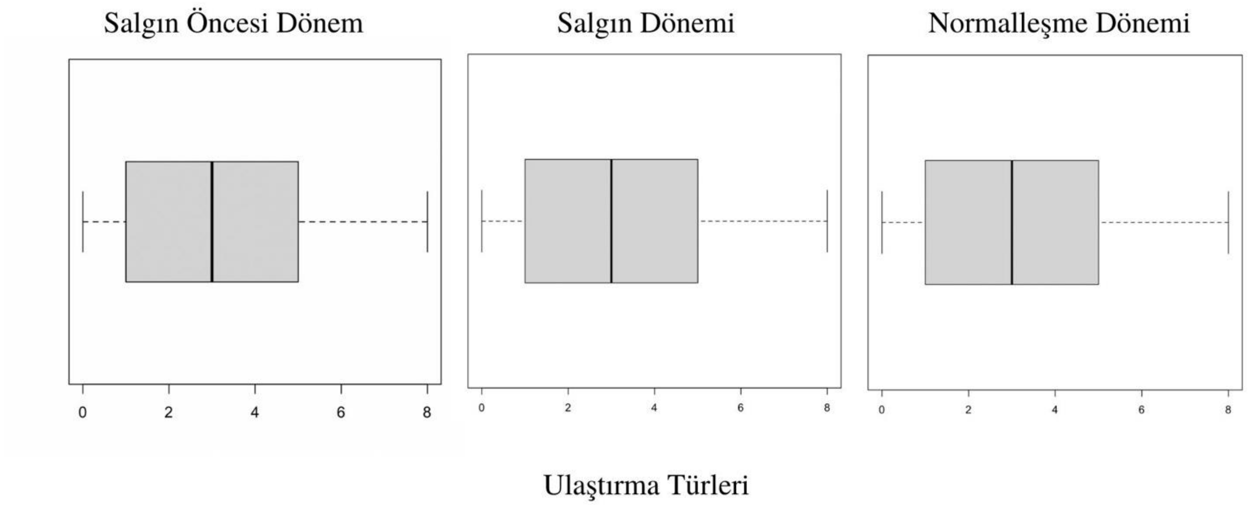

0: Tür Seçimi Yok	4: Taksi	8: Yaya
1: Otobüs	5:Özel Araç	
2: Minibüs	6:Taşıt Paylaşımı (Ortak Araba Kullanımı)	
3: Servis (İşyeri/Okul)	7: Bisiklet	

Şekil 1. Kutu Grafiği (Box-Plot) ile Tür Seçimi Verilerinin Normal Dağılım Kontrolü

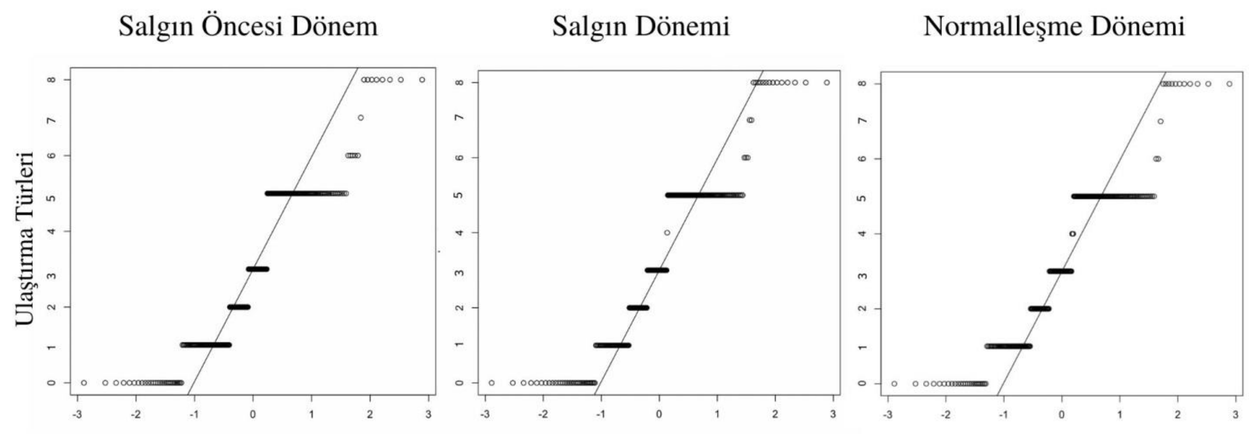

0: Tür Seçimi Yok	4: Taksi	8: Yaya
1: Otobüs	5:Özel Araç	
2: Minibüs	6:Taşıt Paylaşımı (Ortak Araba Kullanımı)	
3: Servis (İşyeri/Okul)	7: Bisiklet	

Şekil 21. Q-Q Grafiği ile Tür Seçimi Verilerinin Normal Dağılım Kontrolü

İkinci aşama değerlendirme ise tanımlayıcı istatistikler üzerinden yapılmaktadır. Bu yaklaşımla, hesaplanan aritmetik ortalama, mod, medyan gibi değerlerin birbirlerine yakın olması ve çarpıklık, basıklık değerlerinin -1,5 ile +1,5 değerleri arasında yer alması istenmektedir. Salgın öncesi dönem, salgın dönemi ve normalleşme dönemleri için ayrı ayrı tanımlayıcı istatistikler incelendiğinde, her bir dönemin mod ve medyanı yakın, aritmetik ortalamaları ise uzak çıkmıştır (Tablo 1). Fakat, çarpıklık-basıklık değerleri ise sınırlar arasında yer almaktadır. Sınır değerlere göre bir değerlendirme yapıldığı zaman, verilerin normal dağılıma uygun olduğu söylenebilse bile, bu değerlendirme yöntemi normallik testlerine göre zayıf kalmaktadır.

Tablo 1. Salgın Dönemlerinin Tanımlayıcı İstatistikleri

Tanımlayıcı İstatistikler	Salgın Öncesi	Salgın	Normalleşme
Ortalama	3,01	3,23	3,19
Standart Hata	0,13	0,14	0,13
Medyan	3	3	3
Mod	5	5	5
Standart Sapma	2,12	2,24	2,10
Varyans	4,49	5,03	4,43
Basıklık	-0,98	-0,88	-0,80
Çarpıklık	0,25	0,18	0,20
Aralık	8	8	8
Minimum	0	0	0
Maksimum	8	8	8
Toplam	779	836	827
Gözlem Sayısı	259	259	259

Normal dağılımı tam olarak tespit edebilmek için üçüncü aşamada normallik testlerinin kullanılması gereklidir. Bu testler, açık kaynak kodlu bir yazılım olan R® Programı kullanılarak yapılmıştır. Burada da üç aşamadan oluşan normallik testinde ilk olarak Kolmogrov-Smirnov Testi uygulanmıştır (Tablo 2). Bu test bağlamındaki araştırma hipotezi, verilerin normal dağılım gösterdiğini ifade etmektedir. Salgın öncesi dönem, salgın dönemi ve normalleşme dönemleri için uygulanan testlerin sonuçları p-değeri ile değerlendirildiğinde, sınır değer olan 0,05'ten küçük çıktığı için verilerin normal dağılmadığı tespit edilmiş; araştırma hipotezi reddedilmiştir.

Tablo 2. Kolmogrov-Smirnov Testi Sonuçları

İstatistikler	Salgın Öncesi	Salgın	Normalleşme
D	0,2319	0,22932	0,2256
p-değeri	$1,597*10^{-9}$	$2,955*10^{-9}$	$7,094*10^{-9}$
Alternatif Hipotez	Çift Kuyruklu	Çift Kuyruklu	Çift Kuyruklu

Parametrik bir testin uygulanabilmesi için yalnızca Normal Dağılım şartının sağlanması yeterli değildir. Bu sebeple ikinci aşamada varyansların homojenliğinin kontrol edildiği Levene Testi yapılmıştır. Testin araştırma hipotezi varyansların arasında anlamlı bir fark olmadığını ileri sürmektedir. Salgının gelişim evrelerinin birbirleri ile kıyaslanarak yapıldığı testin sonucunda, her bir Pr değeri, hesaplanan F değerinden küçük olduğu için, varyansların arasında anlamlı bir fark olduğu saptanmıştır (Tablo 3). Bu sonuca göre parametrik test uygulanma şartlarından biri daha ihlâl edilmiştir.

Tablo 3. Levene Testi Sonuçları

İstatistikler	**[Salgın Öncesi] – [Salgın]**	**[Salgın] – [Normalleşme]**	**[Salgın Öncesi] – [Normalleşme]**
F-Değeri	10,65	3,41	5,91
Pr(>F)	$7{,}211*10^{-10}$	$9{,}815*10^{-4}$	$6{,}138*10^{-4}$

Son aşama ise bağımsızlığın kontrolünün yapıldığı Durbin-Watson testidir. Bu testte de Levene Testi'nde olduğu gibi salgının gelişim evreleri yine ikişerli olarak değerlendirmeye alınmıştır. İlgili testin araştırma hipotezi, gözlemler arasında otokorelasyon olmadığını savunmaktadır. Fakat, test sonucunda hesaplanan DW değerlerinin tamamı 1,5 ile 2 aralığında yer almakta olup, gözlemler arasında bir otokorelasyon olduğu tespit edilmiştir (Tablo 4). Yapılan bütün testler ve incelemeler sonucunda ilgili veri kümesine parametrik bir test uygulanamayacağı görülmüştür. Bu nedenle parametrik olmayan (nonparametric) testlere yönelinmiştir ve ev-iş yolculuklarında ulaştırma türü seçiminde salgının etkisini araştırmak amacıyla, parametrik olmayan testler arasından Wilcoxon İşaretli Sıra Testi (Wilcoxon signed-rank test)'nin yapılmasına karar verilmiştir.

Tablo 4. Durbin-Watson Testi Sonuçları

İstatistikler	**[Salgın Öncesi] – [Salgın]**	**[Salgın] – [Normalleşme]**	**[Salgın Öncesi] – [Normalleşme]**
DW	2,2203	1,8432	2,1755
p-değeri	0,9616	0,1018	0,9212

3. BULGULAR

Wilcoxon İşaretli Sıra Testi'ne geçmeden önce, salgının gelişim evrelerindeki ev-iş yolculukları türel dağılımları incelemek yararlı olacaktır.

Ulaştırma tür seçimlerinde salgın etkisinin ev-iş yolculukları bağlamında araştırılmasının arkasında yatan sebep, Süleymanpaşa kent sakinlerinin her üç dönemde de büyük oranda (ortalama %69) çalışma hayatında aktif rol alması olmuştur (Şekil 3). Salgın öncesi dönemde sakinlerin %68,4'ünün çalıştığı ve bu kesimin de %84,4'ünün yüz yüze çalışma düzenine sahip olduğu saptanmıştır. Bu oranlar salgın döneminin başlaması ile düşüşe geçmiştir. En büyük değişim ise yüz yüze çalışma düzeninde yaşanmıştır. Salgının yayılma hızını kırmak amacıyla esnek veya uzaktan çalışma düzenlerine yönelen kurumlar sebebiyle, kentteki hareketliliğinin büyük bir çoğunluğunu oluşturan ev-iş yolculukları kayda değer miktarda azalmıştır. Normalleşme döneminin başlaması ile yüz yüze çalışma düzenine geri dönülmüş ve yine %85,9'luk büyük bir kesim ev-iş yolculuklarını devam ettirmeye başlamıştır.

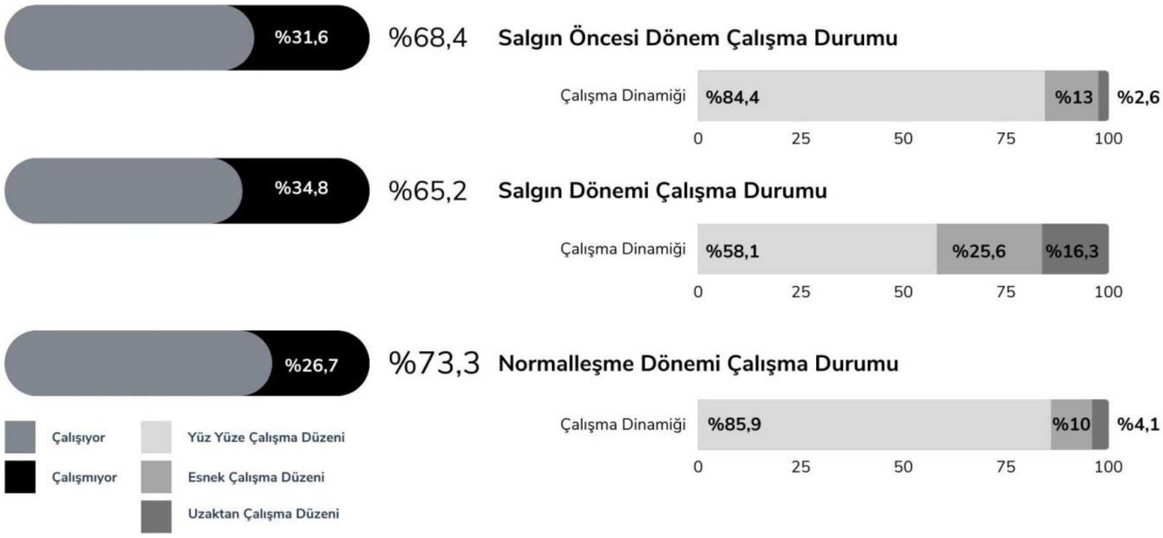

Şekil 3. Süleymanpaşa'da Ev-İş Yolculuklarının Özellikleri

Salgın öncesi dönem, salgın dönemi ve normalleşme dönemi türel dağılımları incelendiğinde her üç dönemde de en çok "Özel Araç"ın tercih edildiği göze çarpmaktadır (Şekil 4). Bu türün seçilmesinde kentin ölçeği, coğrafi yapısı, kentsel ulaşım imkanları vb. birçok faktörün etkisi olabileceği gibi, bu çalışma bağlamında salgın etkisi tartışılmaktadır. Ancak, türlere toplu taşıma (Otobüs, minibüs, servis) ve bireysel ulaşım (Özel araç, taşıt paylaşımı, taksi, bisiklet, yaya) olarak bakıldığında salgın öncesi dönemde ağırlıklı olarak toplu taşımanın tercih edildiği görülmektedir (Şekil 4). Bu manzaraya göre, salgınla ağırlık bireysel ulaşım yönüne kaymış ve toplu taşımada %6,14'lük bir azalma kaydedilmiştir. %6,14'lük bu azalma ise toplu taşıma oranındaki değişimin -%11,3'üne denk gelmektedir. Bireysel ulaşımdaki %6,14'lük artış da bireysel ulaşım oranındaki değişimin +%13,5'ine karşılık gelmektedir. Genel bir değerlendirme yapıldığında da toplu taşımadan bireysel ulaşıma doğru bir yönelim olduğu, normalleşme döneminde eski düzene geri dönülemediği ve salgının ev-iş yolculuğu ulaştırma tür seçiminde kalıcı bir etki bıraktığı salgın öncesi ve normalleşme dönemi toplu taşımadaki %2,21'lik azalmanın -%4,1'lik değişime tekabül etmesinden anlaşılmaktadır (Şekil 4).

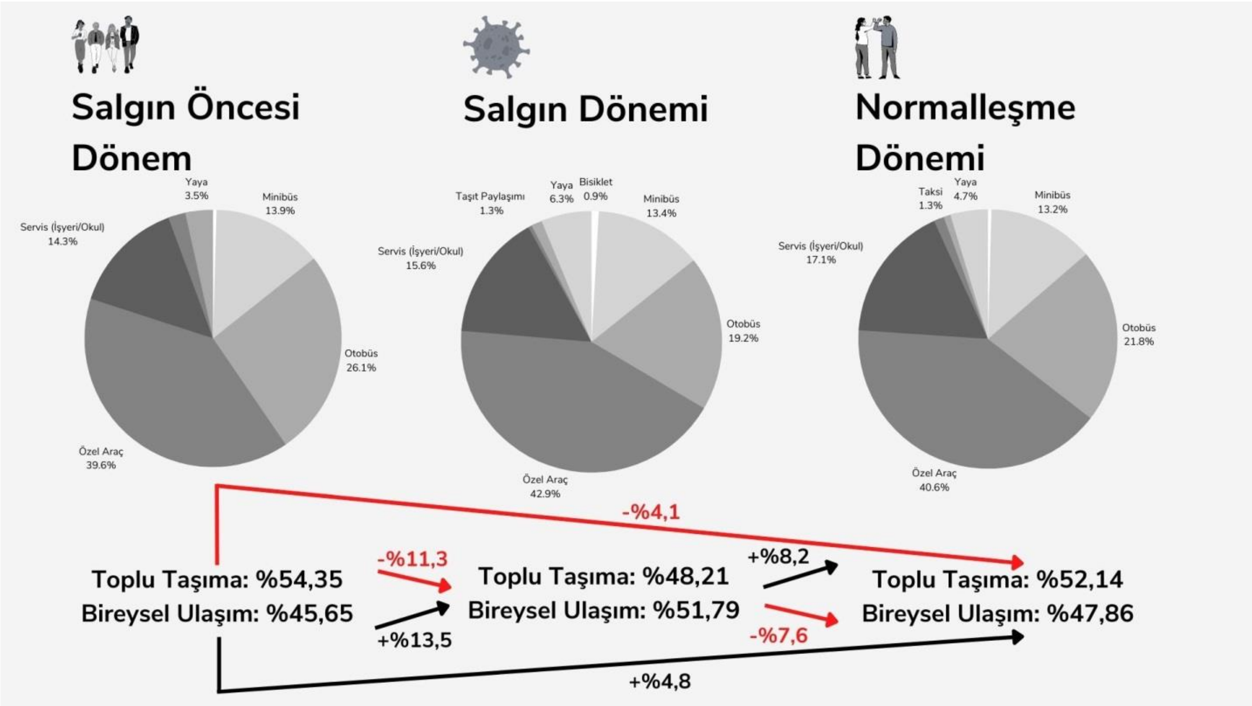

Şekil 4. Salgının Dönemlerine Göre Ev-İş Yolculuğu Türel Dağılımı

Her ne kadar yukarıdaki grafiklerden (Şekil 3, Şekil 4) salgının ev-iş yolculuklarında ulaştırma türü seçiminde etkisi olduğu ifade edilse de bu yargının anlamlılık bağlamında istatistiki testler aracılığı, ile test edilmesi daha güvenilir sonuçlara ulaşmayı mümkün kılacaktır. Bu çerçevede, yukarıda aktarılan Wilcoxon İşaretli Sıra Testi uygulanmıştır. Testin araştırma hipotezi, salgın koşullarının ev-iş yolculuklarında ulaştırma tür seçiminde bir etkisi olduğunu ileri sürmektedir. Salgın öncesi dönem-salgın dönemi, salgın dönem-normalleşme dönemi ve salgın öncesi dönem-normalleşme dönemi olmak üzere üç grupta karşılaştırma yapılmıştır. Yapılan test sonucunda, p değerlerinin sınır değer olan 0,05'ten büyük çıkması, ev-iş yolculuklarındaki ulaştırma tür seçiminde salgının, betimleyici istatistik bulgularındaki değişimlere rağmen etkili olmadığını göstermiştir (Tablo 6). Başka bir deyişle, Wilcoxon İşaretli Sıra Testi sonucunda, grafikler üzerinden yapılan yorumlara konu olan değişimlerin, istatistiki açıdan anlamlı değişimler olmadığı saptanmıştır.

Tablo 2. Wilcoxon İşaretli Sıra Testi Sonuçları

İstatistikler	[Salgın Öncesi] – [Salgın]	[Salgın] – [Normalleşme]	[Salgın Öncesi] – [Normalleşme]
V	1.530	1.650,5	1.154,5
p-değeri	0,1024	0,1087	0,9249

4. SONUÇ

Bu çalışma kapsamında, Covid-19 salgınının ev-iş yolculuklarında ulaştırma türü seçiminde etkili olup olmadığı araştırılmıştır. Salgının gelişim evreleri olan salgın öncesi dönem, salgın dönemi ve normalleşme dönemlerinde, çalışma hayatına aktif katılım gösteren kent sakinlerinin büyük bir çoğunluğunun özel aracı tercih ettiği tespit edilmiştir. Öyle ki salgın, bu kesimin toplu taşımadan bireysel ulaşıma doğru bir yönelim davranışı sergilemesine de ortam hazırlamıştır. Normalleşme döneminde de bu yönelimin tam tersi biçimde işlemesi beklenirken bir kısım toplu taşımaya geri dönmüş, fakat kayda değer miktarda da bireysel ulaşımdan vazgeçmeyen bir kesim doğmuştur. Her ne kadar çeşitli grafikler üzerinden yapılan incelemeler ile birtakım değişimler ve yönelimler tespit edilse

de bu yönelim ve değişimlerin istatistiki açıdan anlamlı değişimler olmadığı sonucuna Wilcoxon İşaretli Sıra Testi ile varılmıştır.
Bu durum, orta ölçekli kentlerin küçük ve büyük ölçekli kentlerden ayrıldığını ve hazırlanan taktik/operasyonel kentsel ulaştırma yönetim planlarında daha farklı bir bakış açısının benimsenmesi gerektiğini işaret etmektedir. Bu çalışmanın çıktıları, literatürdeki birçok çalışmadan, daha çok büyük ölçekli kentlerdeki yolculukların inceleniyor olması ve bu yolculuklarda salgın etkisi ile tür seçimlerinin değiştiğinin ortaya çıkması bağlamında ayrıştığı ve özgün bulgular içerdiği gözlenmiştir.

TEŞEKKÜR

Bu yayın, Dr. Öğr. Üyesi Mustafa Sinan Yardım danışmanlığında, Sahra Başyazgan tarafından yapılan “Covid-19 Salgınının Orta Ölçekli Kentlerde Kentsel Ulaşıma Etkileri: Tekirdağ, Süleymanpaşa Örneği” isimli yüksek lisans tezinden üretilmiş olup, tez çalışması TÜBİTAK 2210/A Genel Yurtiçi Yüksek Lisans Bursu kapsamında desteklenmiştir. İlgili destek için TÜBİTAK’a teşekkür ederiz.

KAYNAKLAR

Eurofound. (2012). *MEDIUM-SIZED CITIES IN EUROPE*. https://www.eurofound.europa.eu/sites/default/files/ef_publication/ field_ef_document/ef9753en.pdf

Fulton, W. (2002). *The Mid-size City: Exploring Its The Unique Place in Urban Policy*. http://livable.nonprofitsoapbox.com/storage/documents/reports/Other/The_Mid-Sized_City_Exploring_its_Unique_Place_in_Urban_Policy.pdf

Gökgür, P., Kaya Altay, İ., & Ulusay Alpay, B. (2016). Çok Merkezlilik/Orta Ölçekli Kent Kavramı; Söke Örneği. *ARTIUM*, *4*(2), 1-12. http://artium.hku.edu.tr/tr/download/article-file/224125

Henderson, V. (1997). Medium Size Cities. *Journal of Regional Science and Urban Economics*, *27*(6), 583-612. https://reader.elsevier.com/reader/sd/pii/S0166046296021692?token=E38C84068FAF212004C798F307E8222C2D71C911214648357F82C5DB5F56F7B9C6481A253EA49FD5BFC063CC050A54B4&originRegion=eu-west-1&originCreation=20221019113558

Marra, A. D., Sun, L., & Corman, F. (2022). The impact of COVID-19 pandemic on public transport usage and route choice: Evidences from a long-term tracking study in urban area. *Transport Policy*, *116*, 258-268. https://doi.org/10.1016/j.tranpol.2021.12.009

Mobility Institute Berlin. (2020). *Beyond the immediate crisis: The SARS-CoV-2 pandemic and public transport strategy A Guideline for Action*. https://mobilityinstitute.com/wp-content/uploads/2020/04/Beyond-the-immediate-crisis-The-SARS-CoV-2-pandemic-and-public-transport-strategy_mib_v1.03.pdf

Özgür, H. (2005). Türkiye’de Orta Ölçekli Kentsel Alanların Yönetimi Sorunu. İçinde H. Özgür & M. Kösecik (Ed.), *Yerel Yönetimler Üzerine Güncel Yazılar –I: Reform* (ss. 471-498). Nobel Yayın Dağıtım.

Seasons, M. (2010). Indicators and Core Area Planning: Applications In Canada’s Mid Sized Cities. *Planning Practice & Research*, *8*(1), 63-80. https://doi.org/10.1080/0269745032000132646

Shabani, A., Shabani, A., Ahmadinejad, B., & Salmasnia, A. (2022). Measuring the customer satisfaction of public transportation in Tehran during the COVID-19 pandemic using MCDM techniques. *Case Studies on Transport Policy*, *10*(3), 1520-1530. https://doi.org/10.1016/j.cstp.2022.05.009

Shen, J., Duan, H., Zhang, B., Wang, J., Ji, J. S., Wang, J., Pan, L., Wang, X., Zhao, K., Ying, B., Tang, S., Zhang, J., Liang, C., Sun, H., Lv, Y., Li, Y., Li, T., Li, L., Liu, H., … Shi, X. (2020).

Prevention and control of COVID-19 in public transportation: Experience from China. *Environmental Pollution*, *266*, 1-5. https://doi.org/10.1016/j.envpol.2020.115291

Sogbe, E. (2021). The evolving impact of coronavirus (COVID-19) pandemic on public transportation in Ghana. *Case Studies on Transport Policy*, *9*(4), 1607-1614. https://doi.org/10.1016/j.cstp.2021.08.010

T.C. Çevre ve Orman Bakanlığı, İBB İmar ve Şehircilik Daire Başkanlığı, Trakya Kalkınma Birliği, & Metropoliten Planlama ve Kentsel Tasarım Merkezi. (2009). *1/100.000 Ölçekli Trakya Alt Bölgesi Ergene Havzası Revizyon Çevre Düzeni Planı Plan Açıklama Raporu*. https://webdosya.csb.gov.tr/db/mpgm/editordosya/file/CDP_100000/trakya_ergene/trakya_100000_cdp_PLANACIKLAMARAPORU.pdf

Transurban. (2020). *Industry Report-Urban Mobility Trends From Covid-19*. https://www.transurban.com/content/dam/transurban-pdfs/03/Urban-Mobility-Trends-from-COVID-19.pdf